

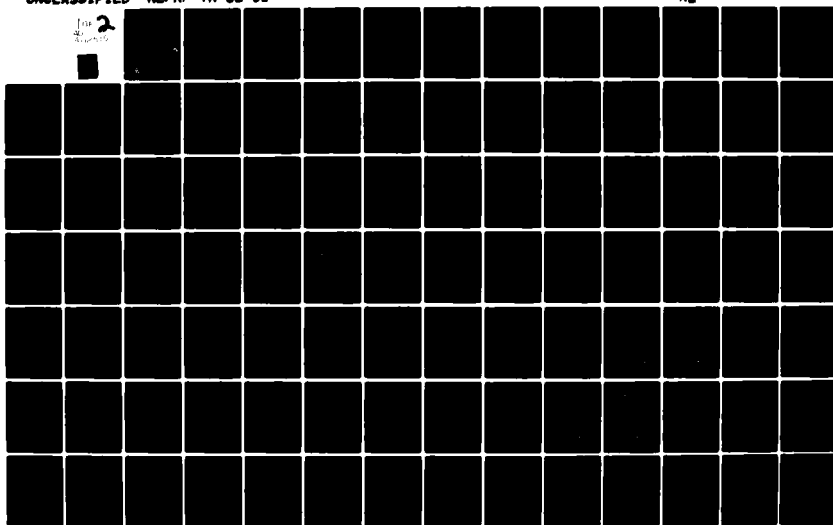
AD-A112 515

NAVAL ENVIRONMENTAL PREDICTION RESEARCH FACILITY MON--ETC F/G 4/2  
A CLIMATOLOGY OF THE REFRACTIVE INDEX STRUCTURE FUNCTION PARAM--ETC(U)  
JAN 82 T BROWN; A K GORUCH  
NEPRF-TR-82-01

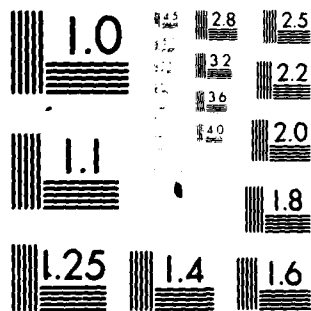
UNCLASSIFIED

NL

100  
2



A/125



MICROCOPY RESOLUTION TEST CHART  
NATIONAL BUREAU OF STANDARDS-1963-A



NAVENVPREDRSCHFAC  
TECHNICAL REPORT  
TR 82-01

12

NAVENVPREDRSCHFAC TR 82-01

# A CLIMATOLOGY OF THE REFRACTIVE INDEX STRUCTURE FUNCTION PARAMETER, $C_n^2$ , IN THE NORTH ATLANTIC OCEAN REGION

Terry Brown and Andreas K. Gorocho  
Naval Environmental Prediction Research Facility

JANUARY 1982

DTIC  
ELECTE  
MAR 25 1982  
H

APPROVED FOR PUBLIC RELEASE  
DISTRIBUTION UNLIMITED

DTIC FILE COPY



NAVAL ENVIRONMENTAL PREDICTION RESEARCH FACILITY  
MONTEREY, CALIFORNIA 93940

82 03 25 006

UNCLASSIFIED

SECURITY CLASSIFICATION OF THIS PAGE (When Data Entered)

REPORT DOCUMENTATION PAGE		READ INSTRUCTIONS BEFORE COMPLETING FORM
1. REPORT NUMBER NAVENVPREDRSCHFAC Technical Report TR 82	2. GOWT ACCESSION NO. ADP-4112515	3. RECIPIENT'S CATALOG NUMBER
4. TITLE (and Subtitle) A Climatology of the Refractive Index Structure Function Parameter, $C_n^2$ , in the North Atlantic Ocean Region	5. TYPE OF REPORT & PERIOD COVERED Final	
7. AUTHOR(s) Terry Brown & Andreas K. Goroch	6. PERFORMING ORG. REPORT NUMBER TR 82-01	
9. PERFORMING ORGANIZATION NAME AND ADDRESS Naval Environmental Prediction Research Facility Monterey, CA 93940	8. CONTRACT OR GRANT NUMBER(s)	
11. CONTROLLING OFFICE NAME AND ADDRESS Naval Sea Systems Command (PMS-405) Department of the Navy Washington, DC 20361	10. PROGRAM ELEMENT, PROJECT, TASK AREA & WORK UNIT NUMBERS PE 62759N PN WF59-551 NEPRF WU 6.2-21	
14. MONITORING AGENCY NAME & ADDRESS (if different from Controlling Office)	12. REPORT DATE January 1982	
	13. NUMBER OF PAGES 100	
	15. SECURITY CLASS. (of this report) UNCLASSIFIED	
	16a. DECLASSIFICATION/DOWNGRADING SCHEDULE	
16. DISTRIBUTION STATEMENT (of this Report)  Approved for public release; distribution unlimited.		
17. DISTRIBUTION STATEMENT (of the abstract entered in Block 20, if different from Report)		
18. SUPPLEMENTARY NOTES Original manuscript received November 1981.		
19. KEY WORDS (Continue on reverse side if necessary and identify by block number) Optical laser propagation Turbulence model Refractive index fluctuations Structure function parameters		
20. ABSTRACT (Continue on reverse side if necessary and identify by block number) The optical refractive index structure function parameter, $C_n^2$ , describes the effects of turbulence on optical propagation. Surface boundary layer turbulence models are used to calculate monthly mean values and standard deviations of $C_n^2$ in the North Atlantic Ocean. $C_n^2$ statistics are presented as isopleths of mean values and standard deviations for day, night, and diurnally averaged values.		

DD FORM 1473

1 JAN 73

EDITION OF 1 NOV 65 IS OBSOLETE  
S/N 0102-014-6601

UNCLASSIFIED

SECURITY CLASSIFICATION OF THIS PAGE (When Data Entered)

# CONTENTS

1. Introduction . . . . .	1
2. Method . . . . .	2
3. Data . . . . .	3
4. Results . . . . .	5
Appendix A - $C_n^2$ Turbulence Model . . . . .	6
References . . . . .	21
Figures . . . . .	22

DTIC  
COPY  
INSPECTED

Accession For	
NTIS	<input checked="" type="checkbox"/>
DTIC	<input type="checkbox"/>
Unannounced	<input type="checkbox"/>
Other	<input type="checkbox"/>
By	
Date	
Avail	
A	

## 1. INTRODUCTION

The shipboard operation of optical laser systems is degraded by turbulence in the marine planetary boundary layer (MPBL). The refractive index structure function parameter,  $C_n^2$ , is a measure of the turbulent fluctuations of refractive index over small distances and is the turbulence parameter related to optical system performance.  $C_n^2$  is defined by:

$$C_n^2 = \overline{[n(x+r) - n(x)]^2} r^{-2/3}, \quad (1)$$

where  $n(x+r)$  and  $n(x)$  are the refractive indices at points separated by a short distance  $r$ . The overbar represents an average value over a spatial region or a time interval. Refractive index fluctuations cause a loss of coherence in a laser beam, a broadening of the beam, and a reduction in power focused on a target.

This climatology presents the means and standard deviations of  $C_n^2$  values for the North Atlantic Ocean region. Locales characterized by large  $C_n^2$  values are identified and indicate areas where optical system performance will be degraded. The diurnal variation of  $C_n^2$  also is presented.

## 2. METHOD

Surface layer turbulence is generated by the fluxes of heat, momentum and moisture in the sea surface boundary layer. The values of these fluxes have been related to commonly observed meteorological variables by the development of surface layer scaling laws. A model using these laws, together with modifications for use of the model in the MPBL, has been described by Burk et al. (1979). A modified form of the model is included as Appendix A.

The meteorological variables required for the model are:

- U - wind speed, usually taken at 10 m height
- T - air temperature
- $T_s$  - sea surface temperature
- q - specific humidity, taken at 10 m height

### 3. DATA

The data base for this study was a subset of the Fleet Numerical Oceanography Center's Consolidated Data Set of marine surface observations. Eleven years of data (1963-1973) were extracted and processed for this analysis. This period was selected to avoid the inclusion of low precision merchant vessel data collected before 1962. Husby (1980) cites such data as a contributor to erroneous heat flux computations.

The accuracy of the data base can be evaluated by comparing simultaneous observations from merchant vessels and ocean station weather ships. Since merchant reports dominate the data base it is important that these observations be reliable. Bunker (1976) found good agreement between means of wind speed, sea surface temperature and air temperature as reported by merchants and weather ships when at least 500 observations are included per average. The uncertainty in the determination of the heat flux can be expected to be about 10% in such cases. This uncertainty increases as the number of observations falls below 500. Mean values of  $C_n^2$  were calculated for each 1° latitude by 1° longitude Marsden subsquare in the study area. Along the major shipping lanes at least 500 observations per month and subsquare generally were reported. Outside these routes the number of reports declined greatly.

Several quality control checks have been made to improve the reliability of the observations. Reports indicating supersaturated conditions were discarded along with air temperatures outside the



range of  $\pm 50^{\circ}\text{C}$ . Reported dew point temperatures were compared to values computed from reported wet and dry bulb temperatures and the report discarded if the disagreement was  $\geq 1^{\circ}\text{C}$ . Reported air-sea temperature differences were similarly screened. Sea surface temperatures  $< -8.0^{\circ}\text{C}$  were eliminated as were sea surface temperatures that deviated from a running mean for each month and subsquare by more than  $9^{\circ}\text{C}$ .

All observations were assumed to have been made at a height of 10 m since actual levels are not reported. The effect of differing heights is probably less significant than other observational errors. A minimum wind speed of 1 meter per second was allowed. Reports of calm conditions were modified accordingly.

Finally,  $C_n^2$  was defined as zero when the air and sea surface temperatures were equal.

The data successfully screened were grouped and analyzed in three categories, daytime, nighttime and all times. Daytime was defined to be from 0601 to 1800 local standard time.

#### 4. RESULTS

The isopleths of mean  $C_n^2$  values are presented for the twelve months for day and night (Figure 1-12), daytime only (Fig. 13-24) and for nighttime only (Fig. 25-36). The units are  $m^{-2/3} \times 10^{15}$ . Standard deviations are shown in Figures 37-72.

The most striking feature of the figures is the strong influence of the Gulf Stream on the turbulence values. The heat flux from the warm sea surface to the colder air is accompanied by higher levels of turbulence than in surrounding areas of colder water. The maximum values of turbulent intensity over the Gulf Stream occurs during winter. This corresponds to the strong heat flux from the warm sea surface to the cold winter air of continental origin.

The diurnal variation of turbulence appears to be greatest during the summer in the area southeast of the Azores. This is an area where there is a small annual variation of sea surface temperature and wind speed. However, insolation does differ between night and day, and this contrast is largest during the summer months. This point leads us to conjecture that the apparent diurnal variation of turbulence levels between the Azores and the African coast is primarily due to ship insolation, and does not indicate the actual variability of  $C_n^2$  in the MPBL. If this is correct, then the isopleths based only on nighttime data most accurately represent the distribution of mean  $C_n^2$  values for the region.

FIGS. 1-72 ARE PRESENTED AS  
A GROUP BEGINNING ON P. 22.

APPENDIX A  
 $C_n^2$  Turbulence Model

This appendix describes a sequence of calculations to compute the refractive index structure function parameter,  $C_n^2$ , from shipboard measurements of air temperature, sea surface temperature, wind speed and specific humidity. The algorithm is a modification of a preliminary model described by Burk et al. (1979) who concluded that the surface layer scaling laws used to predict  $C_n^2$  are accurate to a factor of two and that the accuracy of the shipboard observations introduces the same order of uncertainty into  $C_n^2$  results.

A.1 Refractive index structure function parameter,  $C_n^2$

Since refractive index is related to temperature, moisture and pressure, the fluctuations of the refractive index that compose  $C_n^2$  are caused by fluctuations in these variables. The effect of pressure variations can be neglected while variations of temperature and moisture are described by the temperature structure function parameter,  $C_T^2$ , the moisture structure function parameter,  $C_e^2$ , and the temperature/moisture correlation parameter,  $C_{eT}$ . These component structure parameters are related to  $C_n^2$  by:

$$C_n^2 = B_1 C_T^2 + B_2 C_{eT} + B_3 C_e^2 \quad (A-1)$$

where  $B_1$ ,  $B_2$  and  $B_3$  are functions of temperature, pressure and vapor pressure.

Over the range of normally observed values of these structure parameters,  $C_T^2$  is the largest contributor to  $C_n^2$ . Over land, where moisture sources are relatively unimportant, the contributions of  $C_e^2$  and  $C_{eT}$  are negligible. Over water the contributions of these structure parameters are significant. To calculate  $C_n^2$  in the marine planetary boundary layer (MPBL), it is necessary to calculate  $C_T^2$  and modify it for the contribution made by moisture fluctuations.

In developing the modification used in this model, Wesely (1976) expands the definition of the refractive index structure parameter to provide  $C_n^2$  as a function of the component structure functions and covariances,

$$C_n^2 = C_T^2 \left( \frac{A_1 P}{T} \right)^2 \alpha_v^2; \alpha_v^2 = 1 + 2r_{eT} \left[ \frac{(1-A_2/A_1)C_{eT}}{PC_T} \right] + \left[ \frac{(1-A_2/A_1)C_{eT}}{PC_T} \right]^2 \quad (A-2)$$

where  $T$  is the mean layer temperature in K,  $P$  is the mean layer pressure in mb,

$$A_1 = 78.7 \cdot 10^{-6} \text{K mb}^{-1}, A_2 = 66.7 \cdot 10^{-6} \text{K mb}^{-1} \text{ and } r_{eT} = \frac{C_{eT}}{C_e C_T}.$$

For this analysis it was assumed that  $e$  and  $T$  are perfectly correlated and  $r_{eT} = 1$ . Thus,

$$C_n^2 = C_T^2 \left( \frac{A_1 P}{T} \right)^2 \left( 1 + \frac{0.03}{B} \right)^2 \quad (A-3)$$

where  $B$  is the Bowen ratio defined below.

#### A.2 Temperature structure function parameter, $C_T^2$

In the surface layer, dimensional arguments first introduced by Monin and Obukhov can be used to relate  $C_T^2$  to a temperature scale,  $T_*$ ; a height,  $z$ ; and a stability function,  $g(z/L)$ . Wyngaard et al. (1971) derived a semiempirical relationship of these parameters,

$$C_T^2 = T_*^2 z^{-2/3} g(z/L) \quad (A-4)$$

where  $L$  is the Monin-Obukhov length scale.

#### A.3 Stability Function in $C_T^2$

Using a set of careful observations over uniform terrain in Kansas, Wyngaard et al. (1971) have empirically determined the function  $g(z/L)$  from measurements of  $C_T^2$  and the scaling parameters  $L$  and  $T_*$ . The results have been tested over water by Friehe (1977) and Davidson et al. (1978). The following expressions are used in this analysis,

$$\begin{aligned} g(z/L) &= 4.9(1-7z/L)^{-2/3} & (L \leq 0) \\ g(z/L) &= 4.9(1+2.75(z/L)^{2/3}) & (L > 0). \end{aligned} \quad (A-5)$$

#### A.4 Scaling functions in the surface layer

The Monin-Obukhov theory describes the surface layer using non-dimensional atmospheric variables. Physical variables of length,  $z$ ; wind speed,  $U$ ; temperature,  $T$ ; and specific humidity,  $q$ ; are made non-dimensional by defining a scaling length,  $L$ ; a scaling speed,  $U_*$ ; a scaling temperature,  $T_*$ ; and a scaling humidity,  $Q_*$ . The non-dimensional parameters describe the fluxes of momentum, heat, and humidity in the surface layer.

#### A.5 Monin-Obukhov length, L

In a dry atmosphere the characteristic length  $L_{\text{DRY}}$  is taken as the Monin-Obukhov length,

$$L_{\text{DRY}} = \frac{T U_*^2}{g k T_*} \quad (\text{A-6})$$

where  $T$  is mean surface layer temperature in K,  $g$  is acceleration of gravity, and  $k$  is the von Kármán constant. In unstable air buoyancy generated turbulence dominates at levels above  $-L$ , while mechanical turbulence dominates much below  $-L$ . The length is corrected for moisture by using the Bowen ratio  $B$ ,

$$L = L_{\text{DRY}} \left(1 + \frac{.07}{B}\right)^{-1} \quad (\text{A-7})$$

The Bowen ratio is related to the heat and moisture fluxes and is expressed in terms of the scaling temperature and humidity,

$$B = \frac{C_p T_*}{L_w Q_*} \quad (\text{A-8})$$

where  $C_p$  is specific heat of air at constant pressure and  $L_w$  is latent heat of vaporization.

#### A.6 Scaling wind speed, $U_*$ ; temperature, $T_*$ ; and humidity, $Q_*$

The surface layer is characterized by fluxes of momentum, heat and moisture which are independent of height. These constant fluxes are used to define the scaling velocity,  $U_*$ ; temperature,  $T_*$ ; and humidity,  $Q_*$ ;

$$\begin{aligned} U_* &= \sqrt{-\overline{U'W'}} \\ T_* &= -\frac{1}{U_*} \overline{T'W'} \\ Q_* &= -\frac{1}{U_*} \overline{q'W'} \end{aligned} \quad (\text{A-9})$$

where  $U'$ ,  $T'$  and  $q'$  are fluctuations of horizontal wind, temperature and humidity about their means, and the overbar is an average among all fluctuations. These scaling variables are related to the vertical profiles of each variable,

$$\begin{aligned} U_* &= kU \left[ \ln\left(\frac{Z}{Z_0}\right) - \psi_M(z/L) \right]^{-1} \\ Q_* &= \frac{k}{R}(q - q_s) \left[ \ln\left(\frac{Z}{Z_{0Q}}\right) - \psi_Q(z/L) \right]^{-1} \\ T_* &= \frac{k}{R}(T - T_s) \left[ \ln\left(\frac{Z}{Z_{0T}}\right) - \psi_H(z/L) \right]^{-1} \end{aligned} \quad (A-10)$$

where  $U$  is the wind speed in m/s,  $T$  and  $T_s$  are the air and sea surface temperatures in °C,  $q$  and  $q_s$  are the specific humidities at the observation height  $Z$  and at the sea surface in grams per gram.  $Z_0$ ,  $Z_{0T}$ , and  $Z_{0Q}$  are roughness parameters describing molecular transport of wind, temperature, and moisture near the surface, and  $\psi_M$ ,  $\psi_H$ , and  $\psi_Q$  are empirical profile functions. The constant  $R$  is included in the equations for temperature and humidity. The value of this constant is accepted as 0.74 based on reliable field experiments.

#### A.7 Profile functions

The profile functions,  $\psi$ , were formulated by Businger et al. (1971). These functions have been verified both over land and over water and are given by,

$$\begin{aligned}
& L \leq 0 & L > 0 \\
\psi_H &= \ln \left[ \left( \frac{1+x^2}{2} \right) \left( \frac{1+x}{2} \right)^2 \right] - 2 \arctan(x) + \pi/2 & \psi_H &= -\beta \frac{z}{L} \\
x &= (1 - \gamma_m z/L)^{1/4} & & (A-11) \\
\psi_H = \psi_Q &= 2 \ln \left[ \frac{1 + \sqrt{1 - \gamma_H \frac{z}{L}}}{2} \right] & \psi_H = \psi_Q &= -\frac{\beta}{R} \frac{z}{L}
\end{aligned}$$

Constants in these formulations are determined by fitting the formulations to the data, and correspond best to one particular data set. Universal constants have so far not been found.

The hypothesis that the  $\psi$  are the same for heat and moisture is based mostly on measurements over land. There is considerable controversy whether the assumption is valid over the ocean; but no better hypotheses are available. Fortunately, in all equations, the  $\psi$ 's are small compared to the logarithmic terms, so that extreme accuracy in the  $\psi$ 's is not required. Further,  $\psi_Q$  occurs only in the correction of  $L$  for moisture, which itself is usually a small correction.

#### A.8 Roughness Lengths $Z_0$ , $Z_{0T}$ , $Z_{0Q}$

The molecular transport of momentum, heat and moisture near the surface is described by the values of  $Z_0$ ,  $Z_{0T}$ , and  $Z_{0Q}$  respectively. In the marine environment, the roughness lengths have values on the order of 1 mm or less. The dependence of  $C_n^2$  on  $Z_0$  is included primarily in the function  $\ln \frac{Z}{Z_0}$ , where  $Z$  is the elevation, taken to be 10 meters. Therefore  $C_n^2$  should be insensitive to errors in  $Z_0$ . Separate treatments of  $Z_0$ ,  $Z_{0T}$  and  $Z_{0Q}$  are necessary. The technique developed by Liu (1978) is used



here. Liu derived relations between  $U$  and  $U_*$  and the transfer coefficients for momentum, heat, and moisture, ( $C_D$ ,  $C_H$ ,  $C_Q$ ). These relationships are shown in Figure A-1. The roughness lengths can be related to  $C_D$ ,  $C_H$ ,  $C_Q$ , and the profile functions by,

$$\begin{aligned} Z_o &= Z \cdot \exp\left(\frac{k}{C_D^{1/2}} + \psi_M(z/L)\right) \\ Z_{oT} &= Z \cdot \exp\left(\frac{k}{R} \frac{C_D^{1/2}}{C_H} + \psi_H(z/L)\right) \\ Z_{oQ} &= Z \cdot \exp\left(\frac{k}{R} \frac{C_D^{1/2}}{C_Q} + \psi_Q(z/L)\right). \end{aligned} \tag{A-12}$$

The values of the roughness lengths cannot be obtained in closed form expressions, and the following procedure was used:

- a. An arbitrary, initial value for  $L$  of  $10^{30}$  was chosen. This implies that  $Z/L \approx 0$ , (since  $Z$  was assumed to be 10 m) and indicates neutral conditions.
- b. The profile functions,  $\psi$ , were assigned their neutral values of zero.
- c. The transfer coefficients  $C_Q$  and  $C_H$  were given initial values of  $1.3 \times 10^{-3}$  which is approximately the maximum value shown in Figure A-1.
- d. The curve for  $C_D$  shown in Figure A-1 was approximated by the equation,

$$C_D = 10^{-3} \cdot (0.62375 + 0.8414 \cdot \log_{10}(U)) \tag{A-13}$$

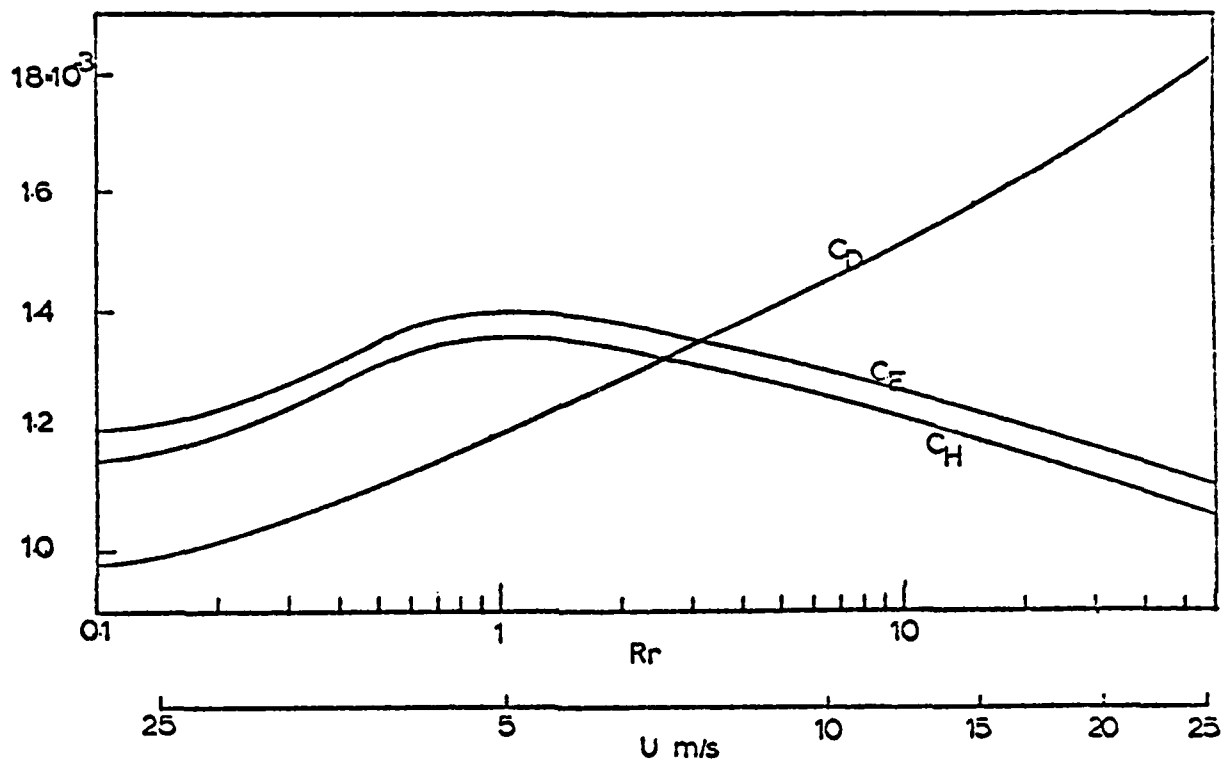


Fig. A-1. Bulk transfer coefficients at neutral conditions versus 10 m wind  $U$  and roughness Reynolds number  $R_r$  (Liu, 1978). The transfer coefficients are approximately calculated from wind  $U$ ; when scaling speed  $U^*$  and roughness length  $Z_0$  are found, transfer coefficients are found from  $R_r$  using formulas in the text.

where  $U$  is the wind speed. For this calculation only, reported values of  $U < 2.5$  m/s were changed to a minimum value of 2.5 m/s to correspond to the lower limit of the diagram. Using Eq. (A-13), an initial value of  $C_D$  was computed.

e.  $Z_o$ ,  $Z_{oT}$  and  $Z_{oQ}$  were calculated from equation (A-12).

A maximum value of 1 mm was allowed for all roughness lengths. Larger values were reduced to this limit.

f. The initial roughness lengths were used to calculate new values for the transfer coefficients,  $C_D$ ,  $C_H$  and  $C_Q$ . These values in turn were used to compute the scaling parameters  $U_*$ ,  $T_*$  and  $Q_*$ . At this point the roughness Reynolds number was found by,

$$R_r = \frac{Z_o U_*}{\nu} \quad (A-14)$$

where  $\nu$  is the kinematic viscosity of air. As shown in Figure A-1, a minimum value of 0.1 was allowed for  $R_r$ .

g. A new set of roughness lengths was calculated using another approximation to the curve for  $C_D$  in Figure A-1 and the arbitrary values of  $C_H = .0011$  and  $C_Q = .0012$ . The equation for  $C_D$  is

$$C_D = 10^{-3} \cdot (1.233 + 0.336 \cdot \log_{10}(R_r)). \quad (A-15)$$

A minimum value of  $0.75 \times 10^{-3}$  was allowed. This corresponds to the lower limit in Figure A-1.

#### A.9 Sea Surface Temperature, $T_s$

In most cases, bucket temperature,  $T_w$ , rather than the surface temperature is measured.  $T_s$  was estimated from a theory by Liu (1978). Liu, (Figure A-2) gives  $T_s - T_w$  as a function of the wind speed and the difference between bucket temperature and air temperature at 10 m height,  $\Delta T$ .

Liu's diagram was approximated by the following equations:

$$T_w - T_s = .025\Delta T + 0.1 \quad (U > 6 \text{ m sec}^{-1}) \quad (\text{A-16})$$

$$T_w - T_s = 0.1\Delta T + .8 - U(.117 + .0125\Delta T) \quad (U \leq 6 \text{ m sec}^{-1})$$

where the temperature is in  $^{\circ}\text{C}$  and the wind speed is in  $\text{m sec}^{-1}$ .

#### A.10 Evaluation of constants

Certain empirical constants were introduced in the definition of scaled quantities, the vertical flux profiles, and in the  $C_T^2$  stability function. These constants depend on the particular data set from which they were determined, and there is no uniform agreement in the literature on the best values of each. In choosing the constants, a set of values corresponding to one particular data set should be chosen because the constants are interdependent. Table 1 provides the values of the constants used in this analysis.

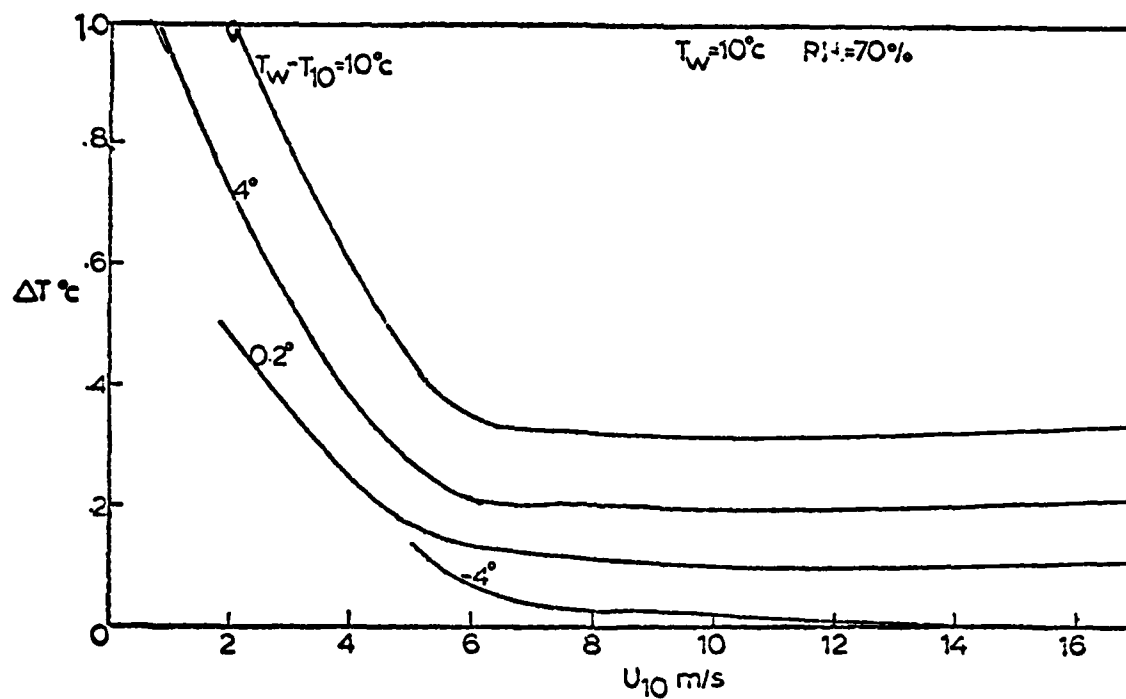


Fig. A-2. Temperature difference across the aqueous sublayer versus 10 m wind for values of air-bulk water temperature difference  $T_w - T_{10}$  (Liu, 1978). These formulas account for radiation and molecular effects in the surface layer.

Table 1

<u>Constant</u>	<u>Value Used</u>
For Scaling Functions	
k	0.35
R	.74
For Profile Functions	
$\gamma_m$	15
$\gamma_H$	6
$\beta$	4.7
For Stability Function	
b	.667

#### A.11 Calculation of $C_n^2$

The step-by-step procedure used to calculate  $C_n^2$  is given below.

- a. Modify the sea surface temperature measurement to an actual sea surface temperature value using Eq. (A-16) and  $T_s$ ,  $T_w$  and  $U$ .
- b. Set initial stability to neutral, i.e.,  $L=10^{30}$ ,  $Z/L=0$ , and  $\psi_M = \psi_H = \psi_Q = 0$ .
- c. The bulk wind speed determines an initial value of  $C_D$  using Eq. (A-13). Initial values for  $C_H$  and  $C_Q$  are set to .0013.
- d. Calculate  $Z_o$ ,  $Z_{oT}$ , and  $Z_{oQ}$  from  $C_D$ ,  $C_H$ ,  $C_Q$  with Eq. (A-12).
- e. Calculate new values for  $C_D$ ,  $C_H$ , and  $C_Q$  by rearranging Eq. (A-12).
- f. Evaluate scaling parameters  $U_*$ ,  $T_*$  and  $Q_*$  using Eq. (A-10).

- g. Evaluate Bowen ratio,  $B$ , using Eq. (A-8).
- h. Evaluate Monin-Obukhov length for moist atmosphere using Eqs. (A-6) and (A-7).
- i. Test if the new  $L$  is within 0.1% of the last value of  $L$ .
- L. If so, go to statement m. If not, go to statement j.
- j. Calculate stability functions  $\psi_M$ ,  $\psi_H$ ,  $\psi_Q$  using Eq. (A-11).
- k. Calculate roughness Reynolds number  $R_r$  from Eq. (A-14).
- l. Evaluate  $C_D$  from Eq. (A-15) using  $R_r$  and set  $C_H$  and  $C_Q$  to .0011 and .0012 respectively. Go to statement d.
- m. Evaluate  $C_T^2$  stability function,  $g(z/L)$ , using Eq. (A-5).
- n. Evaluate  $C_T^2$  using Eq. (A-4).
- o. Calculate  $C_n^2$  using Eq. (A-3).

This procedure is graphically outlined in Figure A-3.

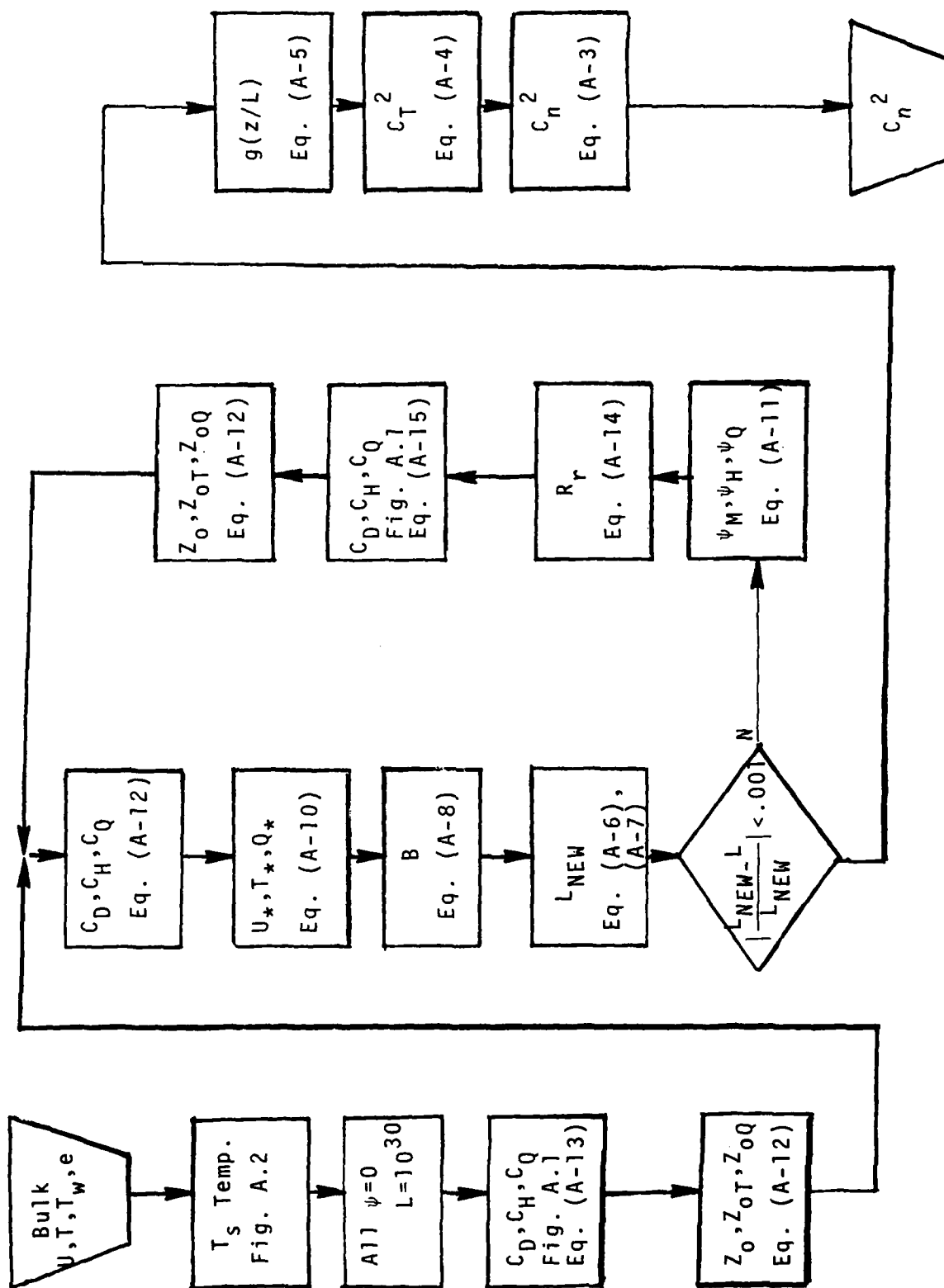


Figure A-3. Flow chart of surface layer  $C_n^2$  calculation. Symbols, equation numbers, and figure numbers are those used in text.



## Glossary and Values for $C_n^2$ Turbulence Model

B	- Bowen ratio
$C_D, C_H, C_Q$	- bulk transfer coefficients
$C_e$	- moisture structure function parameter
$C_{eT}$	- temperature/moisture correlation parameter
$C_n^2$	- index of refraction structure function parameter
$C_p$	- specific heat of air at constant pressure (0.24 cal/g K)
$C_T^2$	- temperature structure function parameter
g	- acceleration of gravity ( $9.8 \text{ m/s}^2$ )
K	- von Kármán constant (.35)
L	- Monin-Obukov length (m)
$L_w$	- latent heat of vaporization (591.7 cal/g)
n	- optical index of refraction
P	- atmospheric pressure (mb)
q	- specific humidity (g per g)
$Q_*$	- scaling humidity (g per g)
R	- scaling constant (.74)
$R_r$	- roughness Reynolds number
T	- temperature (K or °C)
$T_s$	- sea surface temperature (°C)
$T_w$	- bucket temperature (°C)
$T_*$	- scaling temperature (K)
U	- wind speed (m/sec)
$U_*$	- scaling velocity (m/sec)
Z, z	- observation height (assumed 10 m)
$Z_o$	- roughness lengths (m)
$\beta$	- profile function constant (4.7)
$\gamma_H$	- heat flux profile parameter (6.0)
$\gamma_m$	- momentum flux profile parameter (15.0)
$\nu$	- kinematic viscosity of air ( $1.35 \times 10^{-5} \text{ m}^2/\text{s}$ )
$\psi$	- profile functions

## REFERENCES

- Bunker, A., 1976: Computations of surface energy flux and annual air-sea interaction cycles of the North Atlantic Ocean. Mon. Wea. Rev., 104, 1122-1140.
- Burk, S., A. K. Goroch, A. I. Weinstein, and H. A. Panofsky, 1979: Modeling the refractive index structure parameter in the marine planetary boundary layer. NAVENVPREDRSCHFAC Technical Report TR 79-03.
- Businger, J. A., J. C. Wyngaard, Y. Izumi, and E. F. Bradley, 1971: Flux profile relationships in the atmospheric surface layer. J. Atmos. Sci., 22, 181-189.
- Davidson, K. L., T. M. Houlihan, C. W. Fairall, and G. E. Schacher, 1978: Observations of the temperature structure function parameter,  $C_T^2$ , over the ocean. Naval Postgraduate School Technical Report NPS 63-78-005, 37 pp.
- Friehe, C., 1977: Estimation of the refractive index temperature structure parameter over the ocean. Appl. Optics, 10, 334-340.
- Husby, D., 1980: A comparison of surface heat flux estimates over ocean weather station V and merchant vessels in its vicinity in the western North Pacific region 1956-1970. J. Phys. Oceanogr., 10, 6, 971-975.
- Liu, W. T., 1978: The molecular effects on air-sea exchanges. Ph.D. Thesis, University of Washington, Seattle.
- Wesely, M. L., 1976: The combined effect of temperature and humidity fluctuations on refractive index. J. Appl. Meteor., 15, 43-48.
- Wyngaard, J. C., Y. Izumi, and S. Alloblis, Jr., 1971: Behavior of the refractive index structure parameter near the ground. J. Opt. Soc. Am., 61, 1646-1650.

## FIGURES

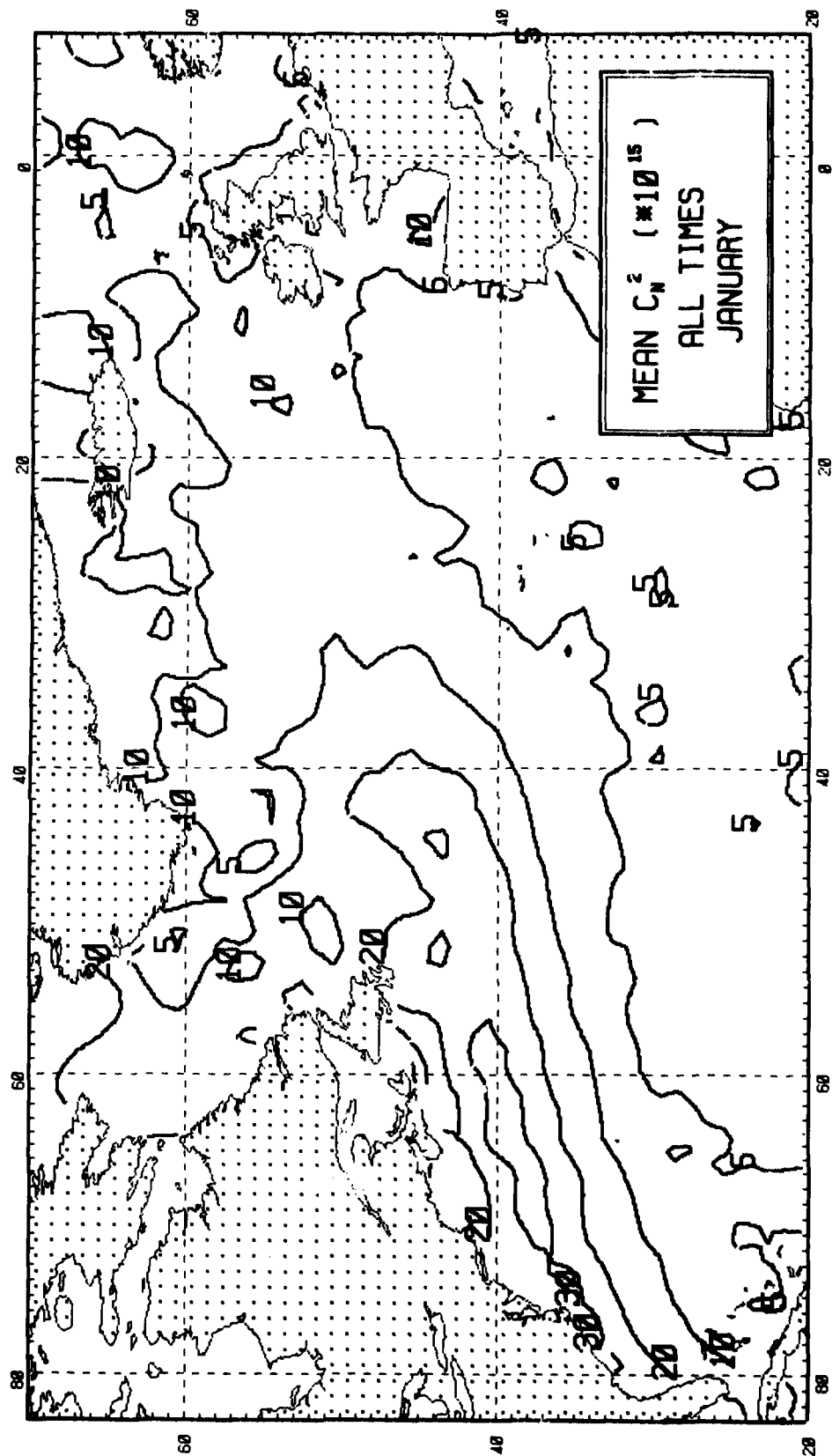
Figures showing isopleths of mean  $C_n^2$  values and of standard deviations are sequenced numerically for the twelve months of the calendar year as follows:

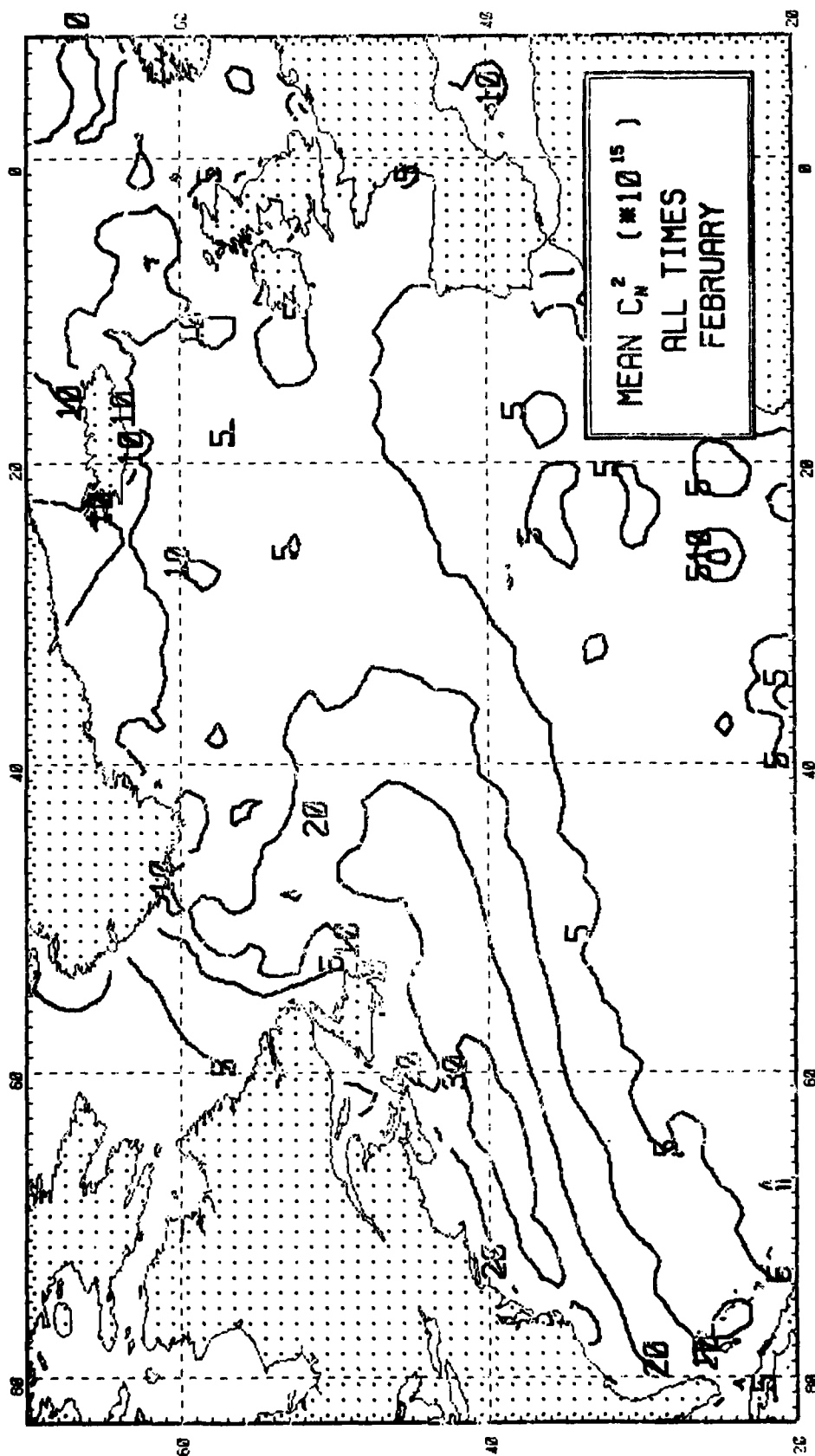
### Means

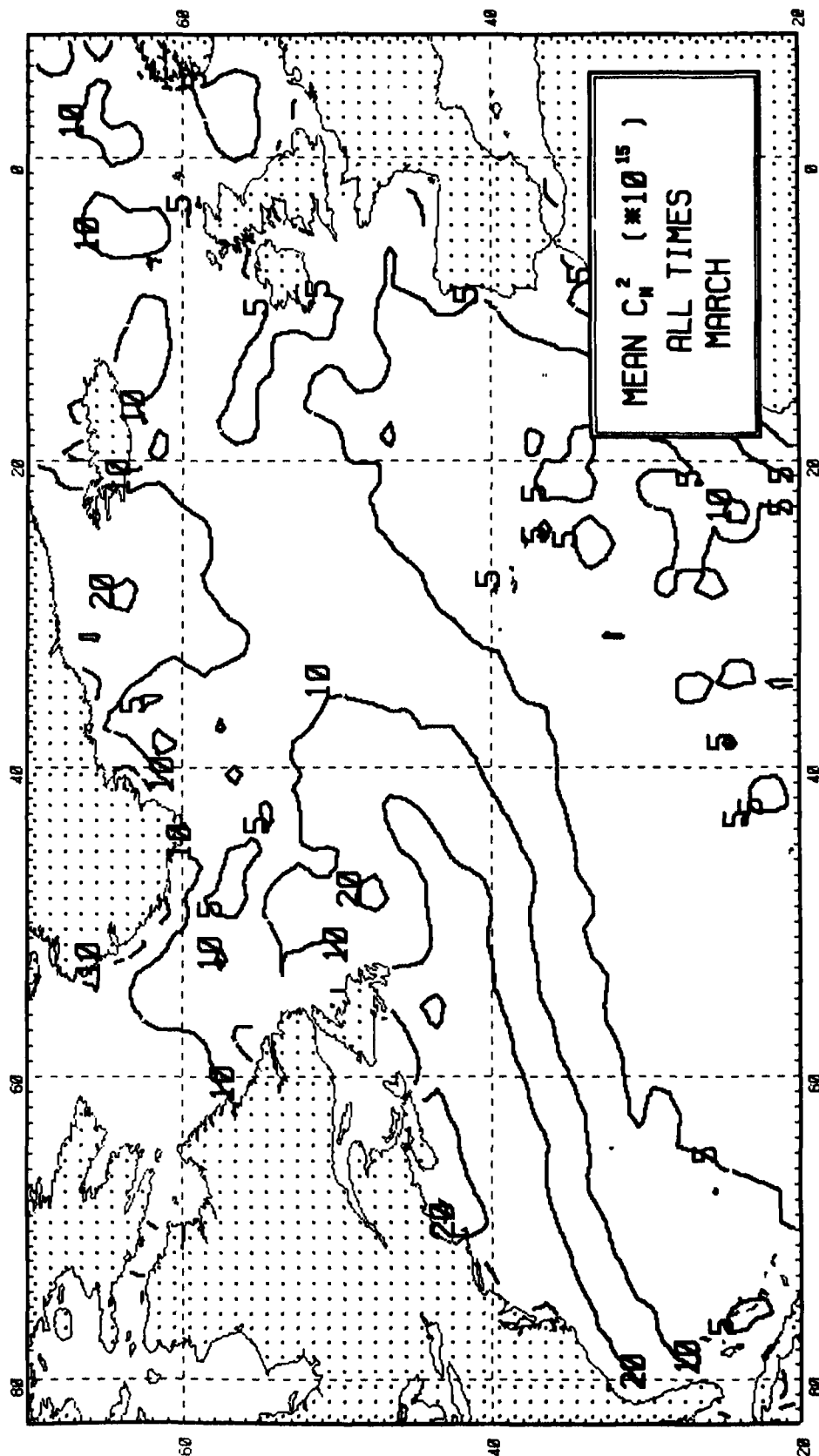
Day and Night -- Figs. 1-12 ("All Times")  
Daytime Only -- Figs. 13-24  
Nighttime Only - Figs. 25-36

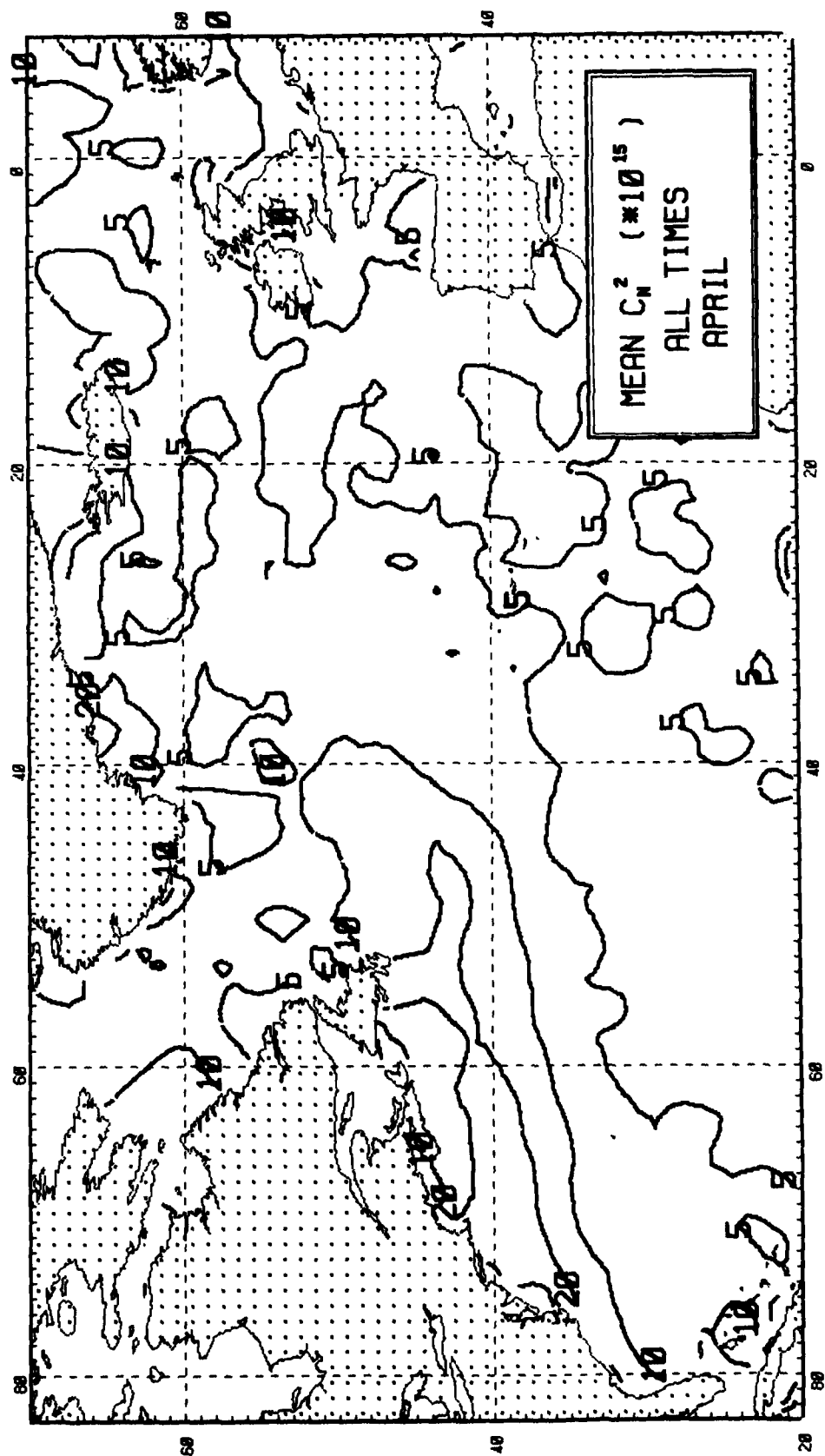
### Standard Deviations

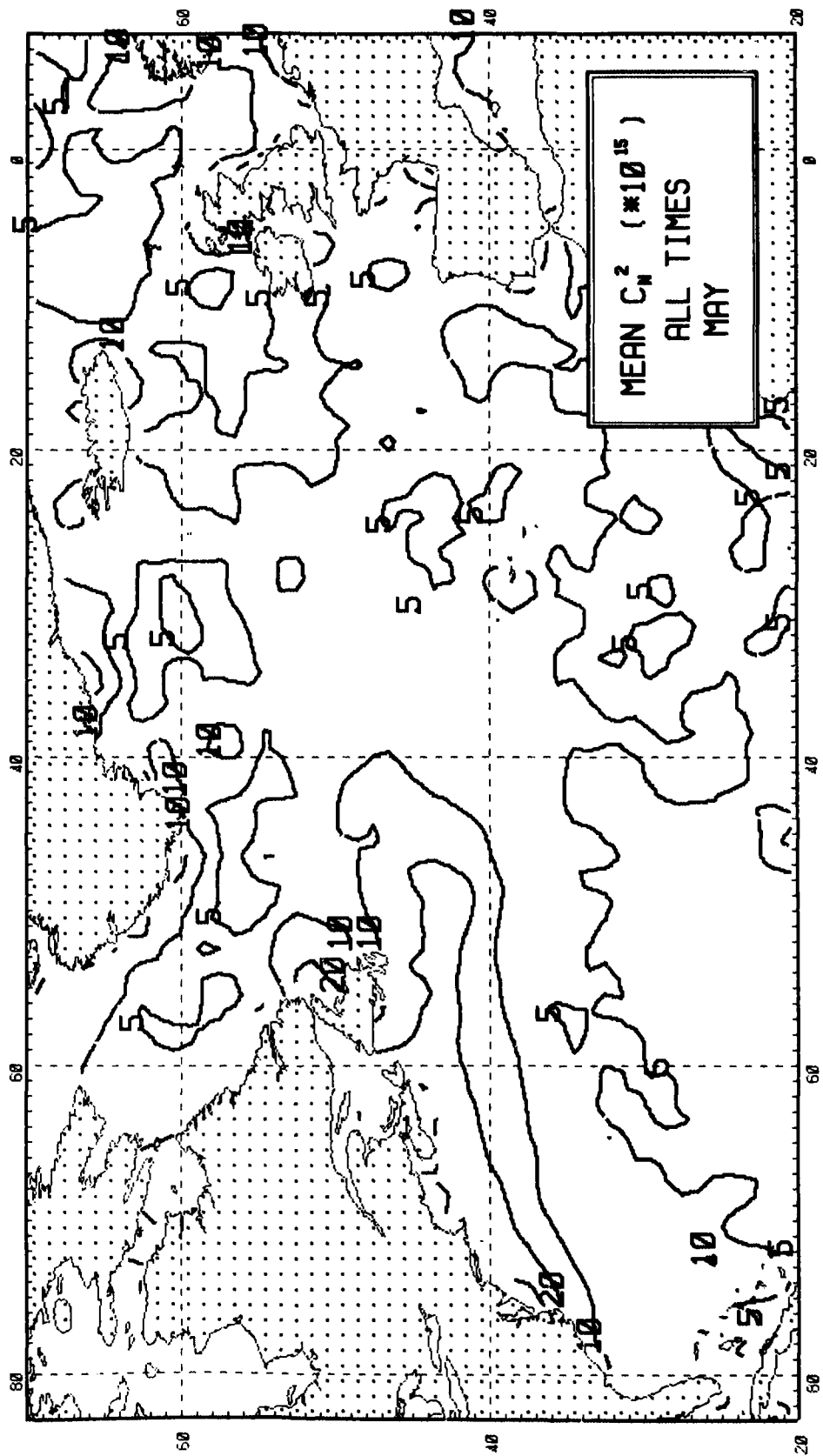
Day and Night -- Figs. 37-48 ("All Times")  
Daytime Only -- Figs. 49-60  
Nighttime Only - Figs. 61-72



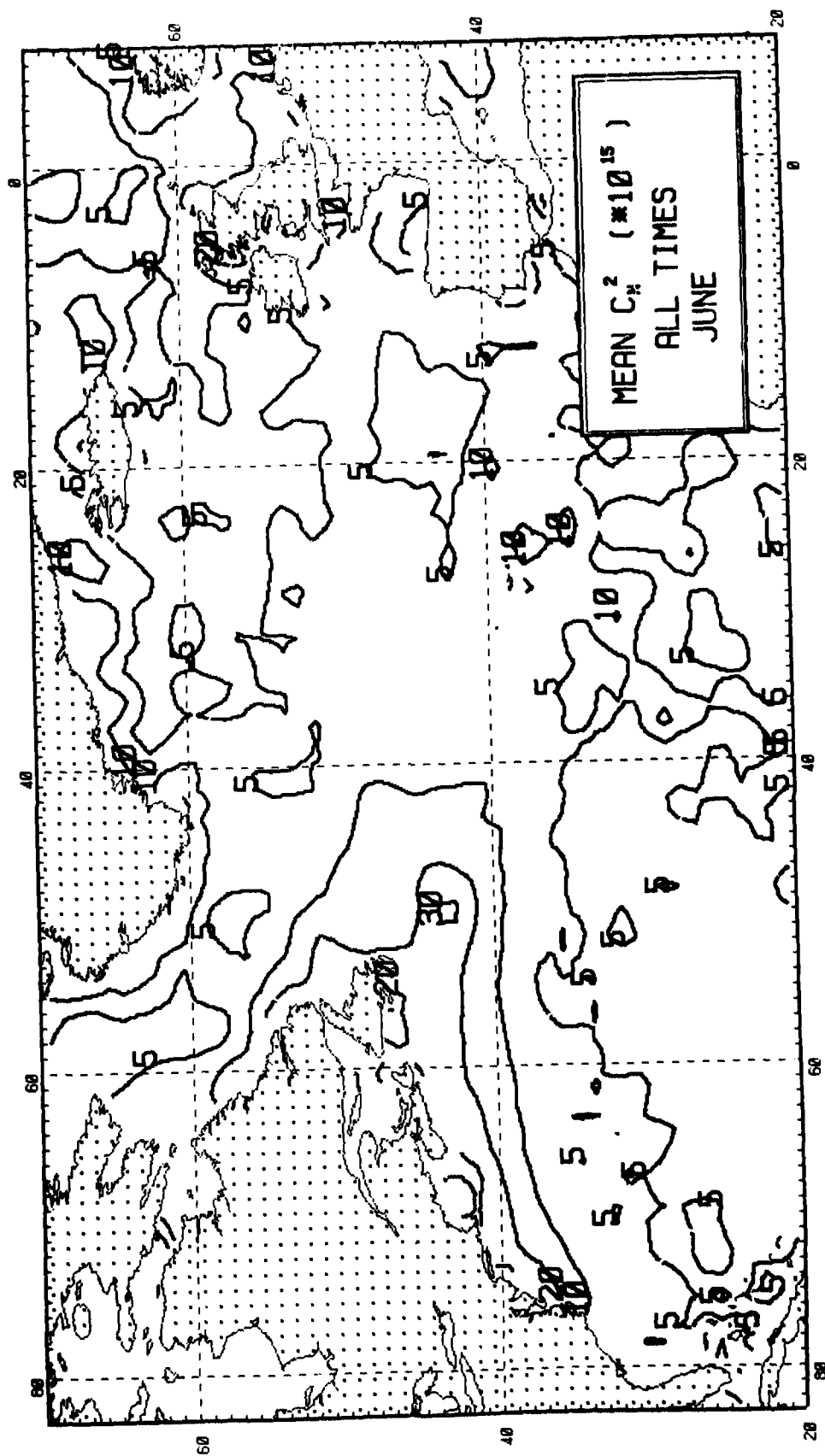


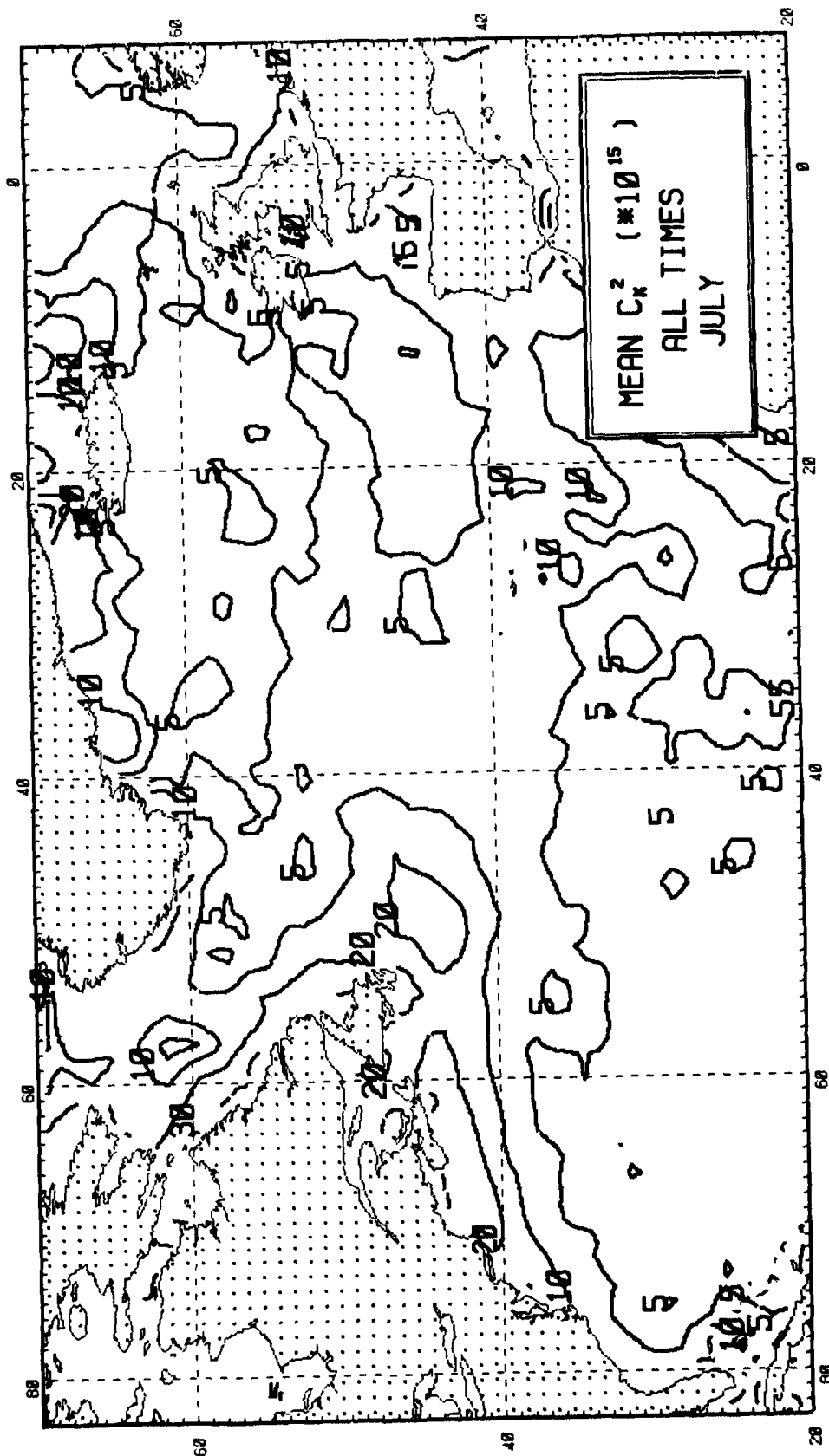


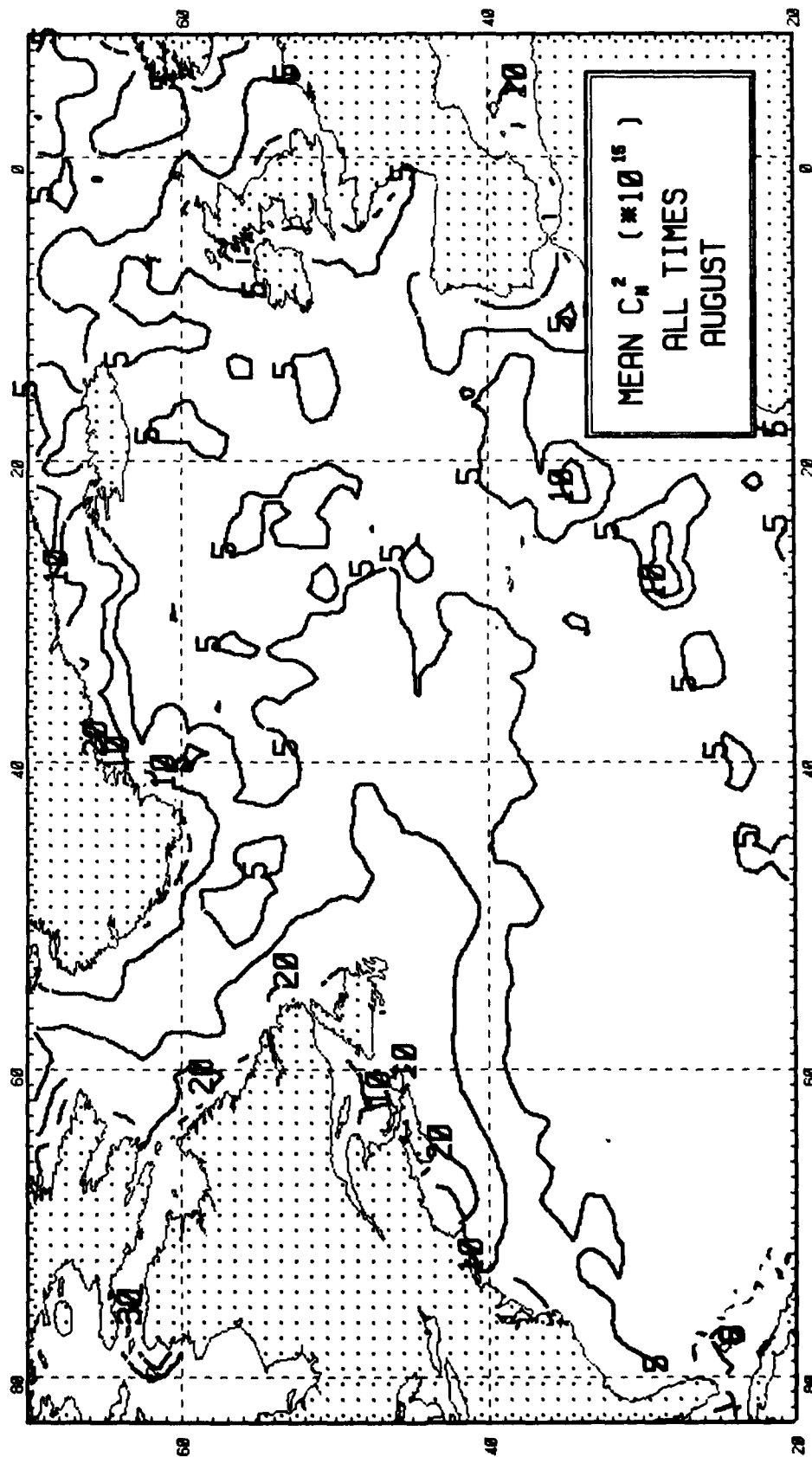


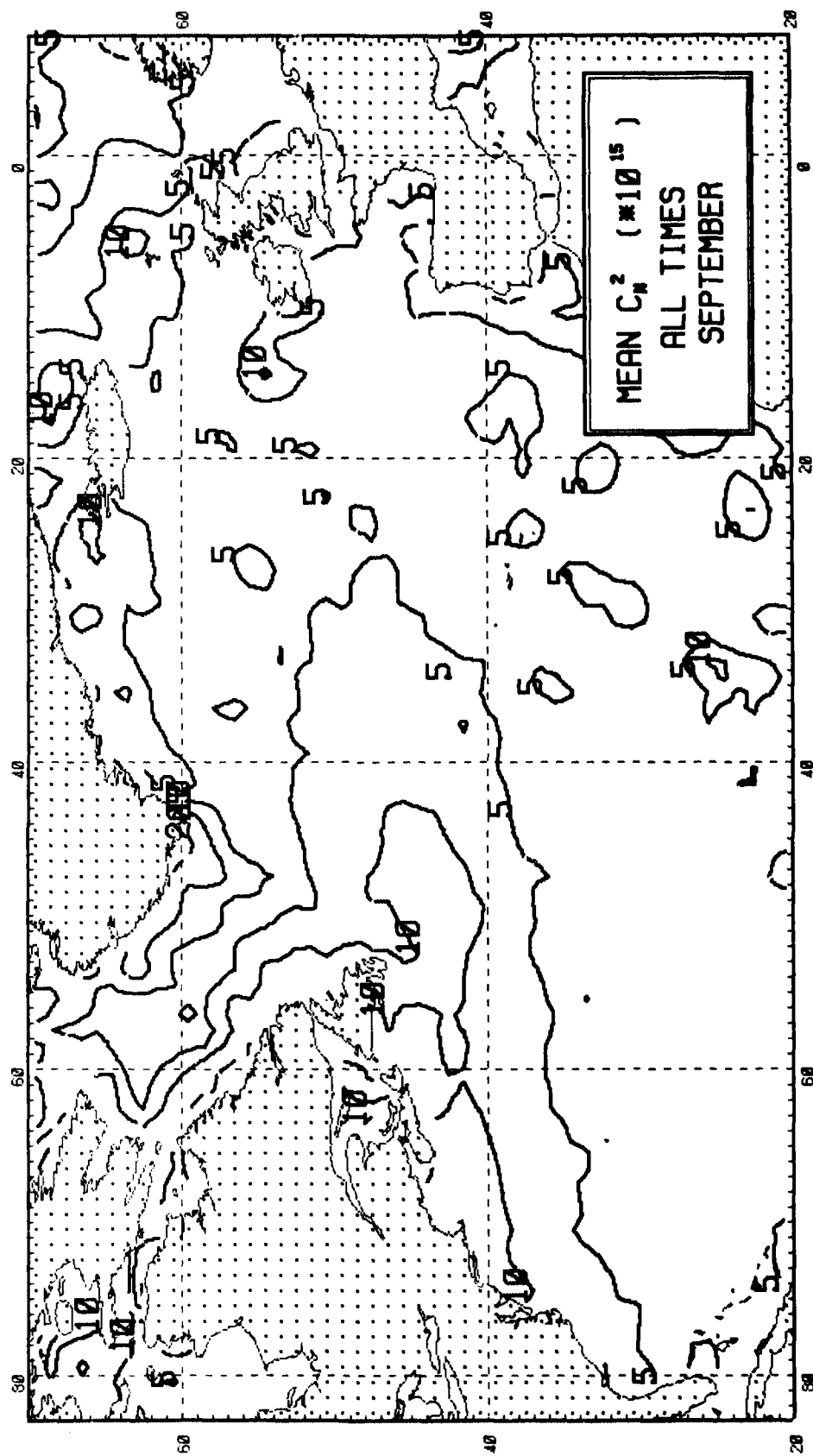


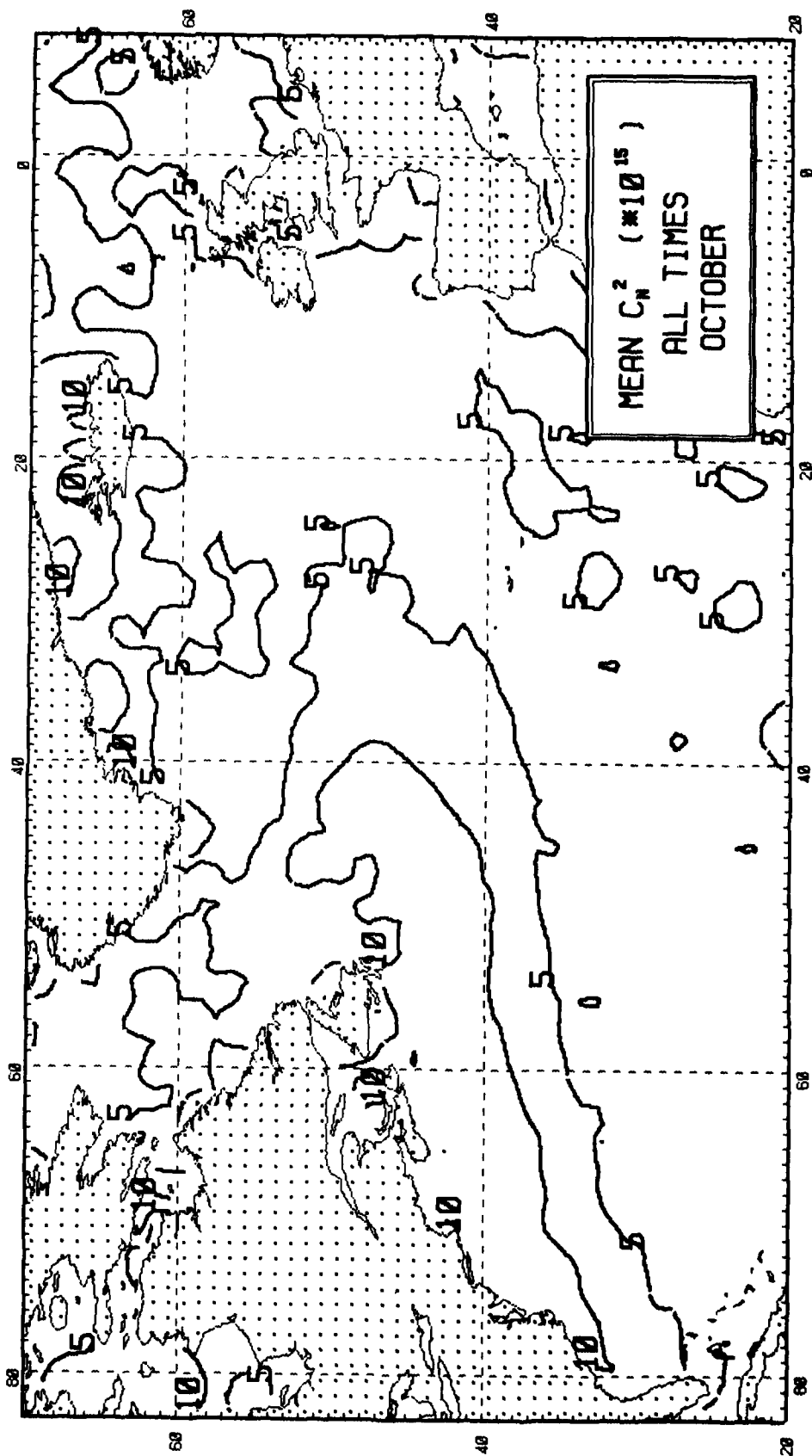


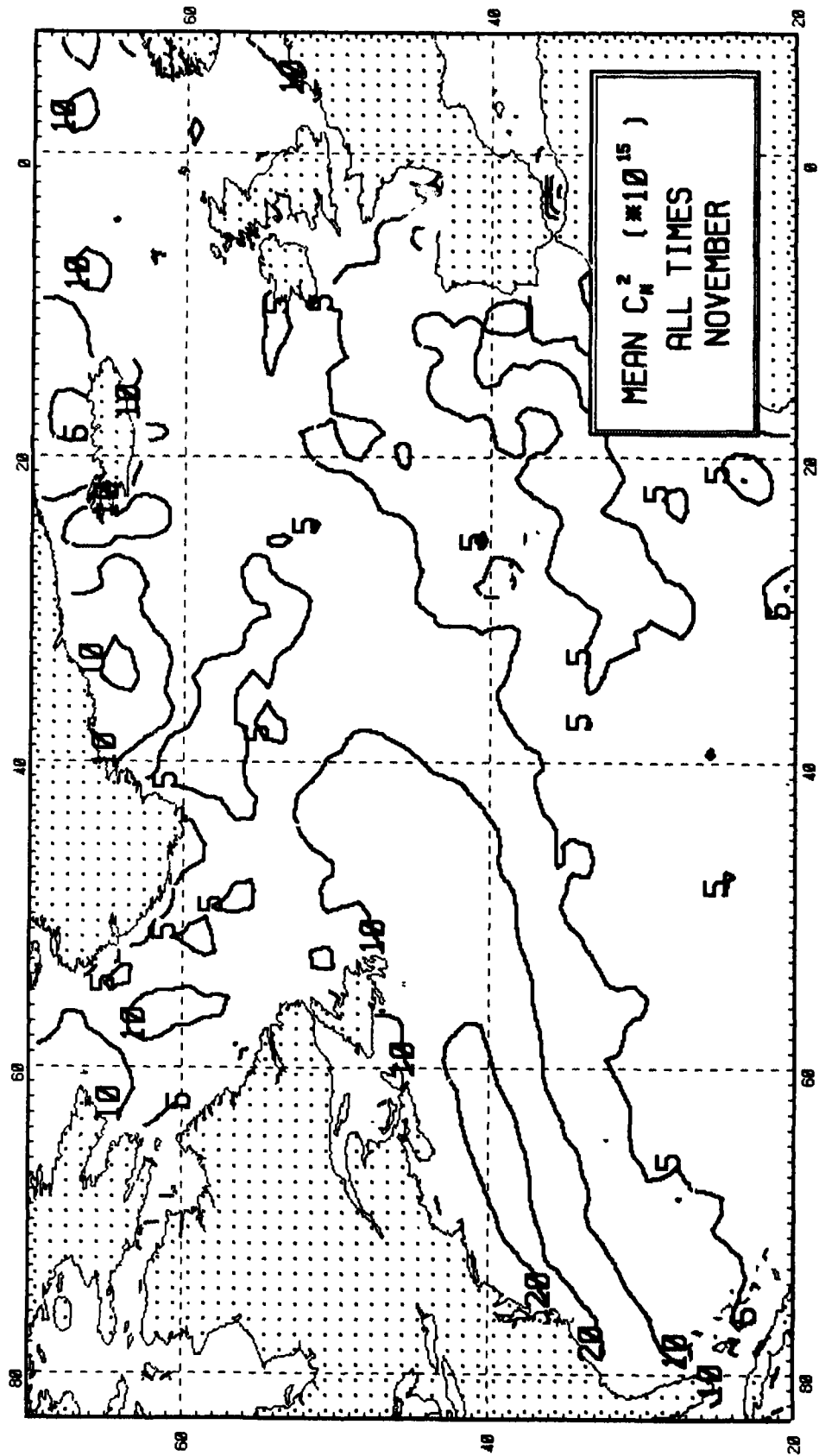


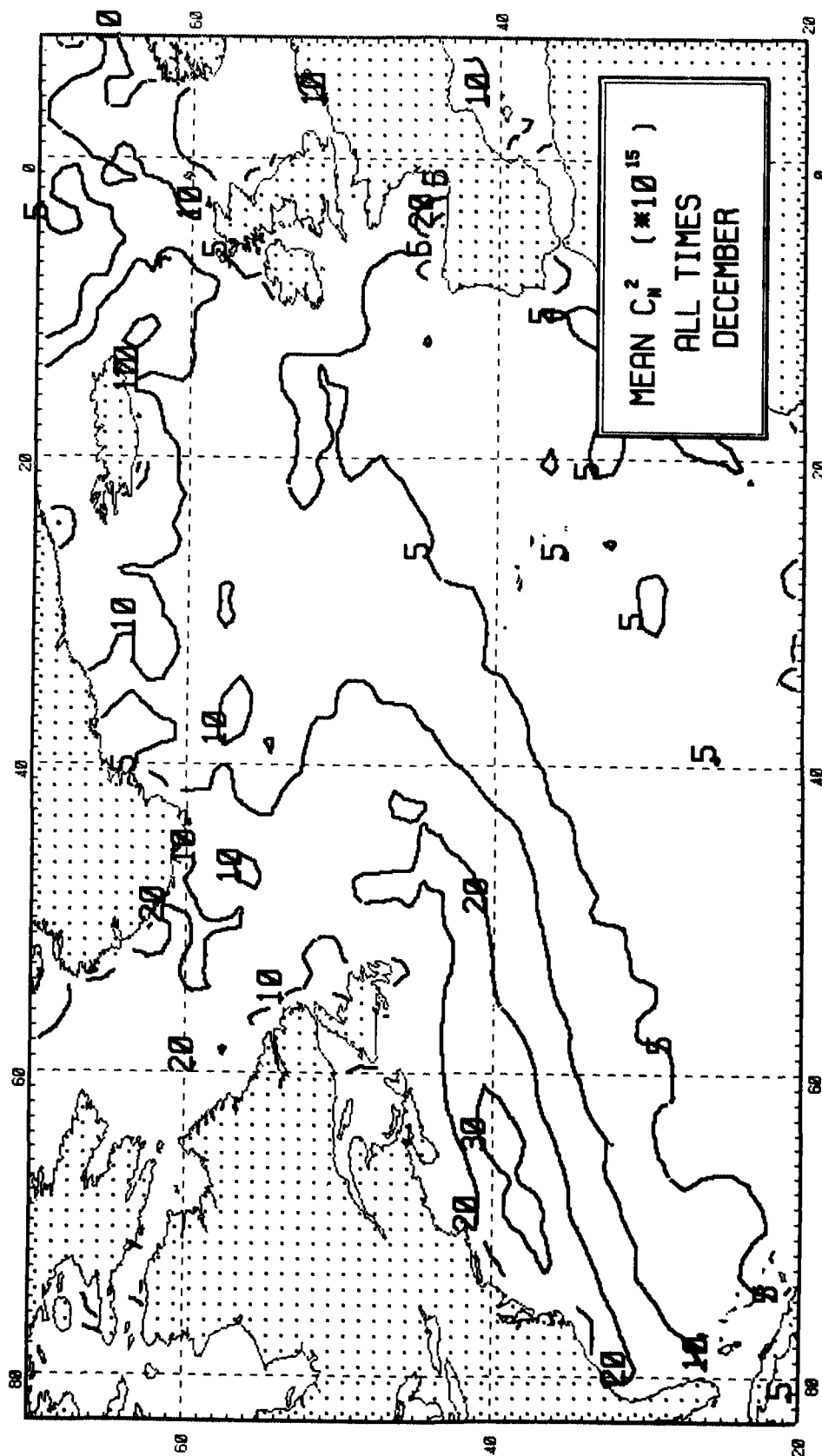


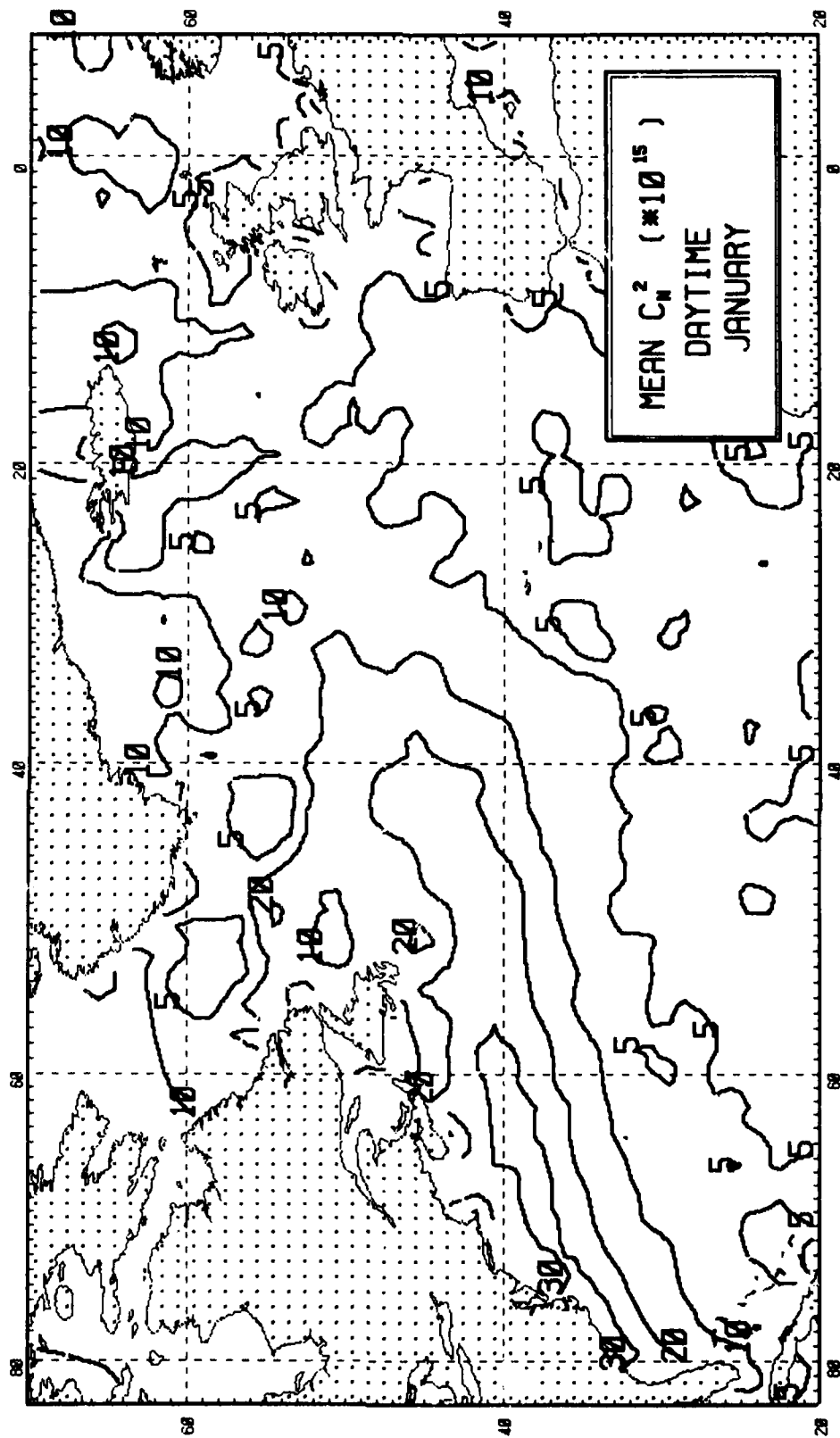




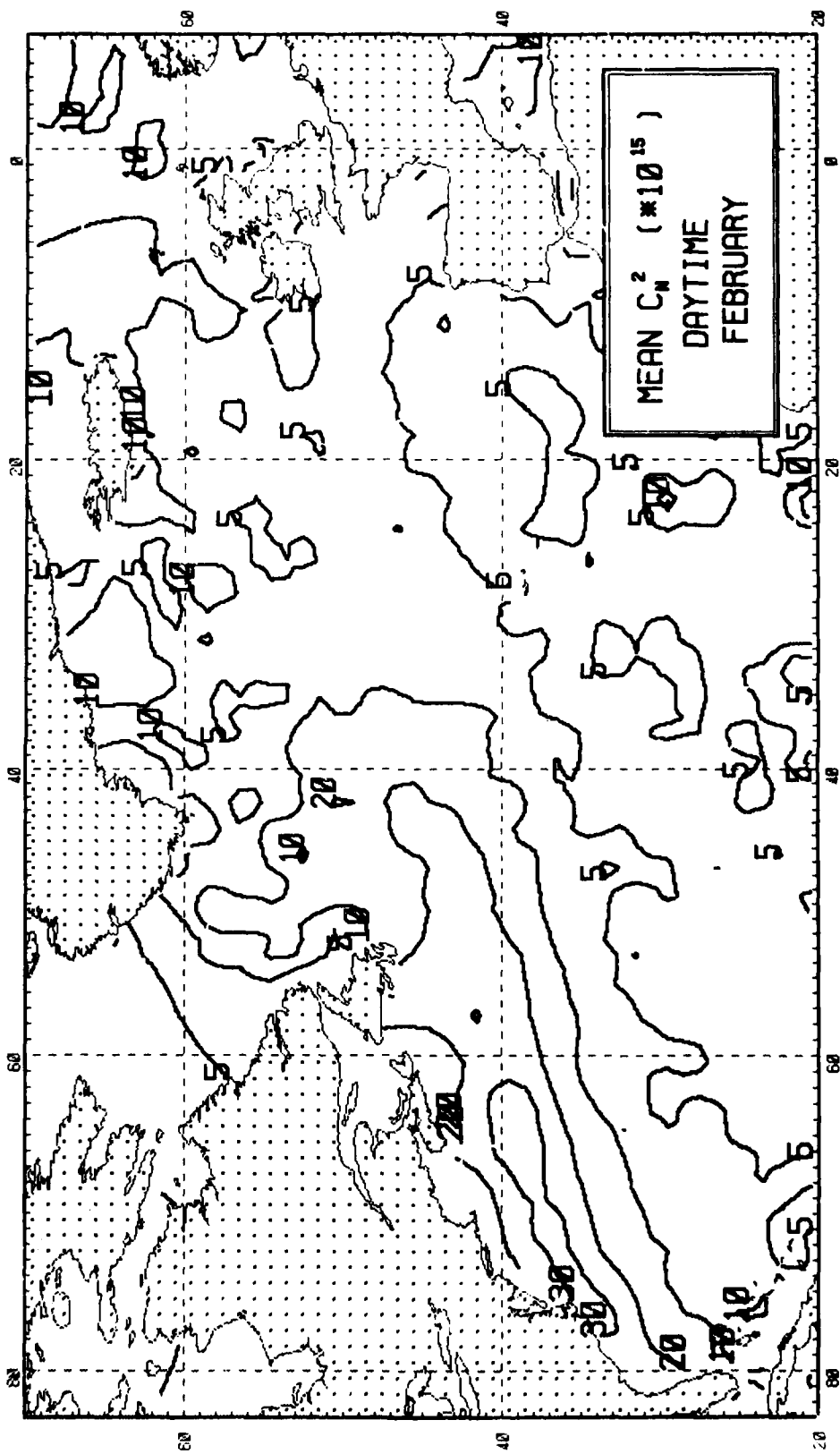


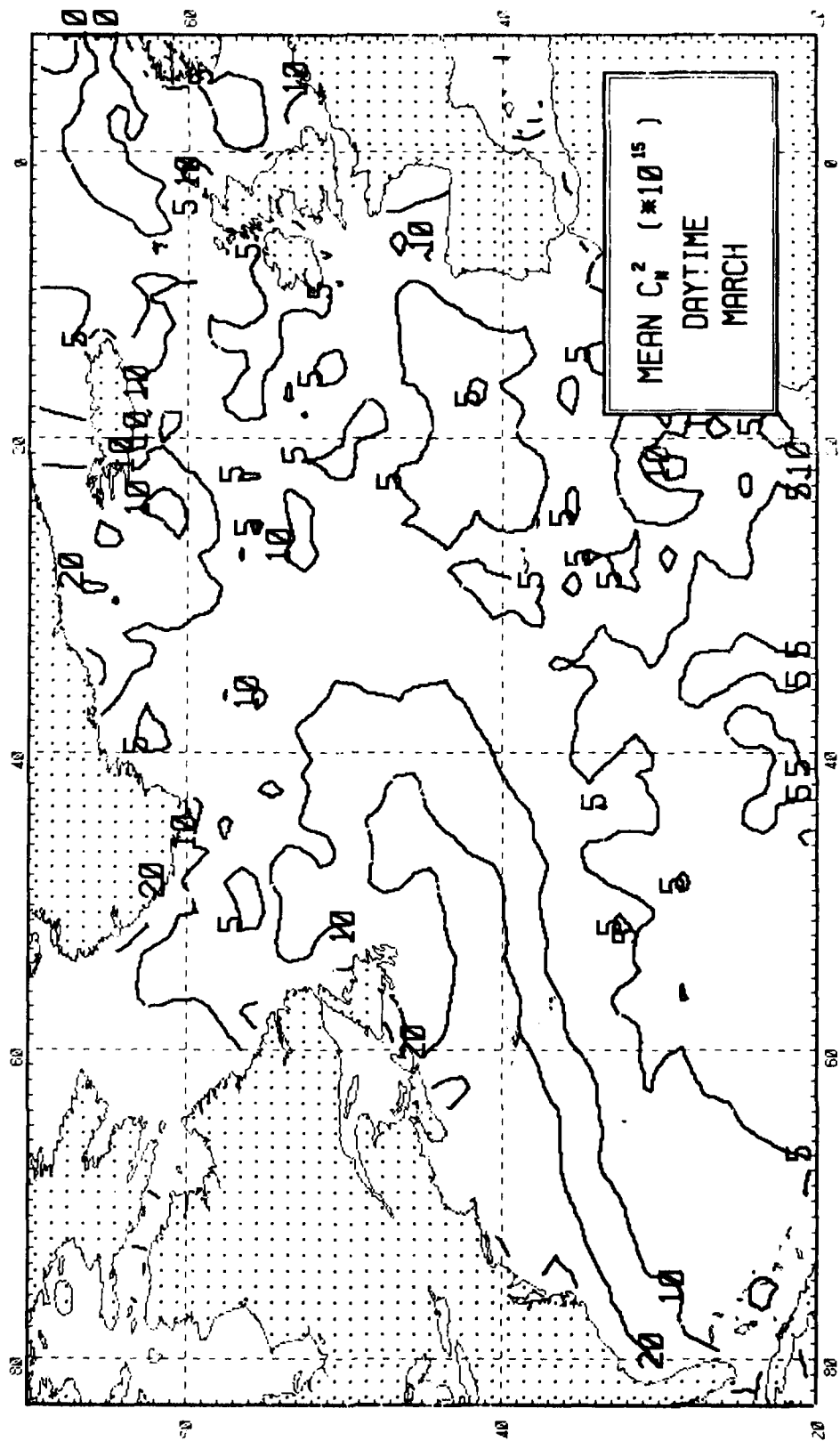


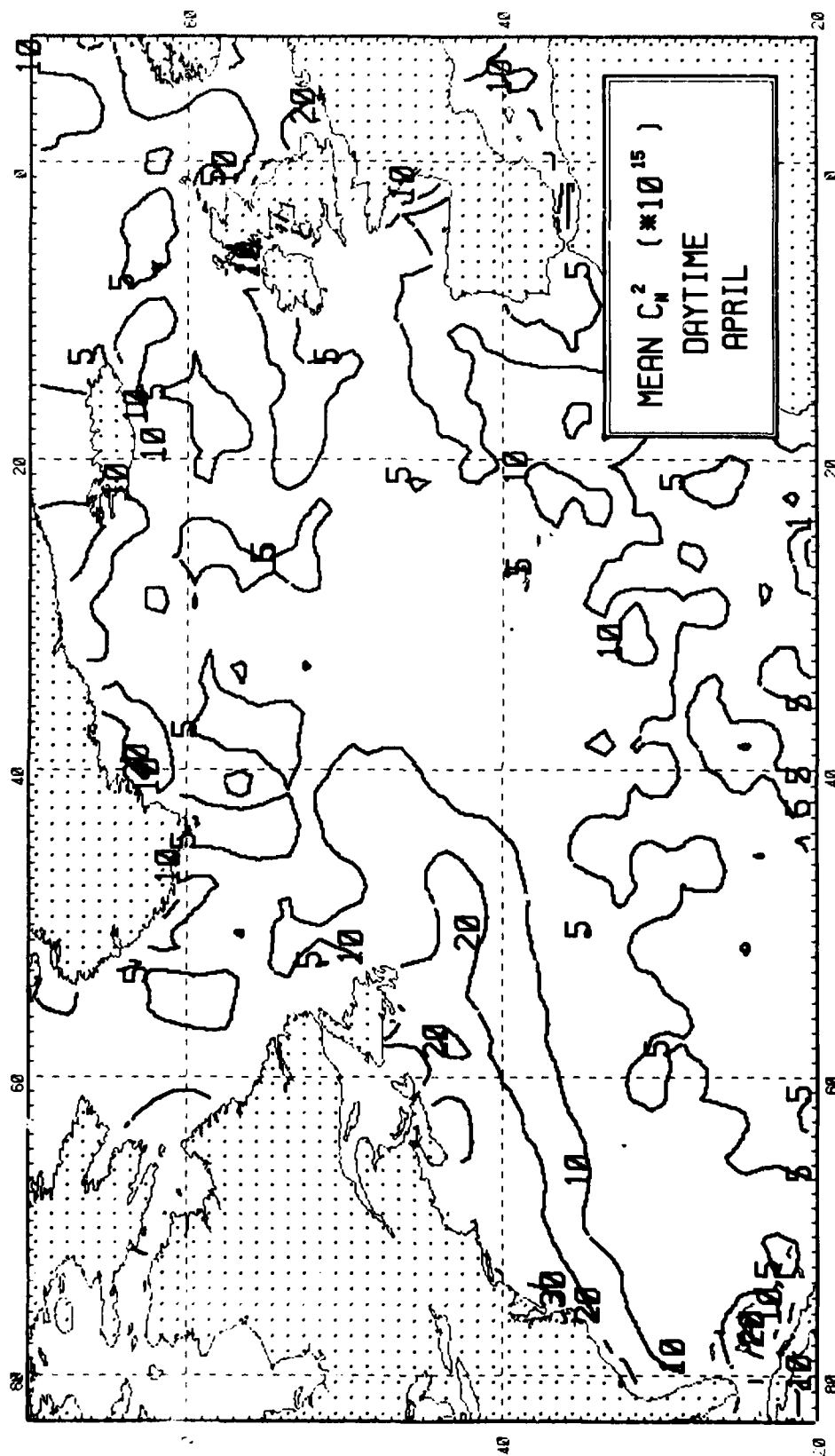


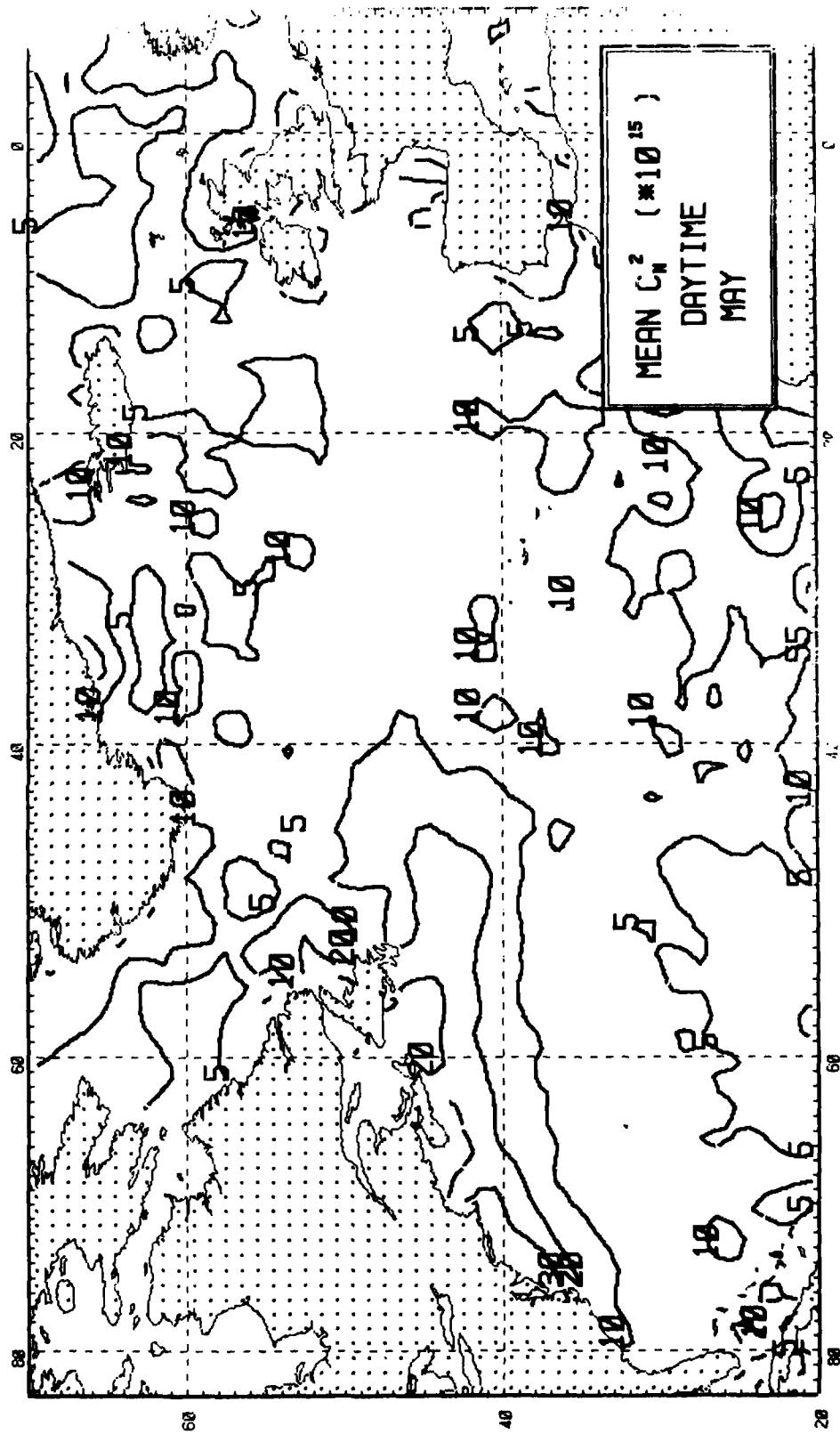


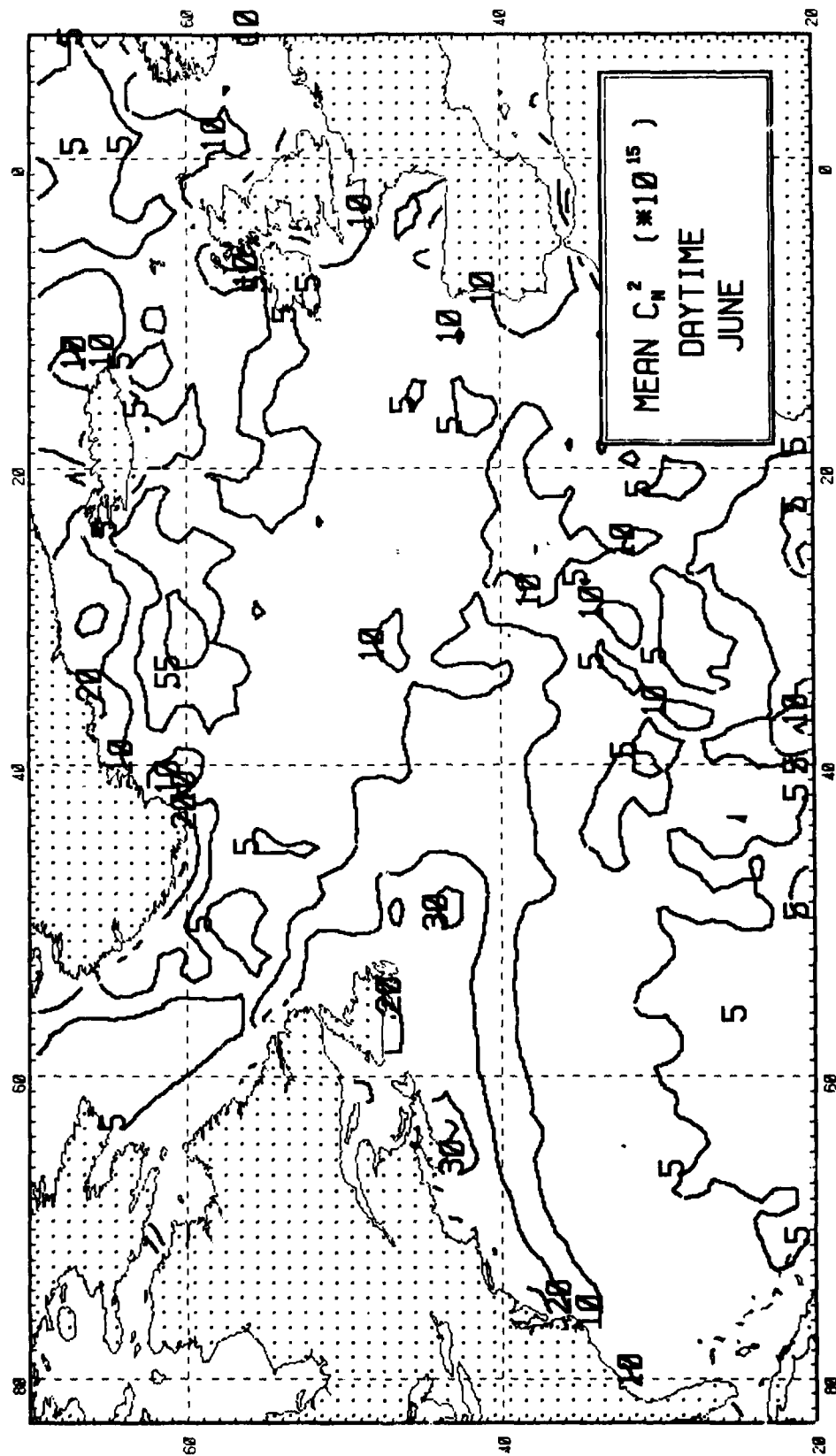


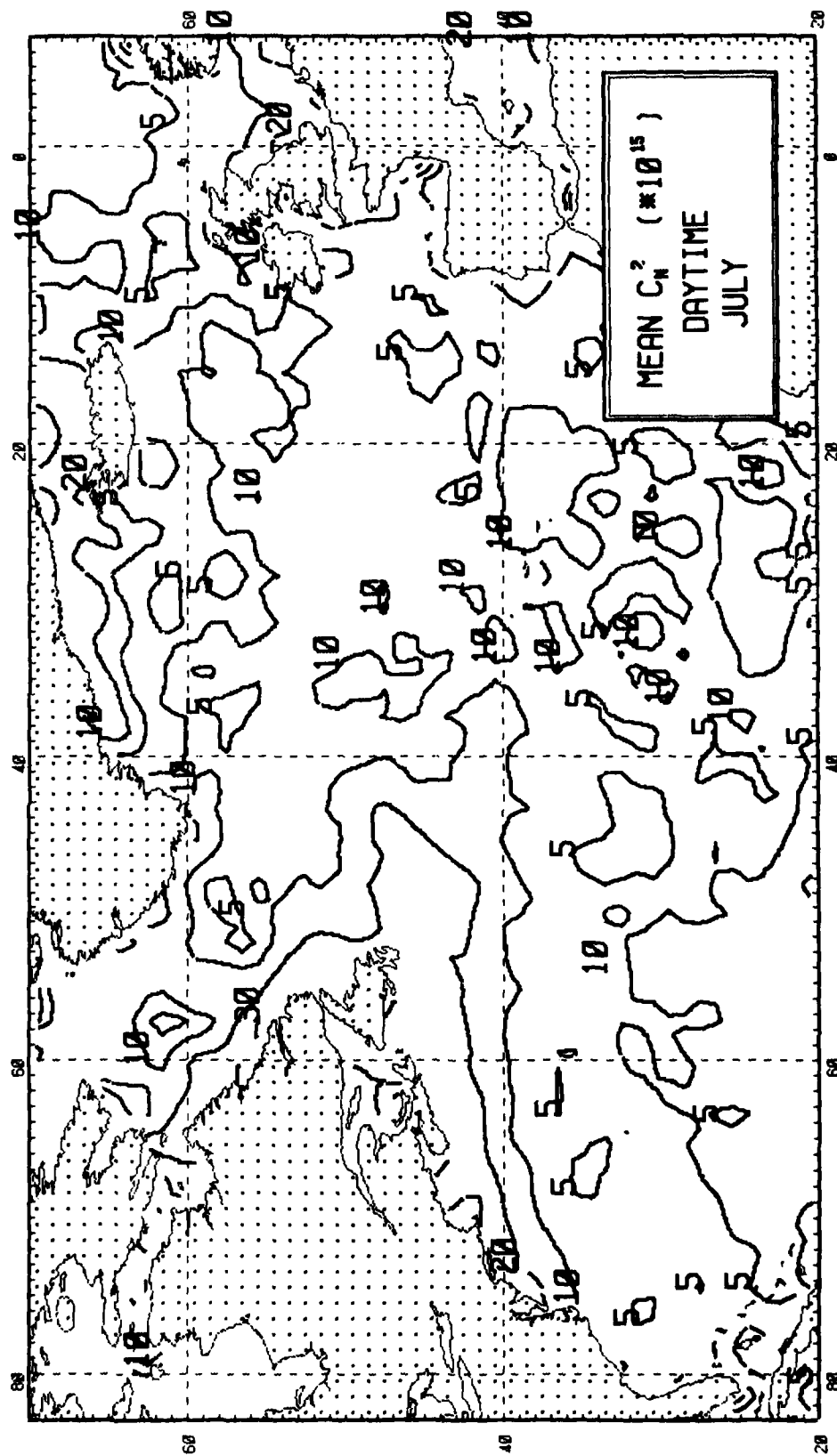


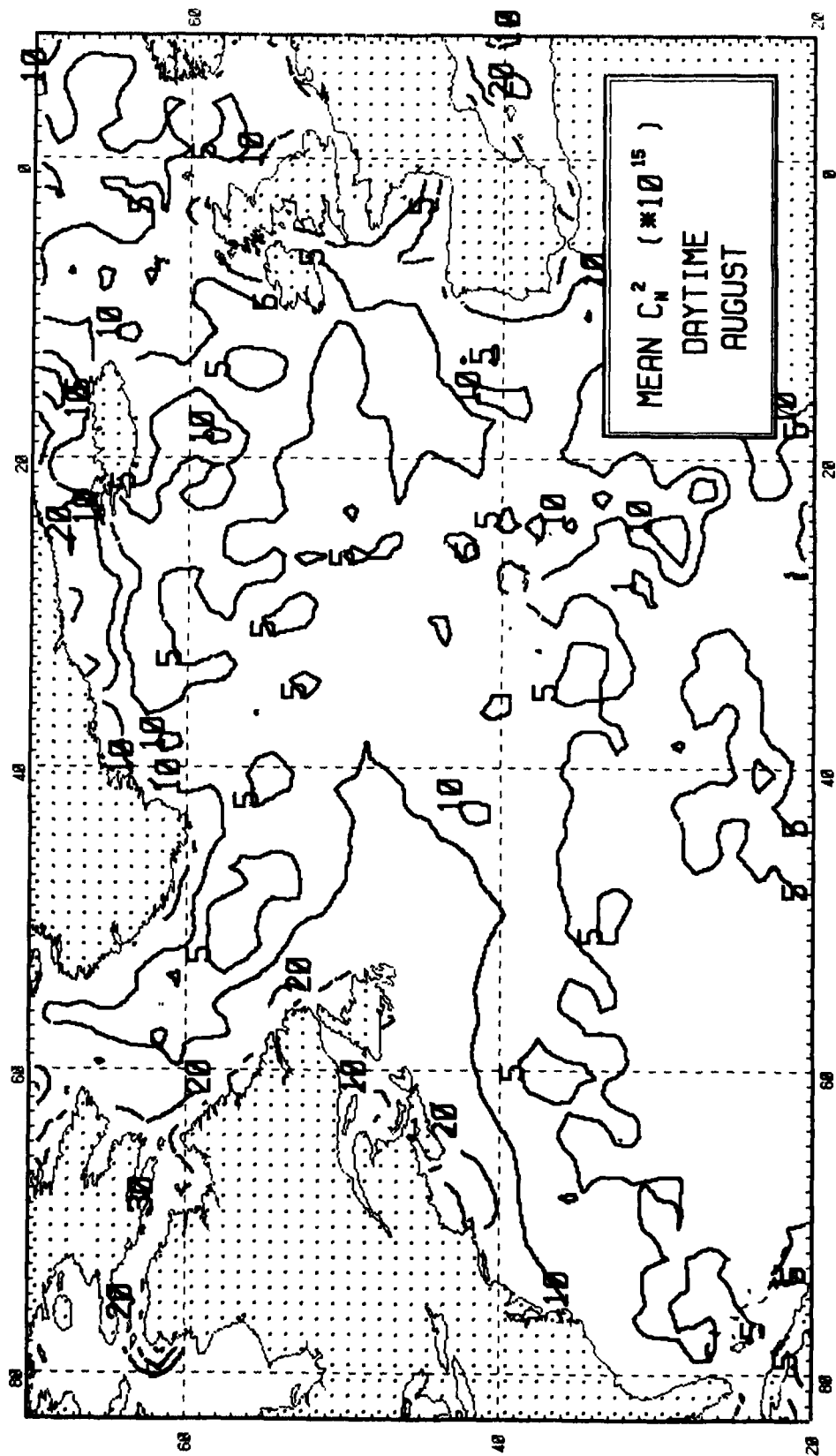


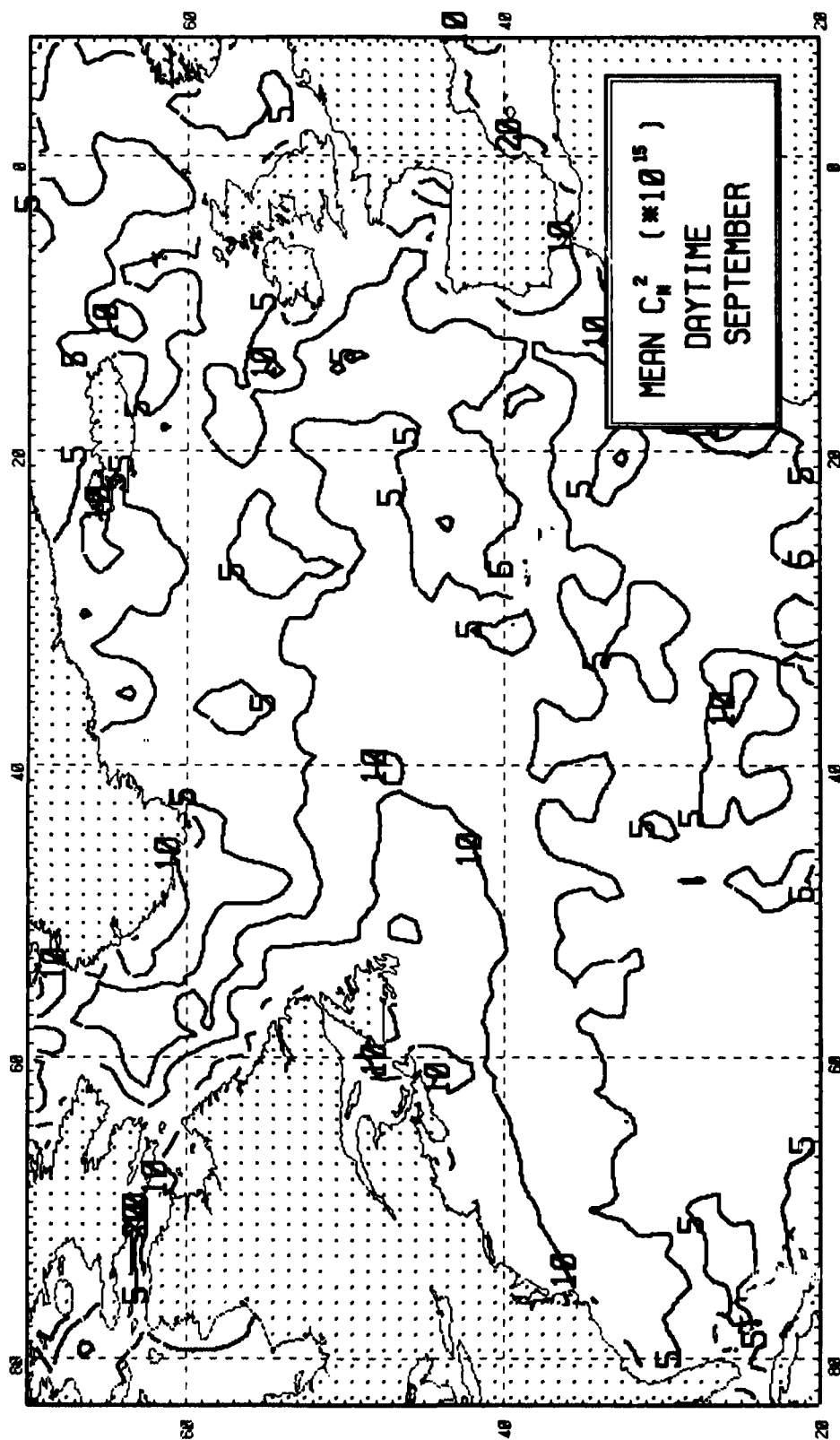




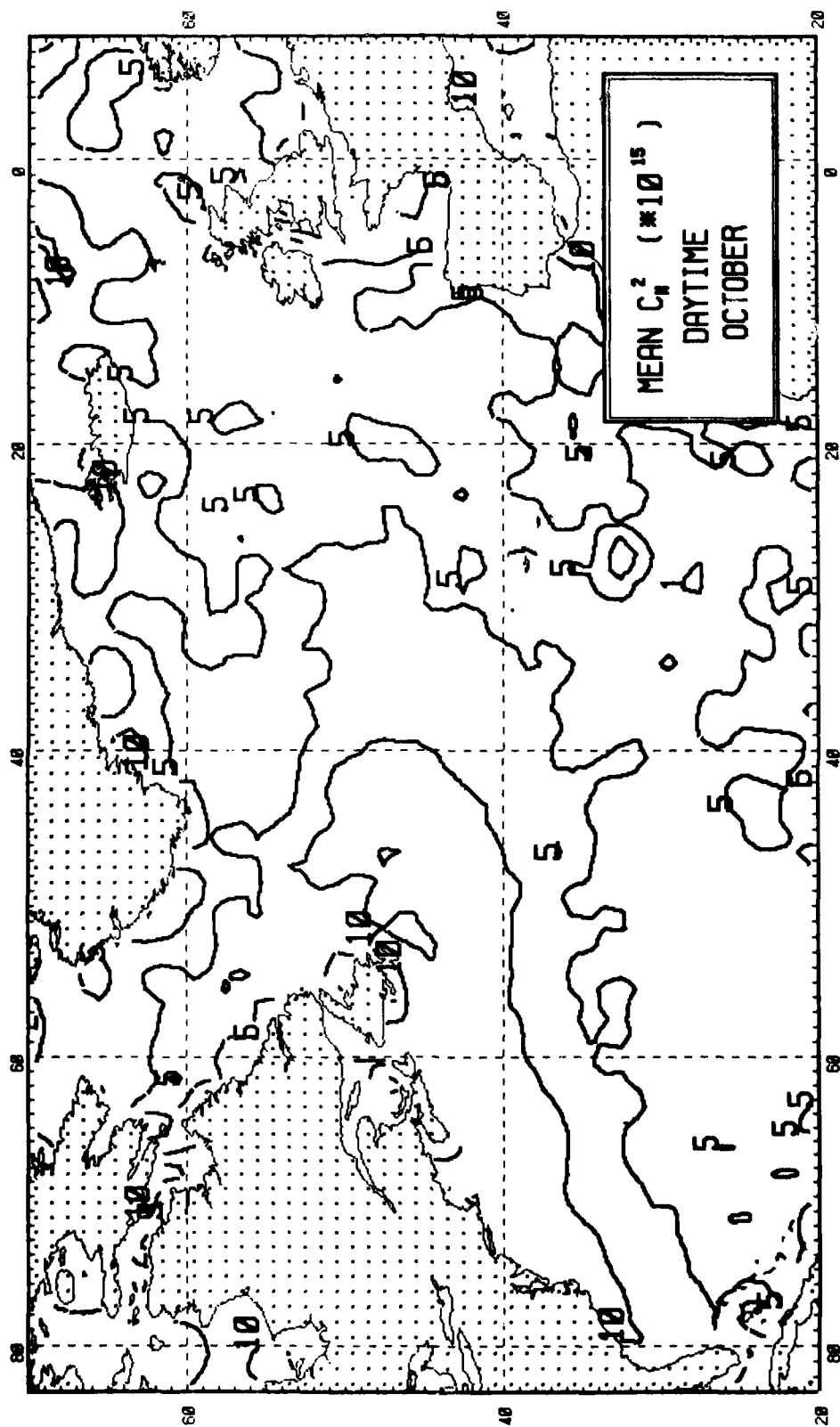


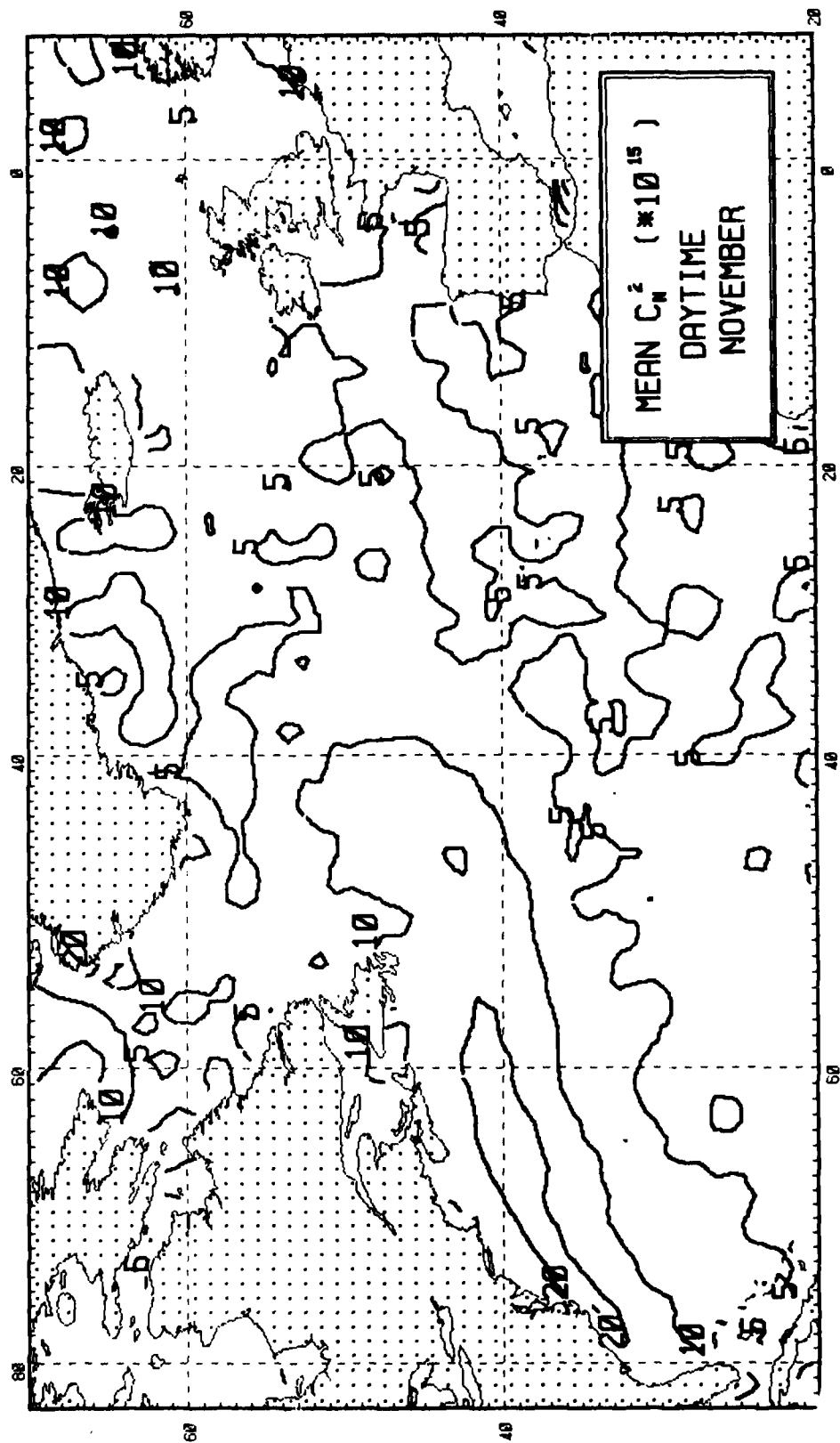


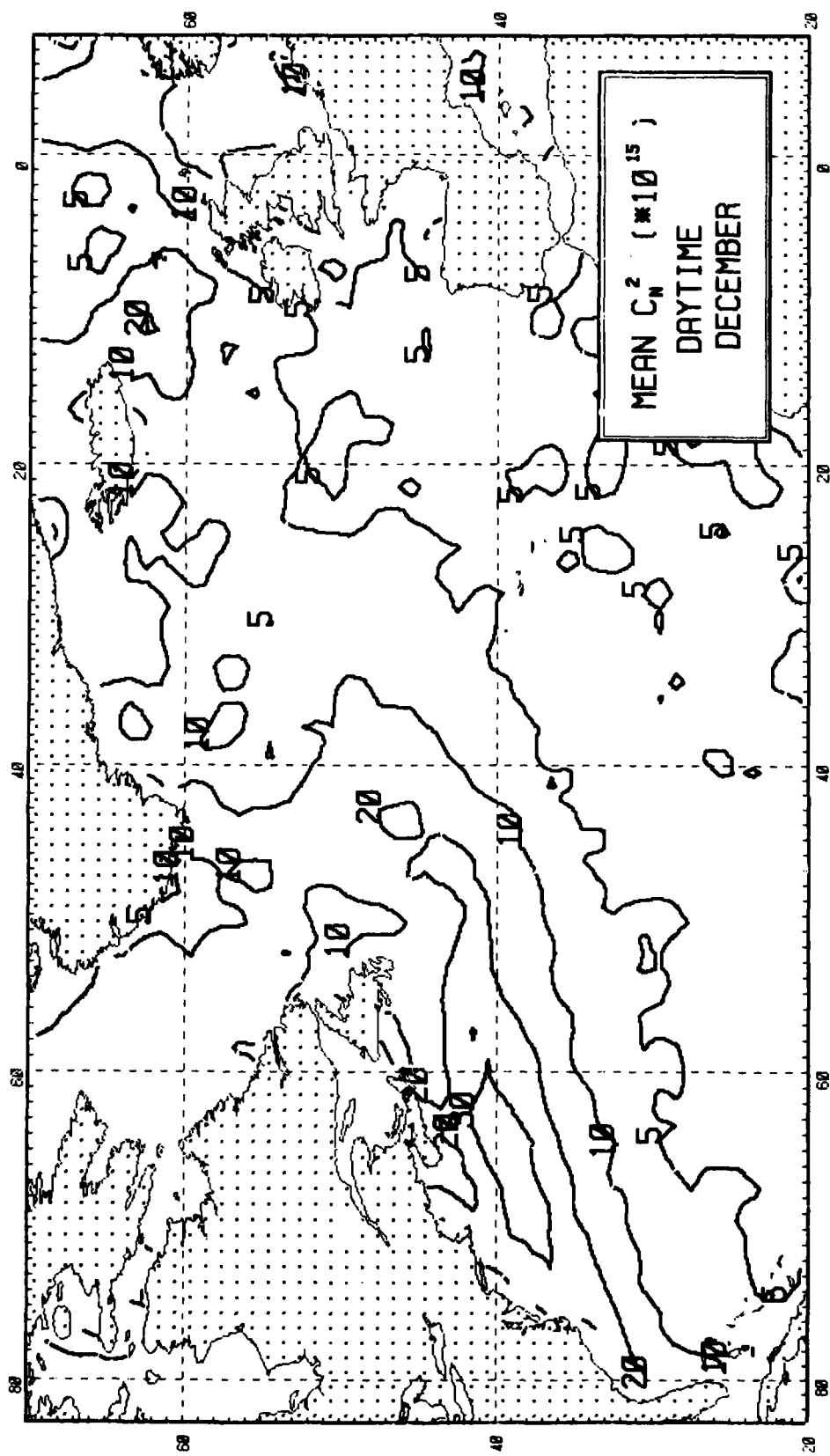


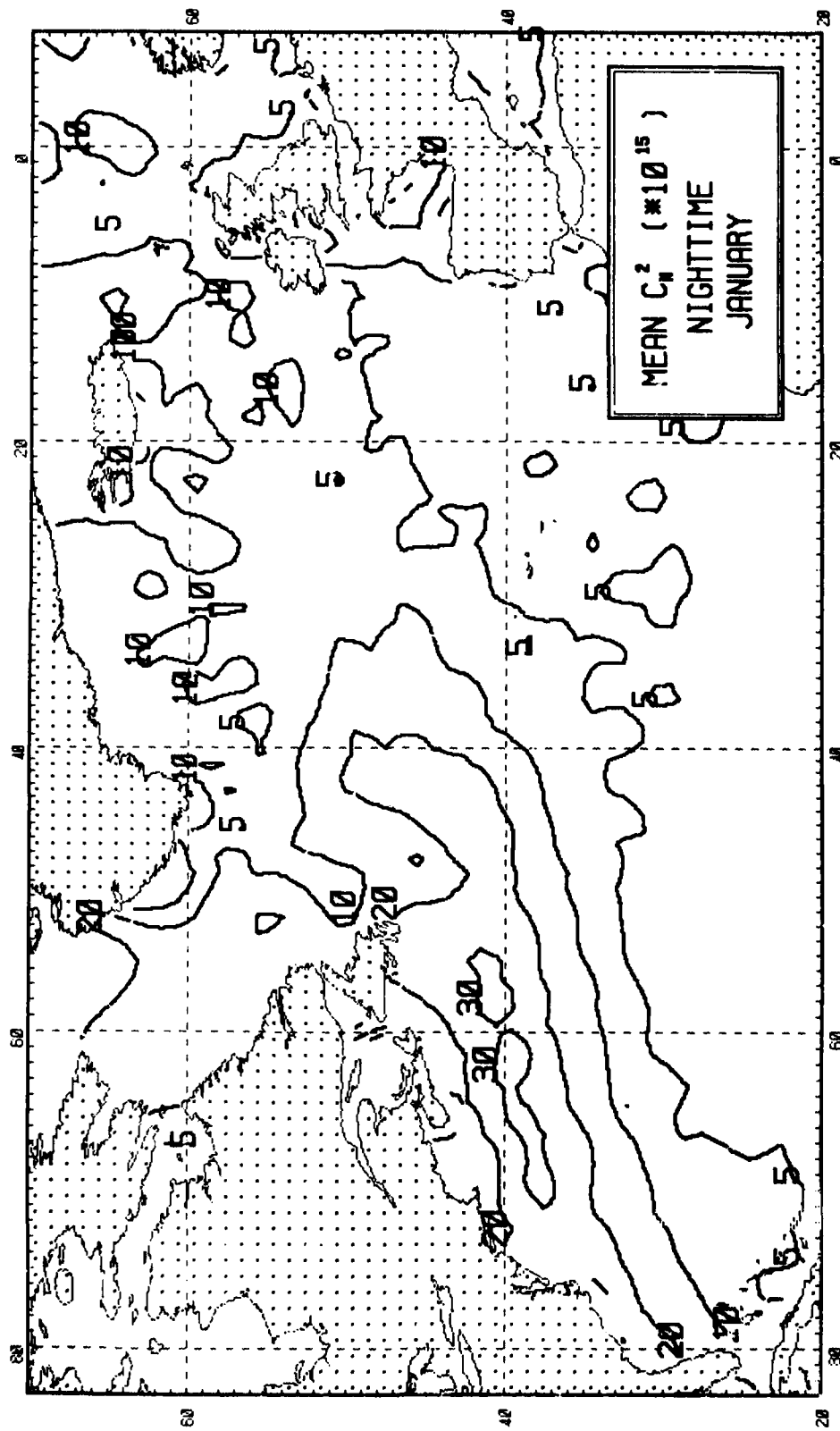


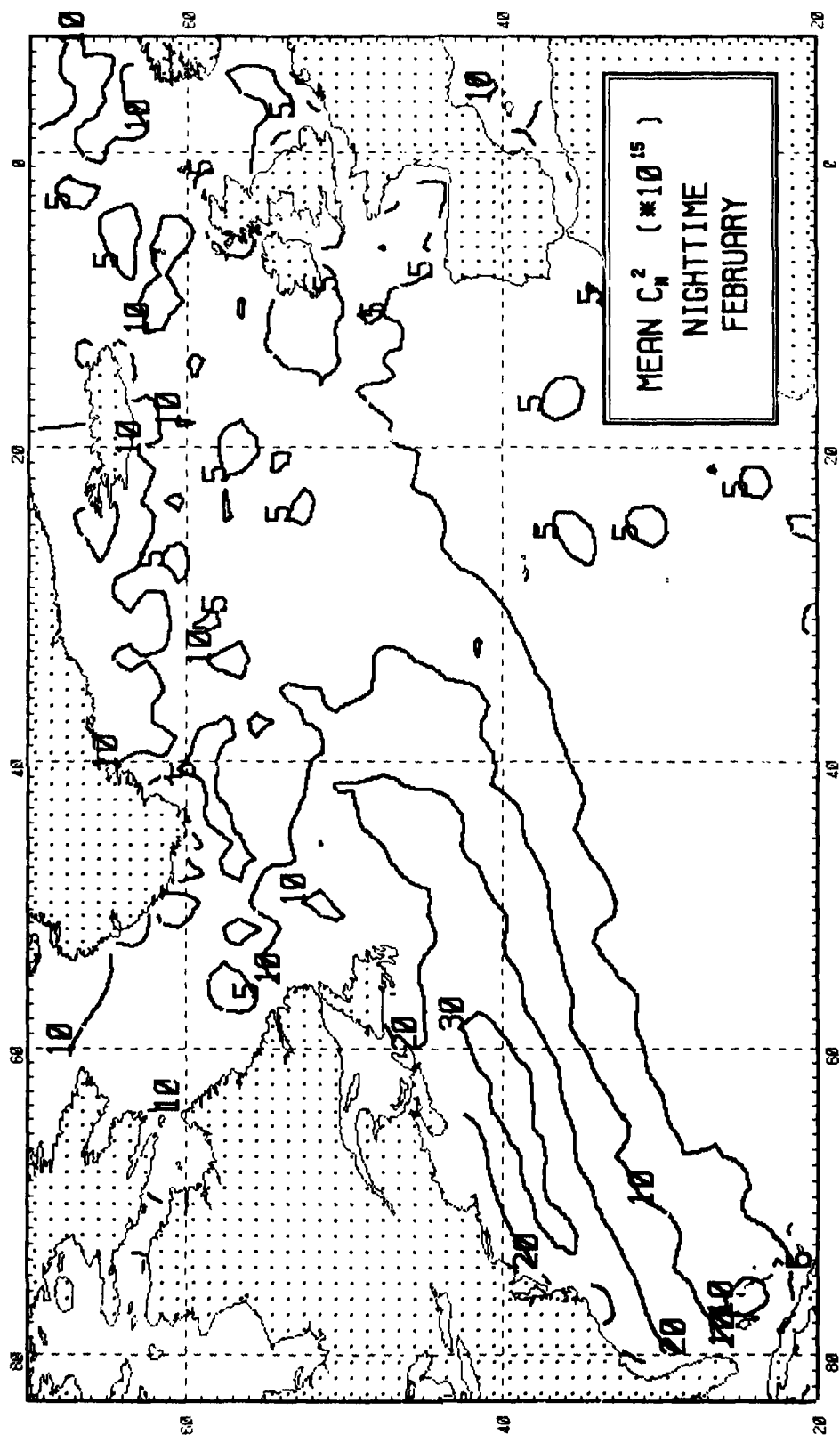


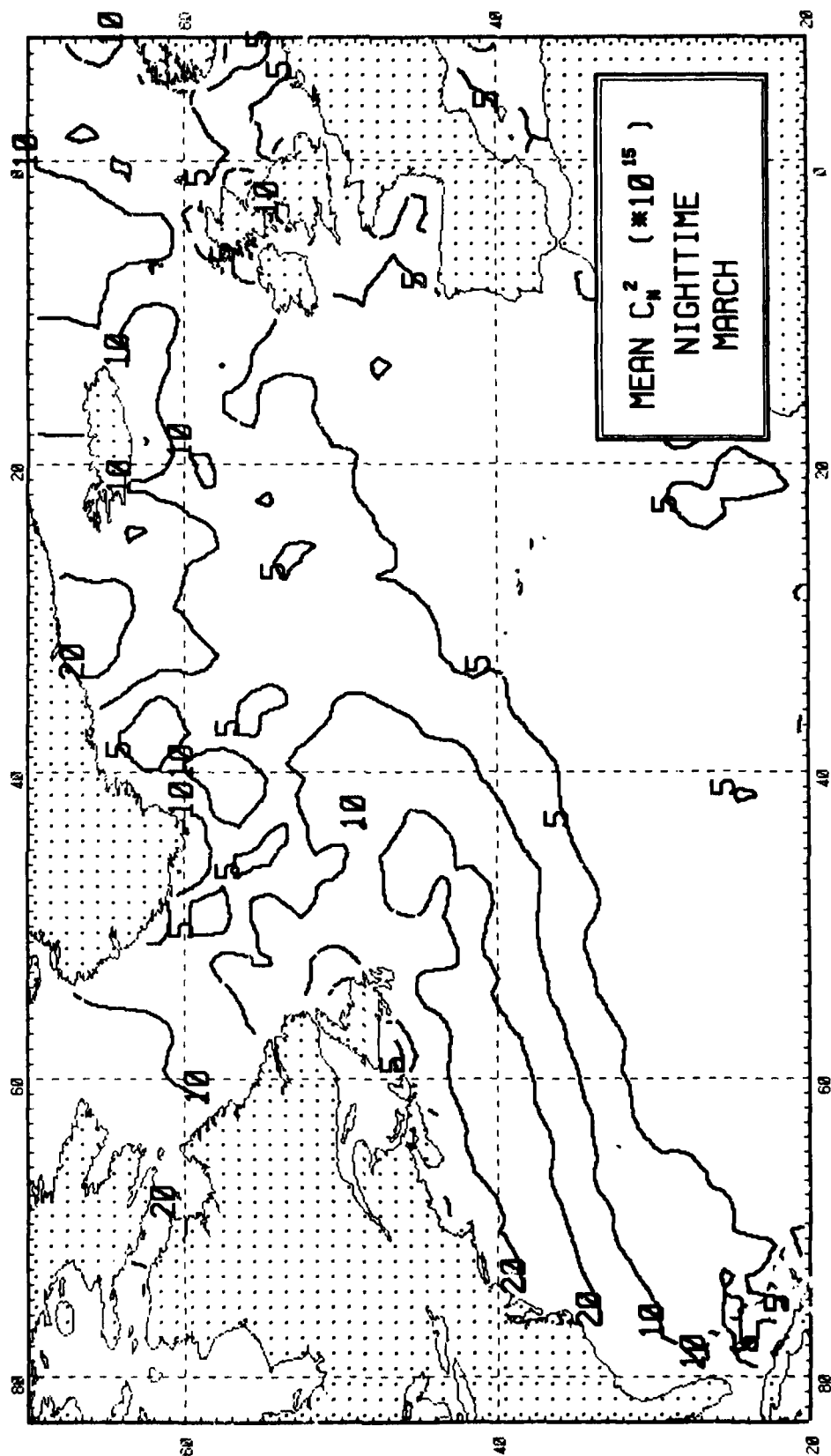


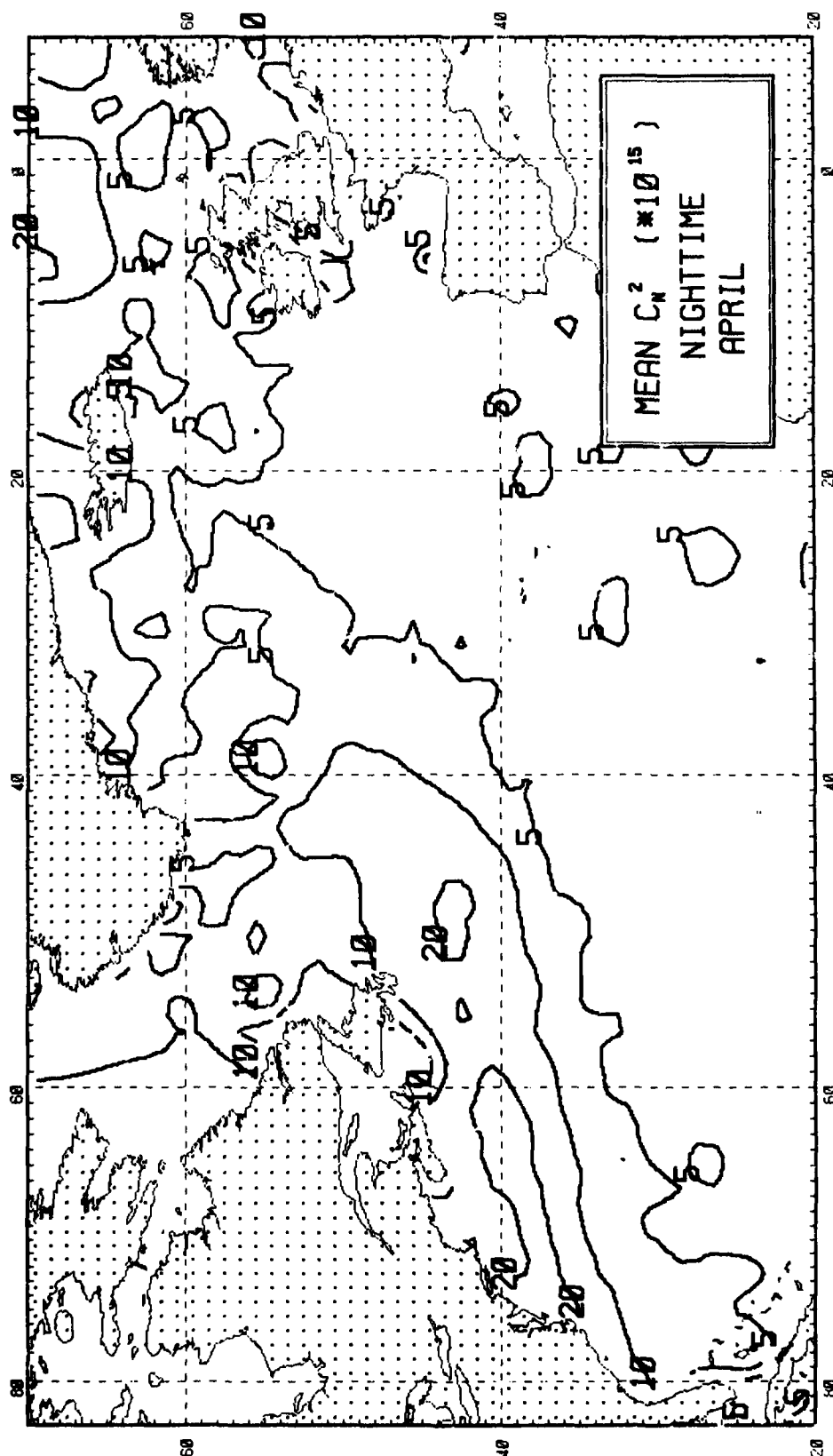


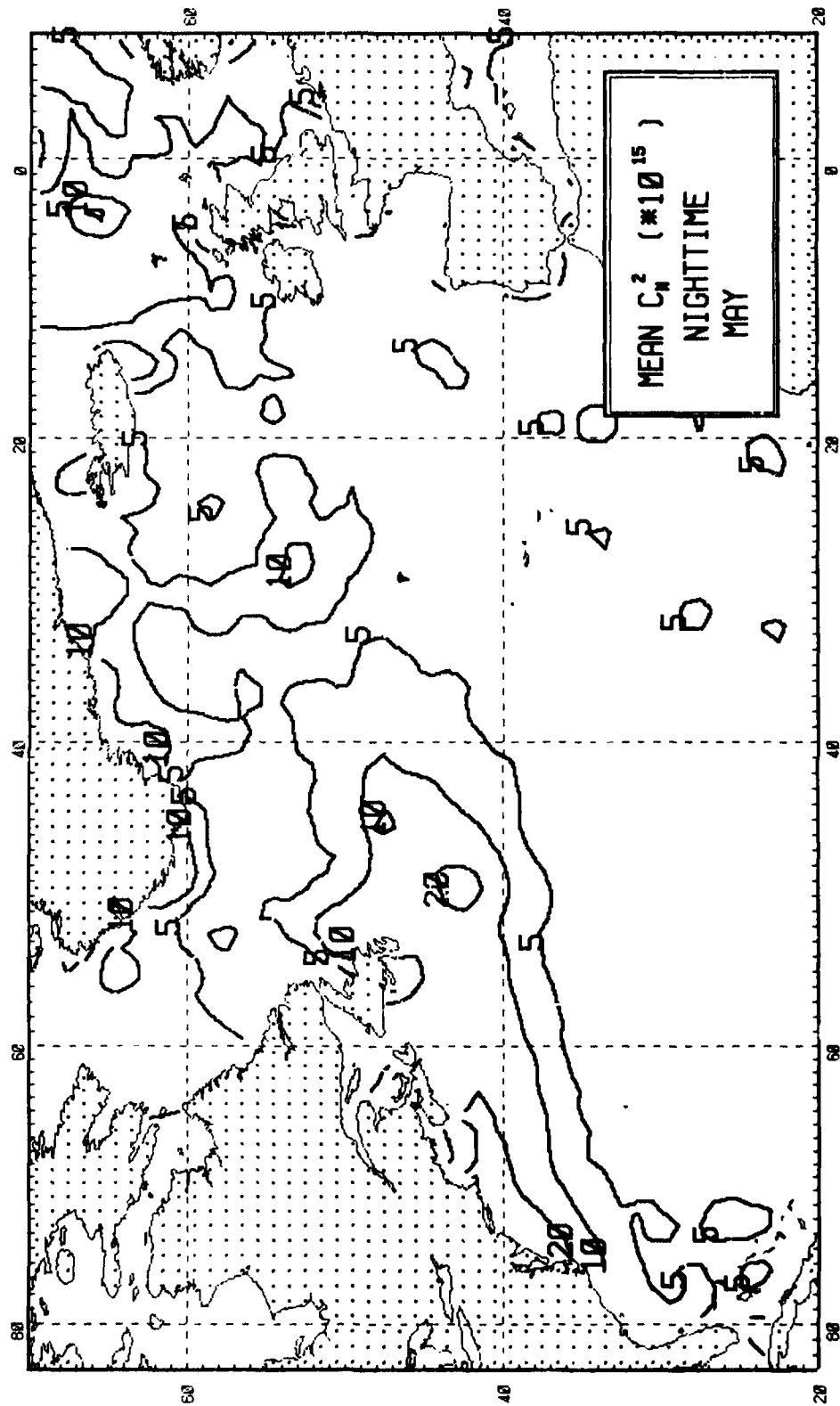




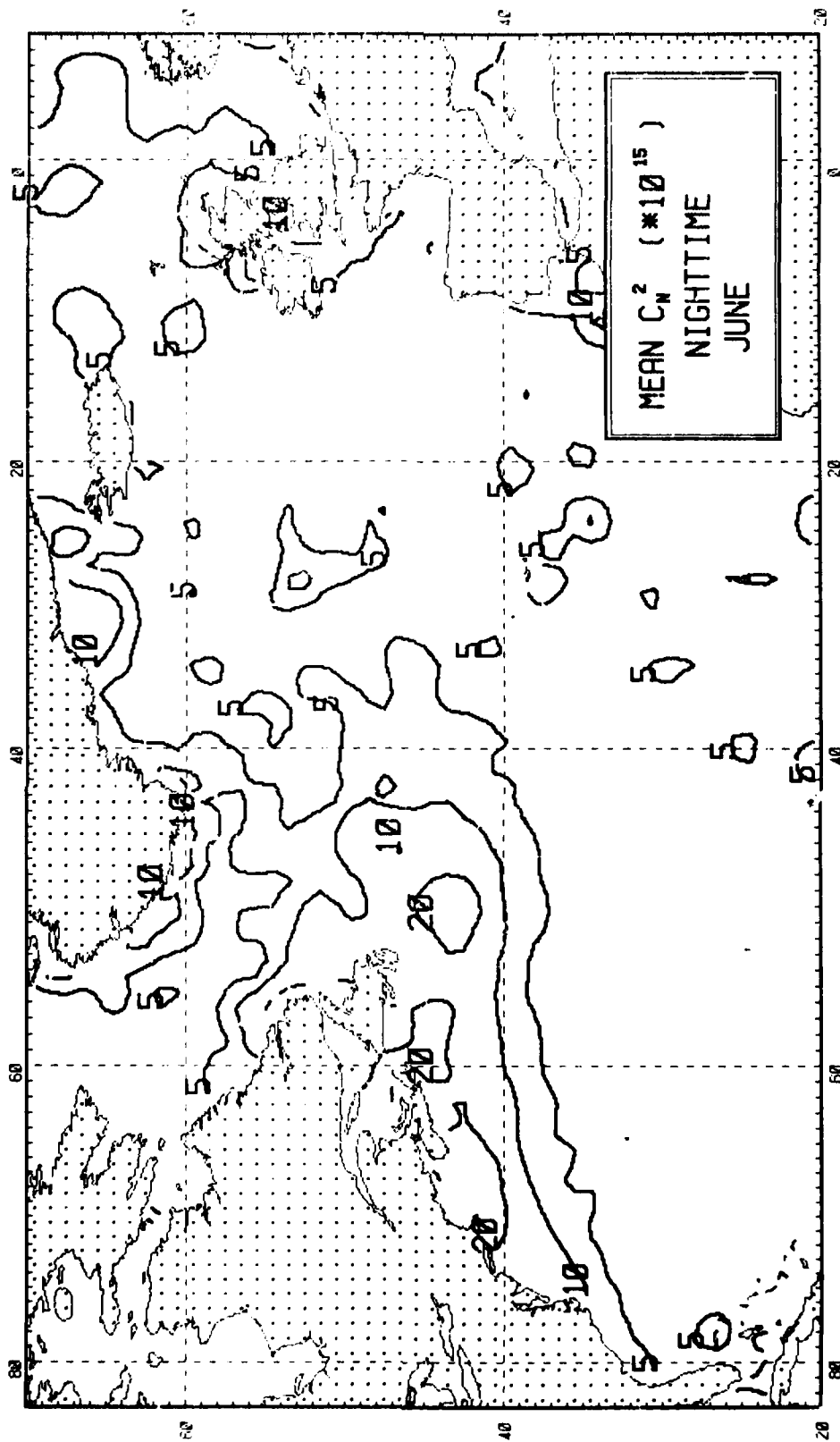


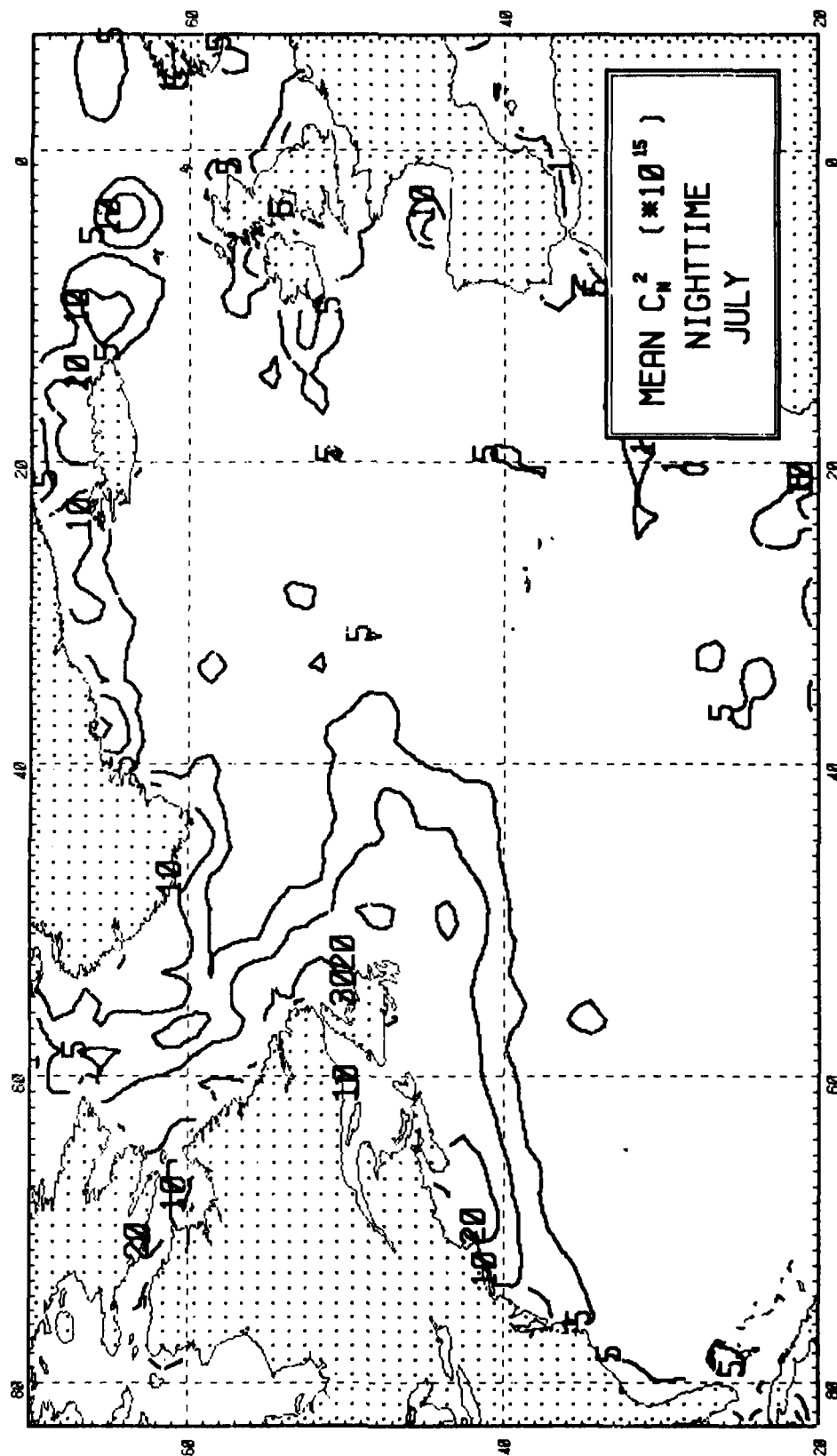


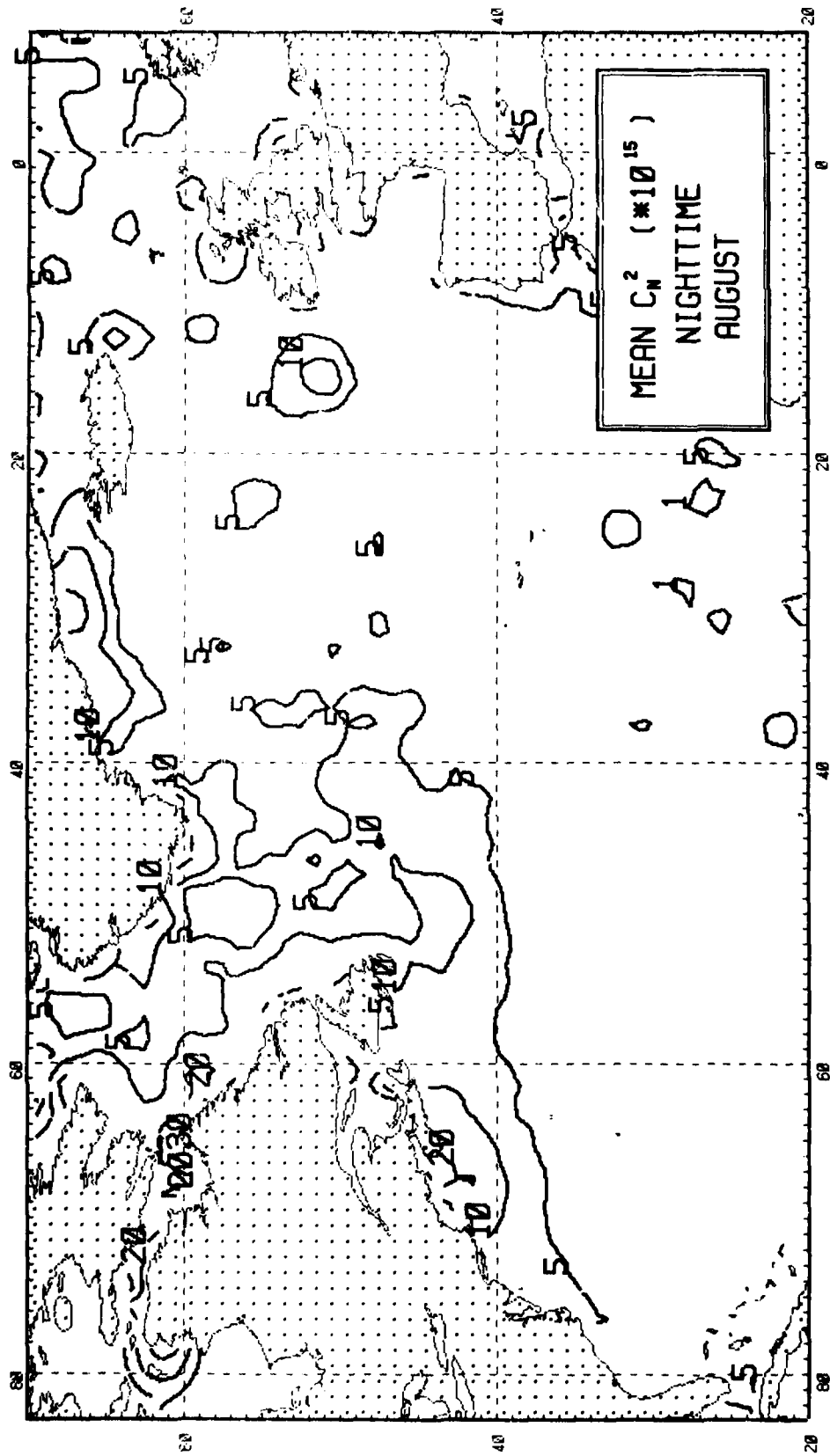












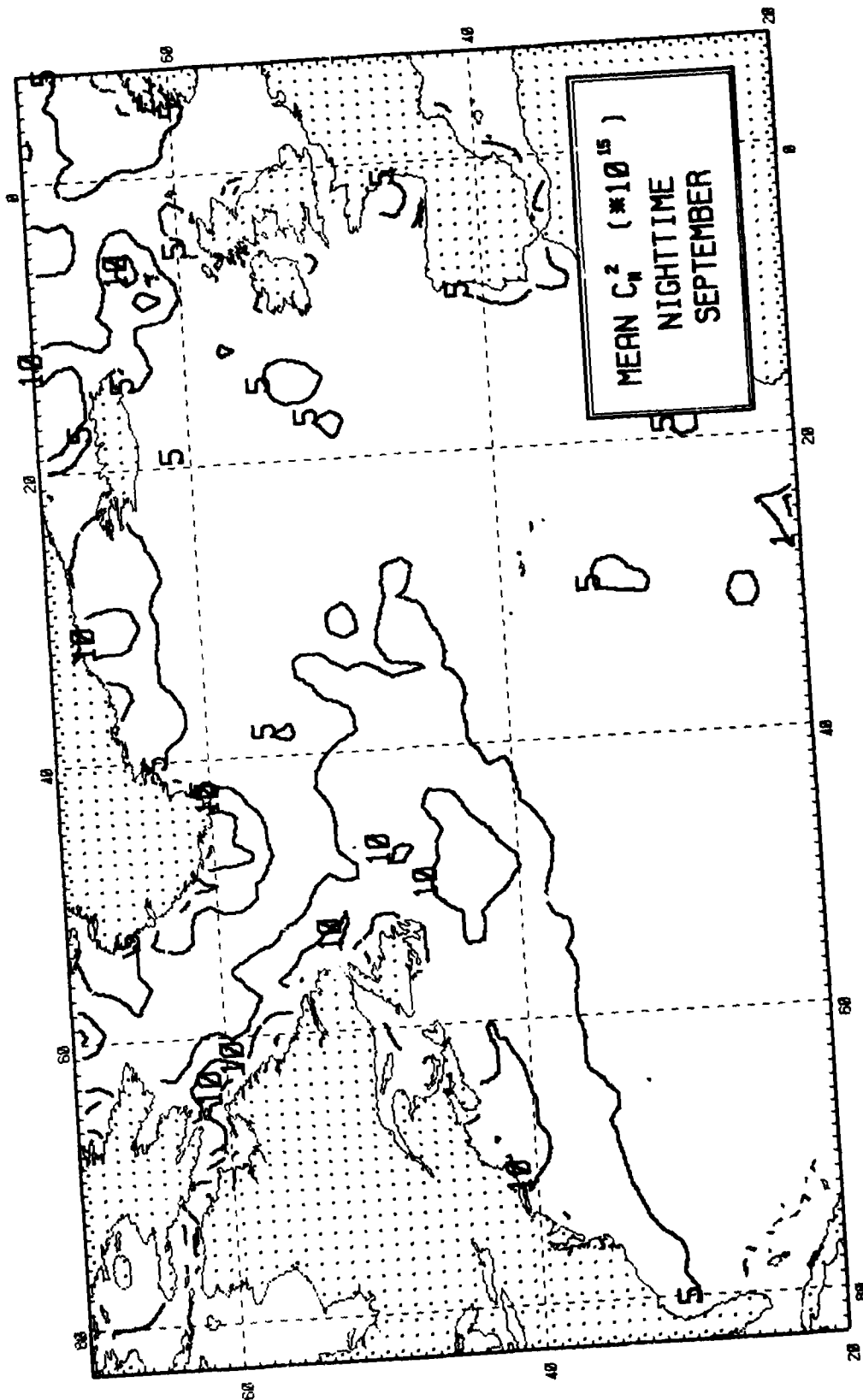
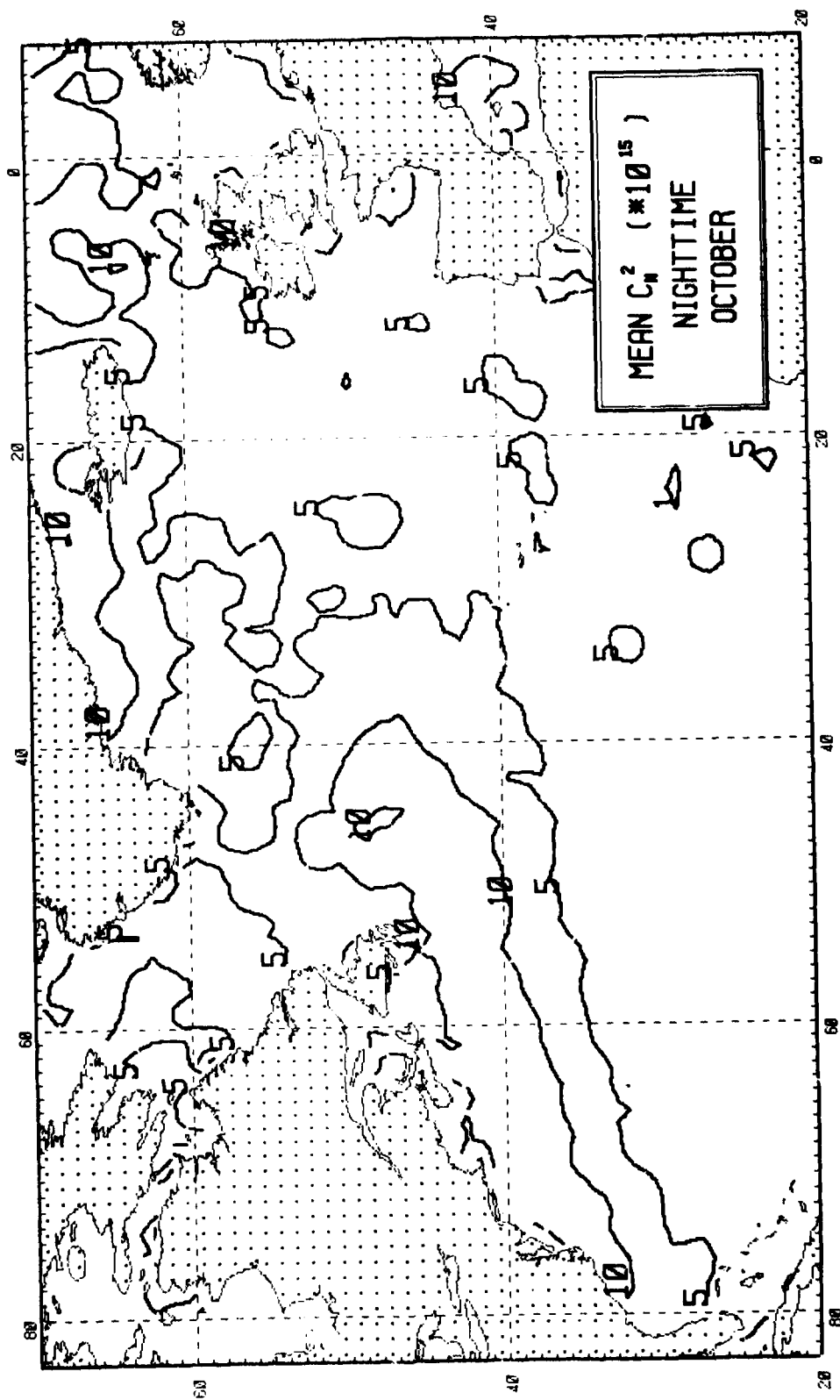
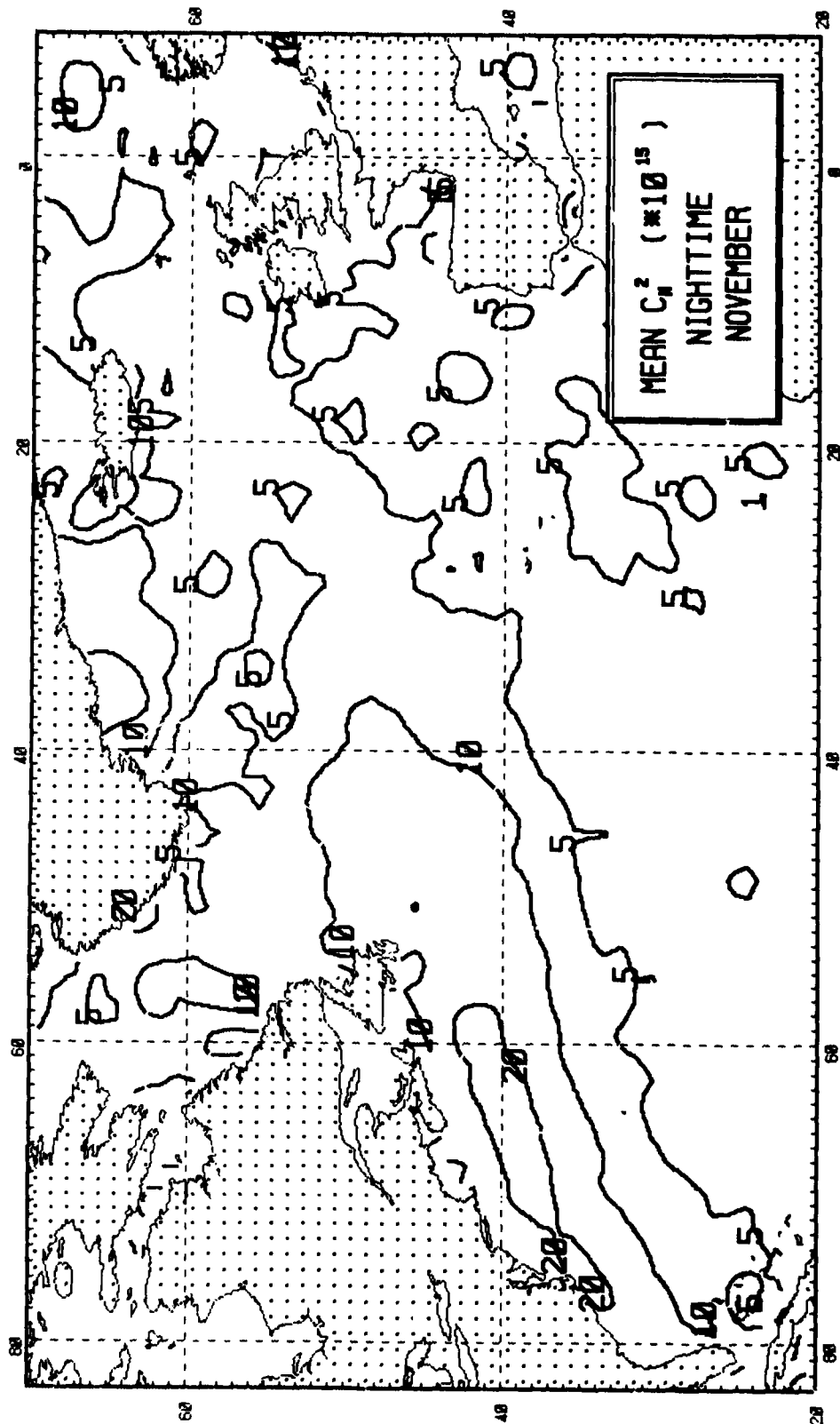
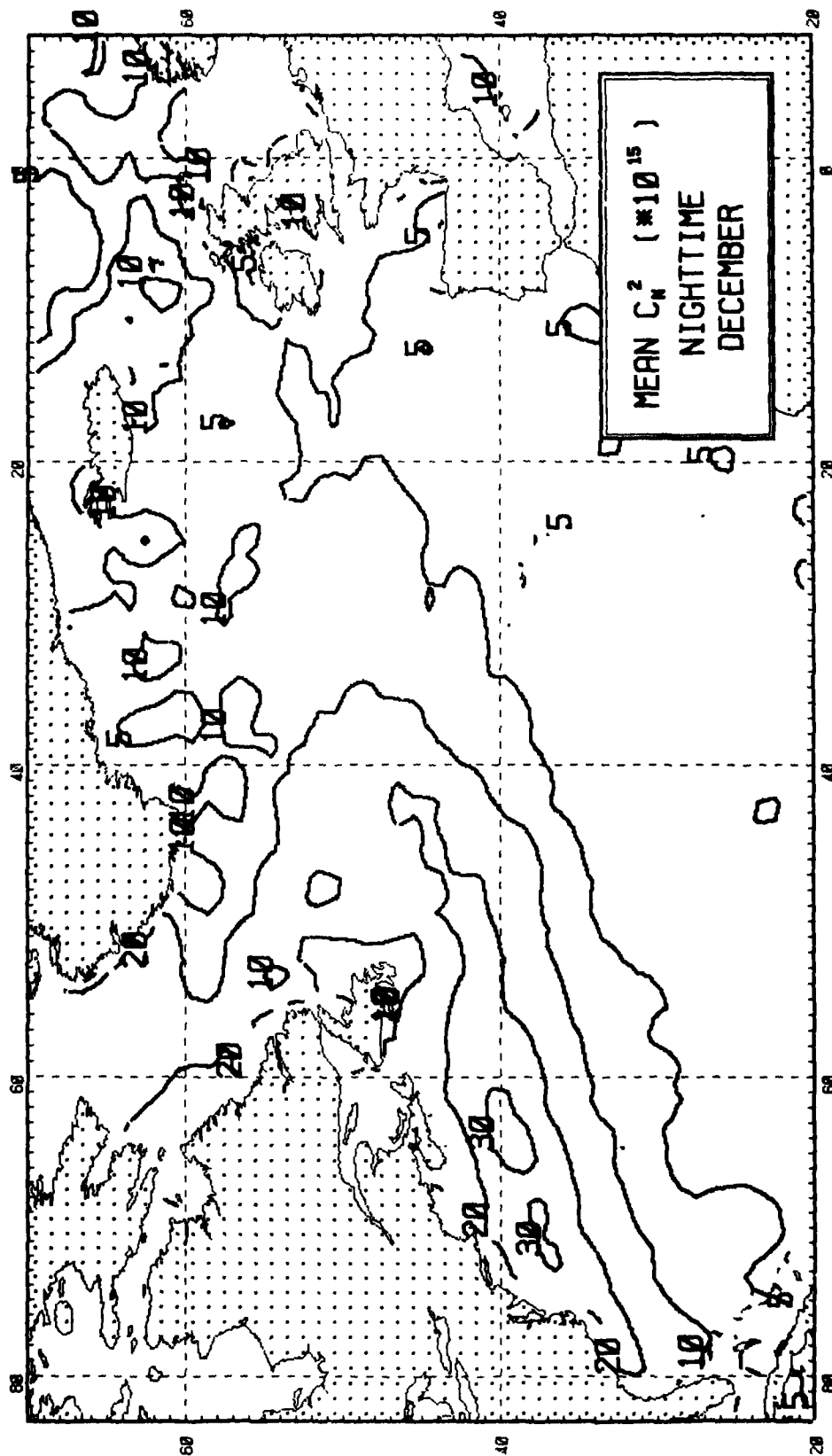
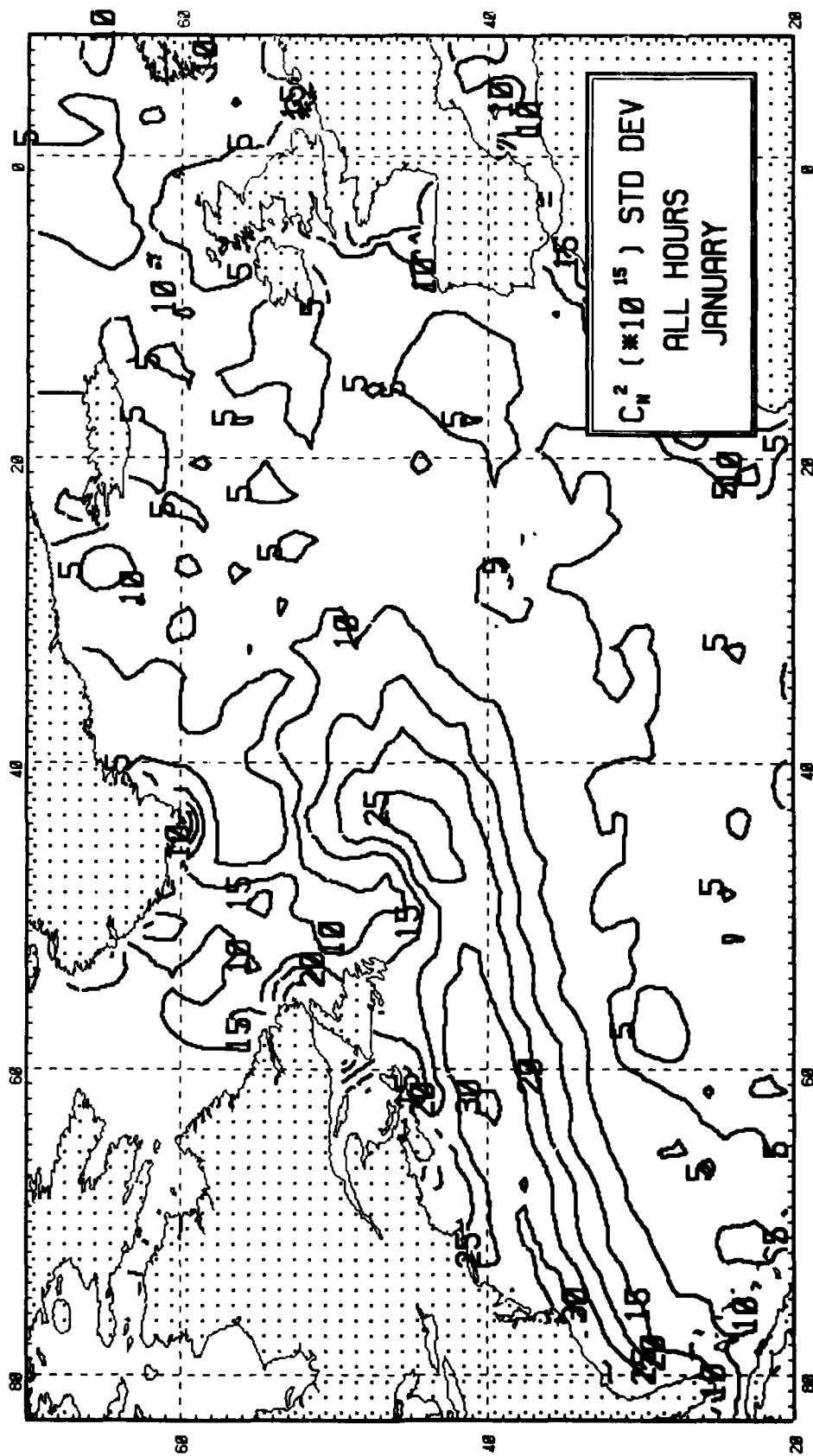


FIGURE 33

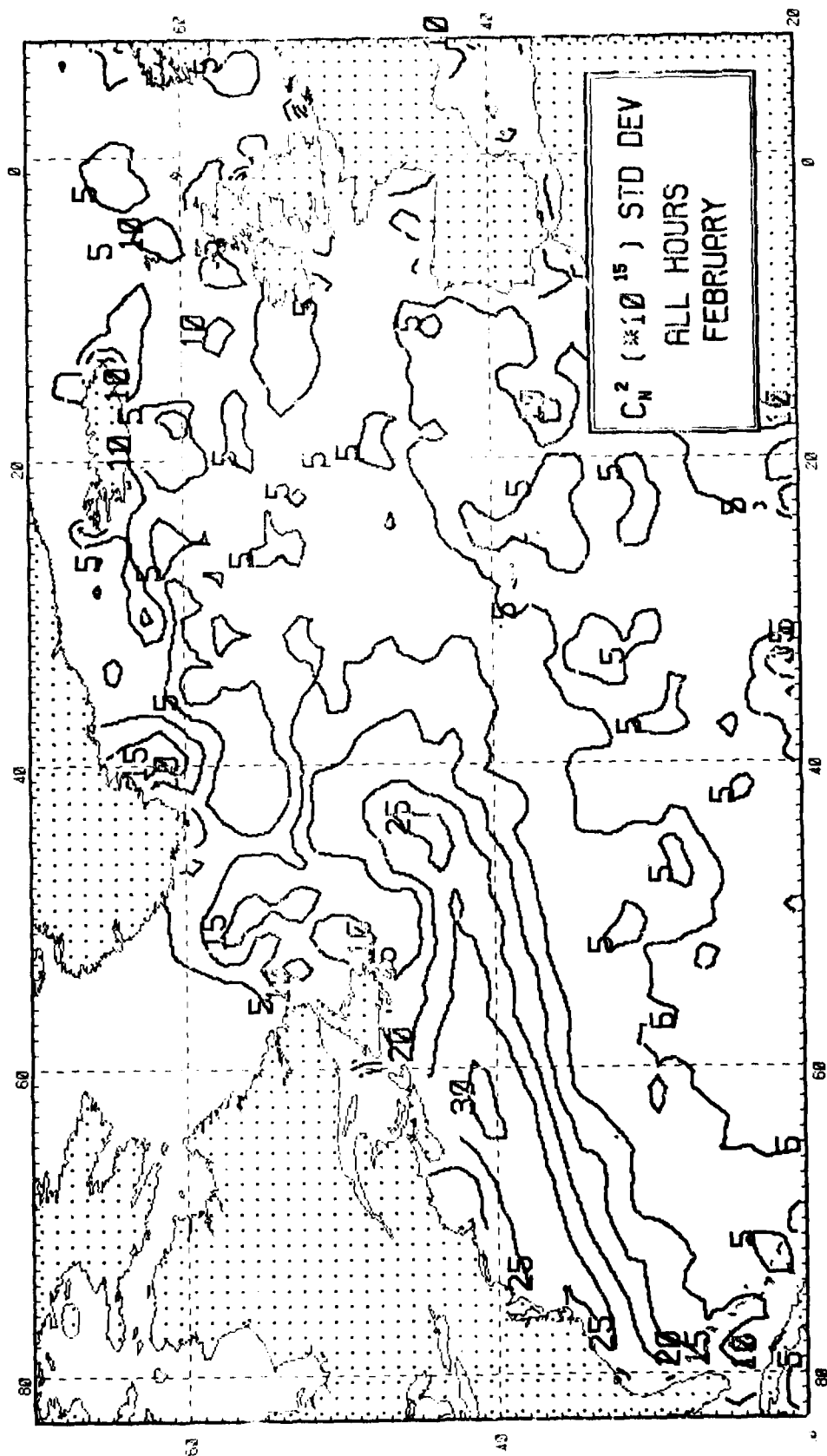


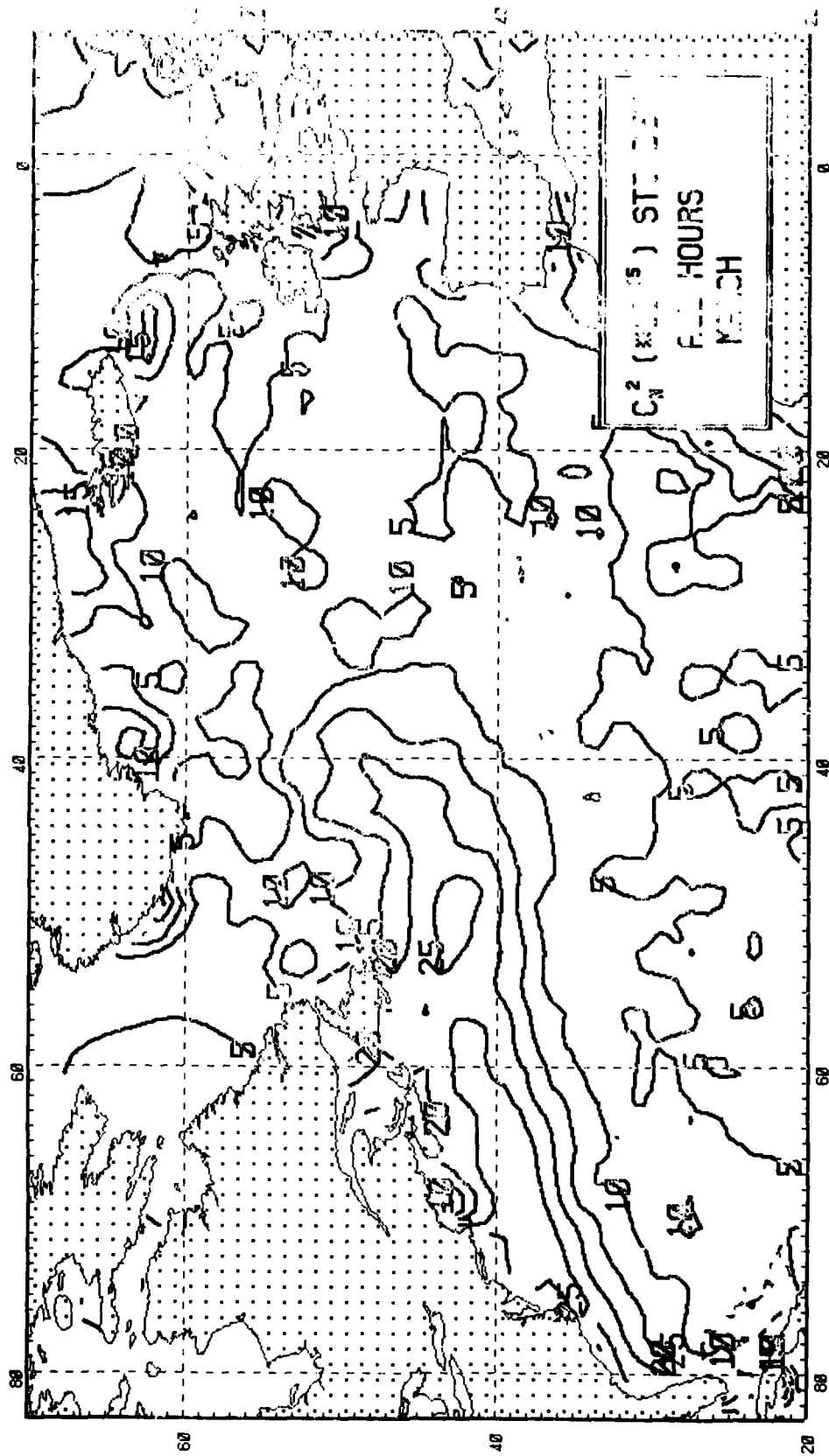


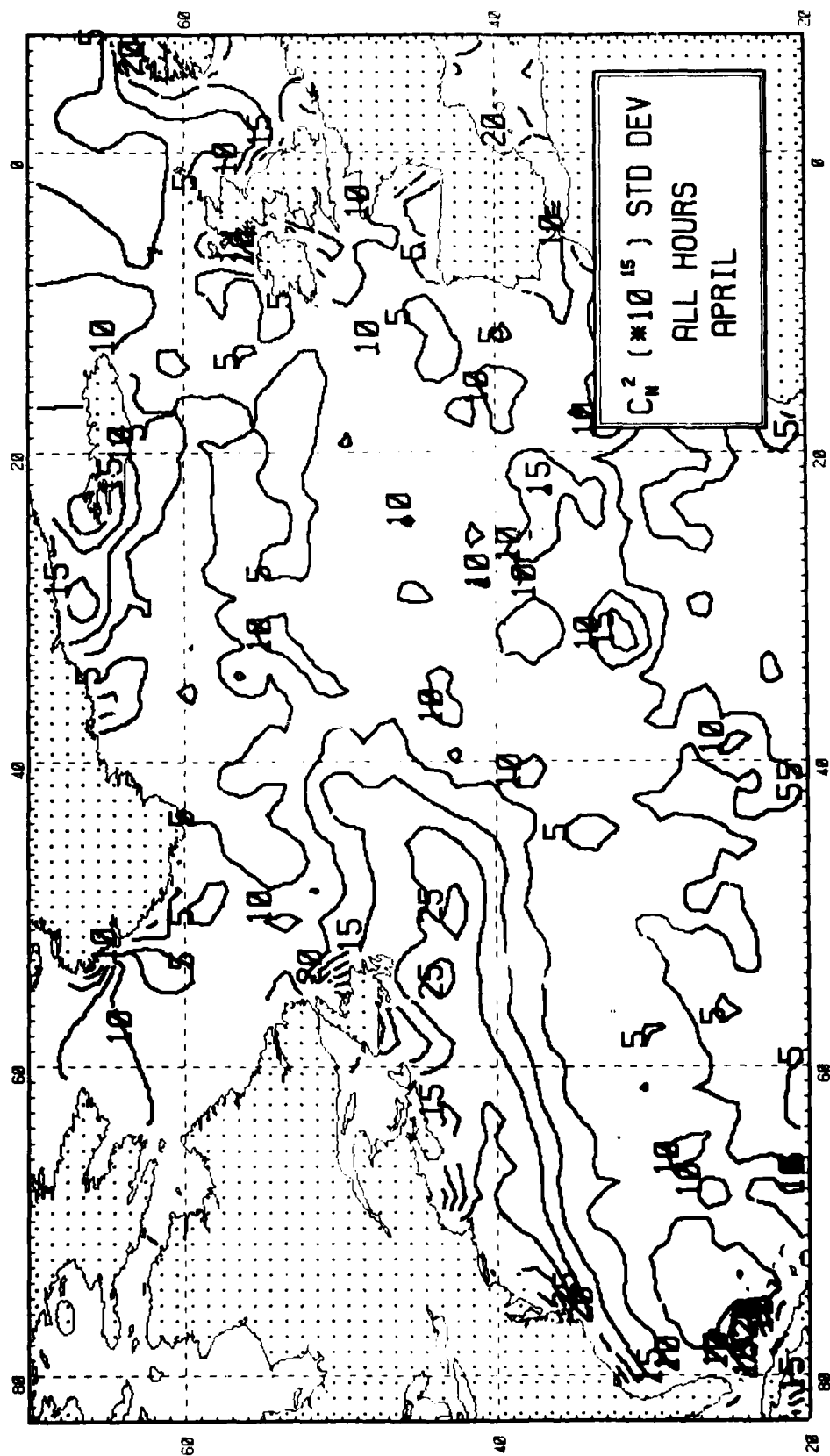


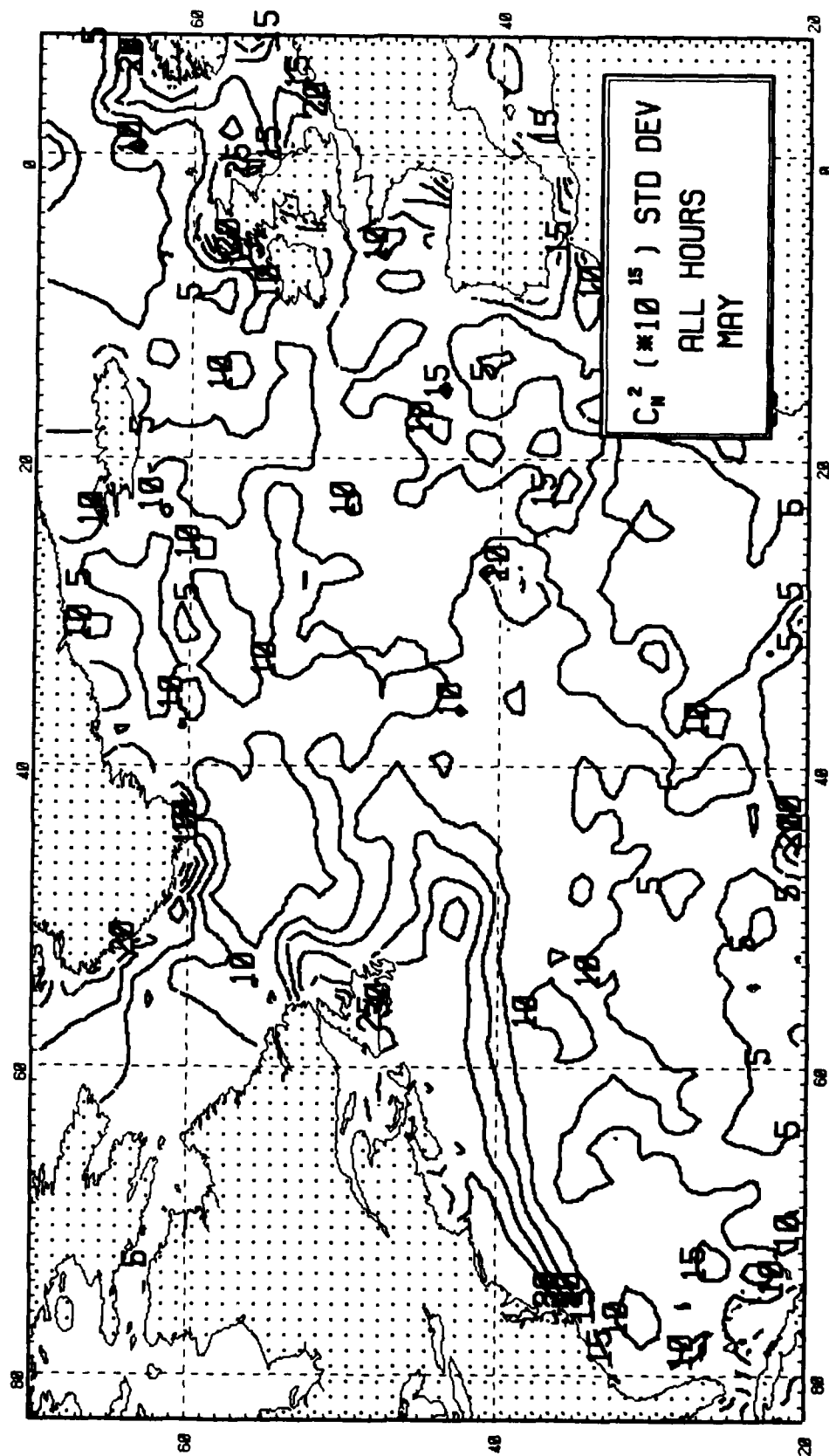


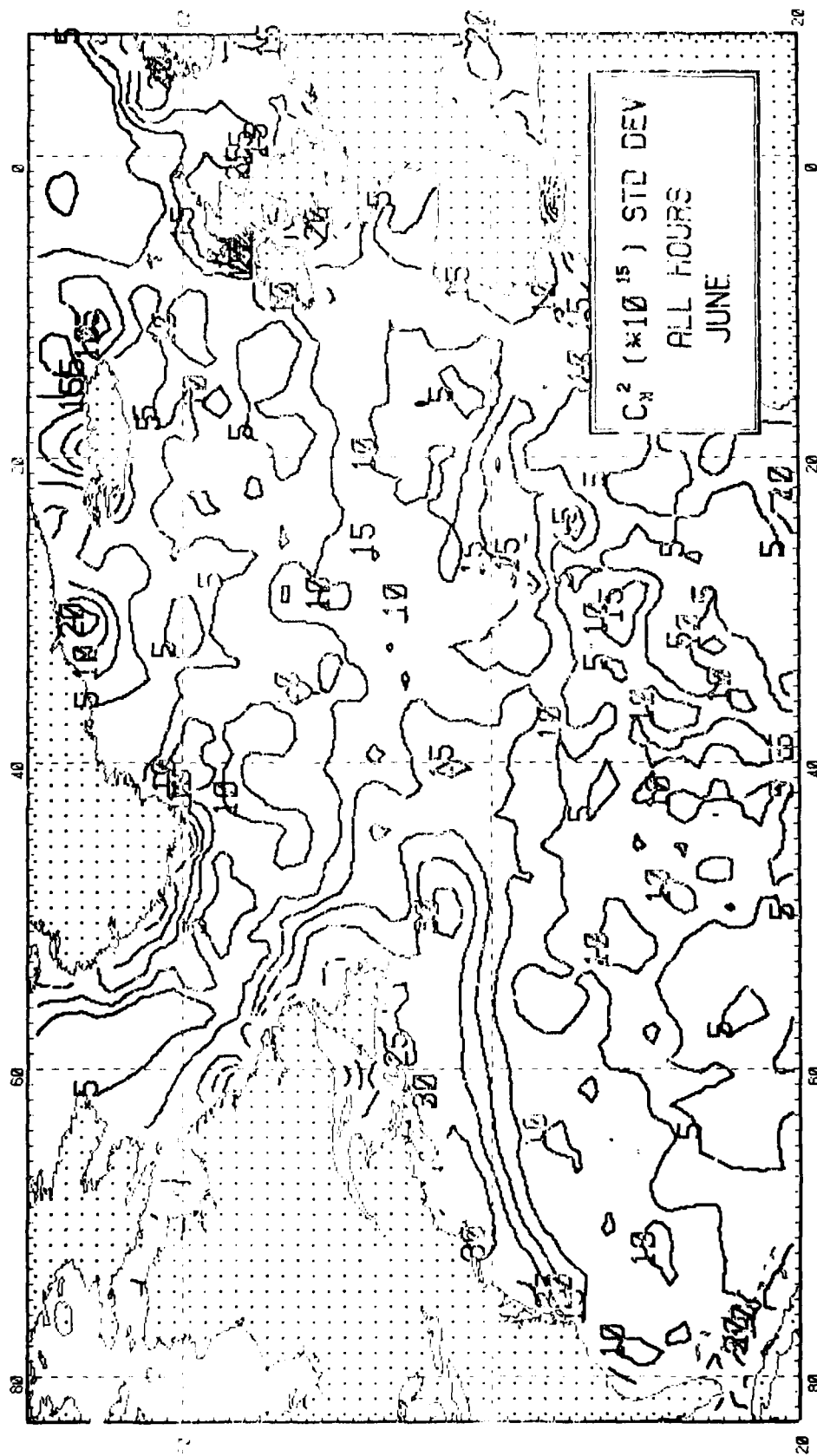


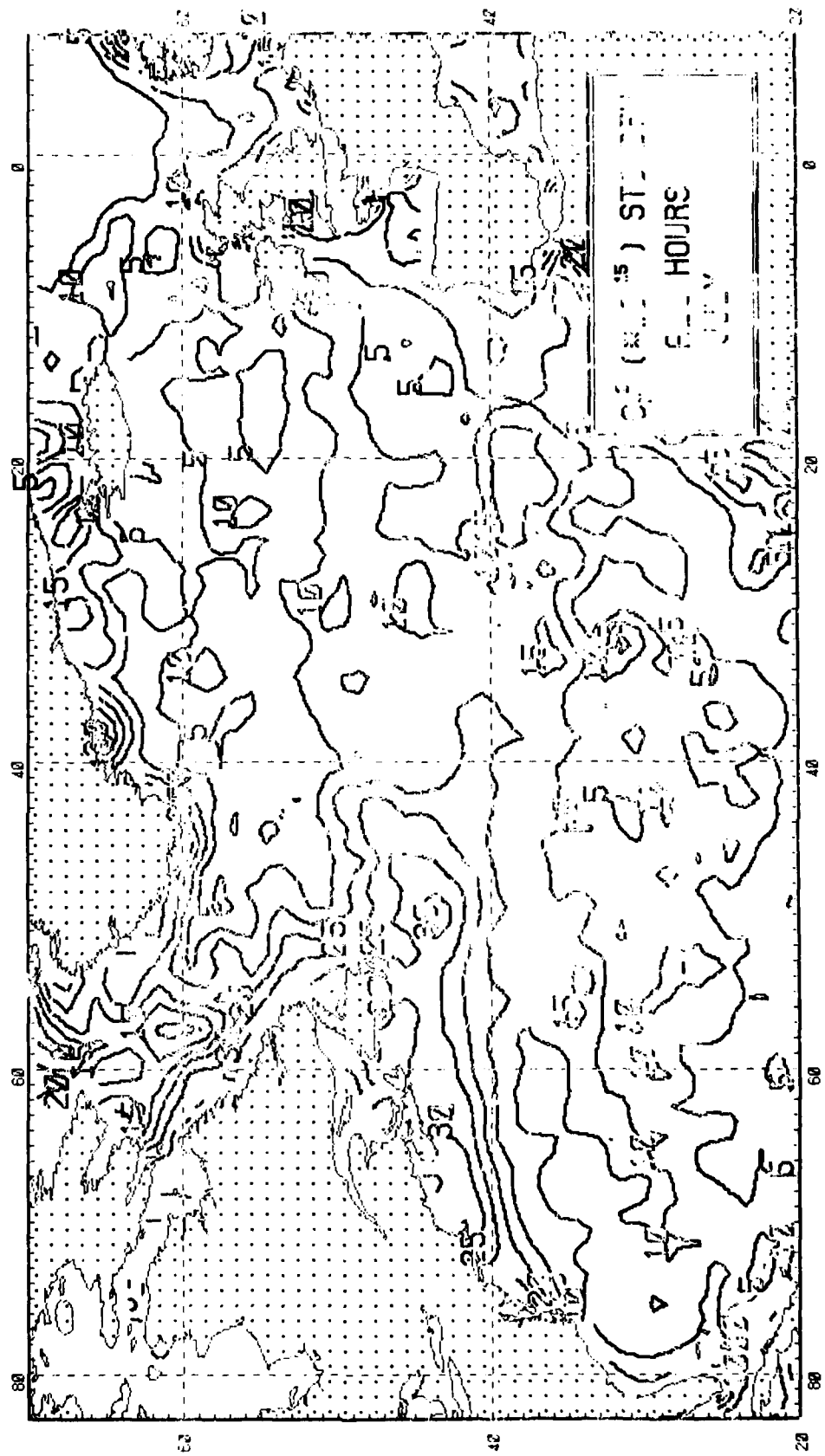


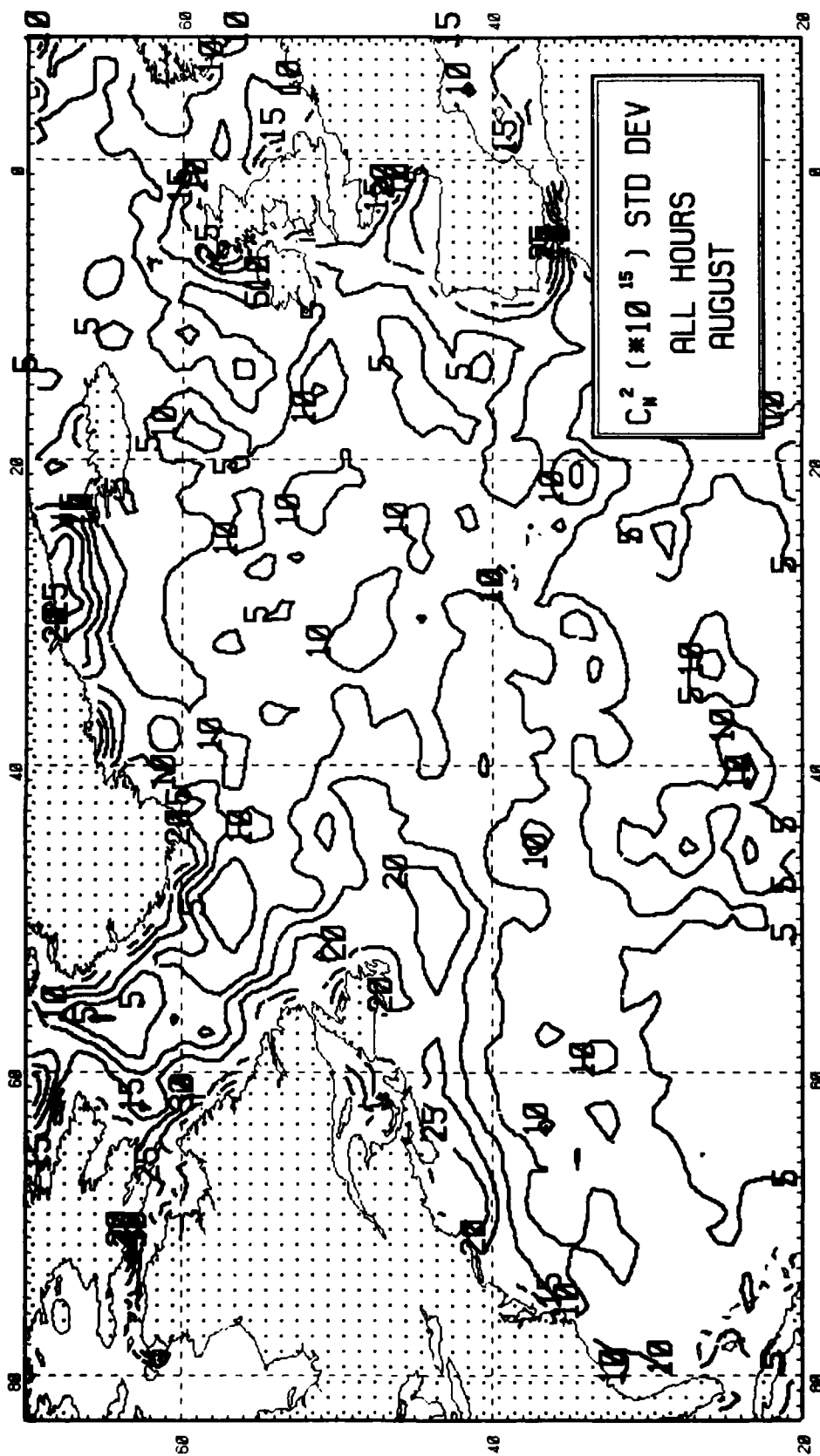


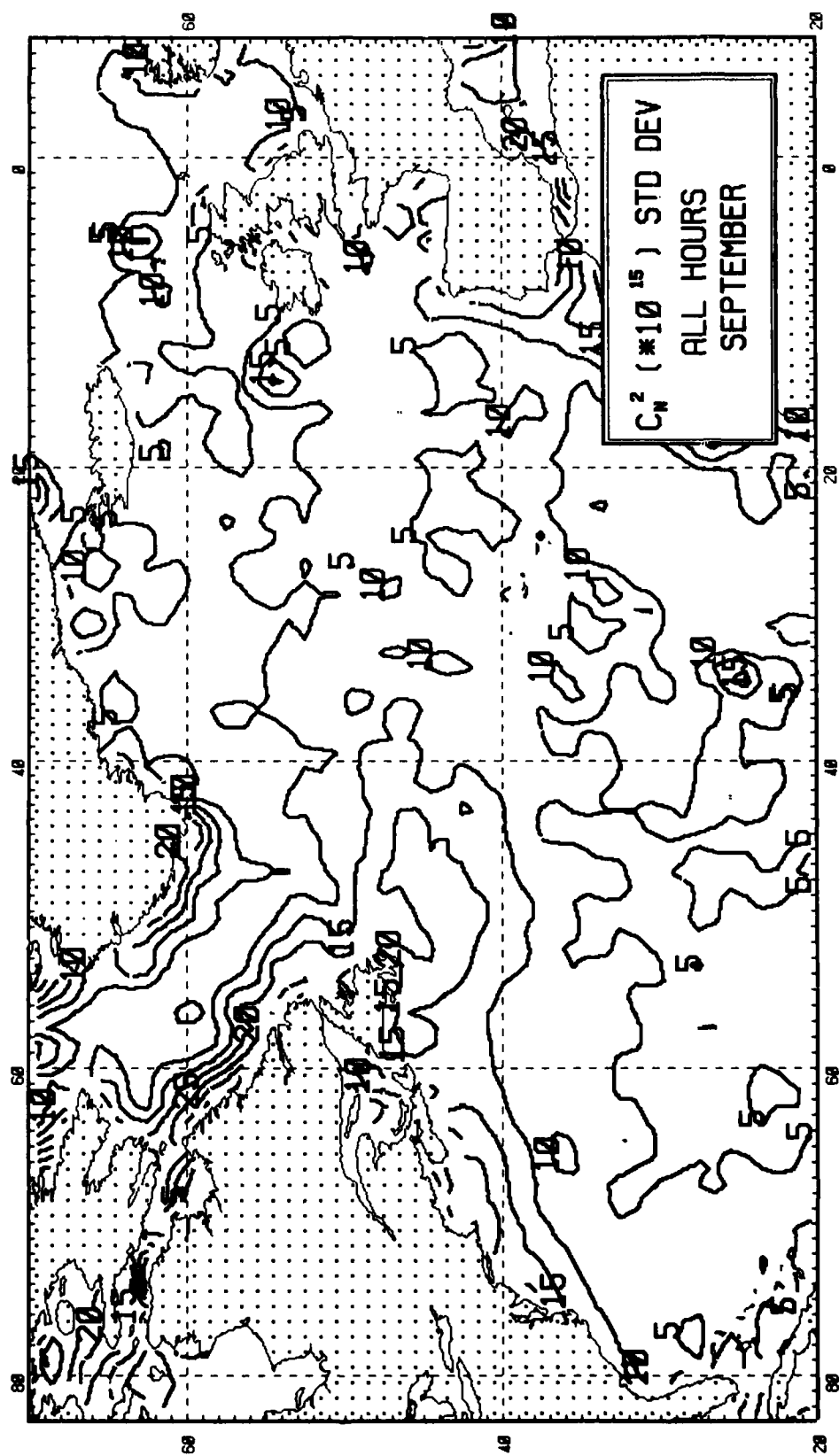




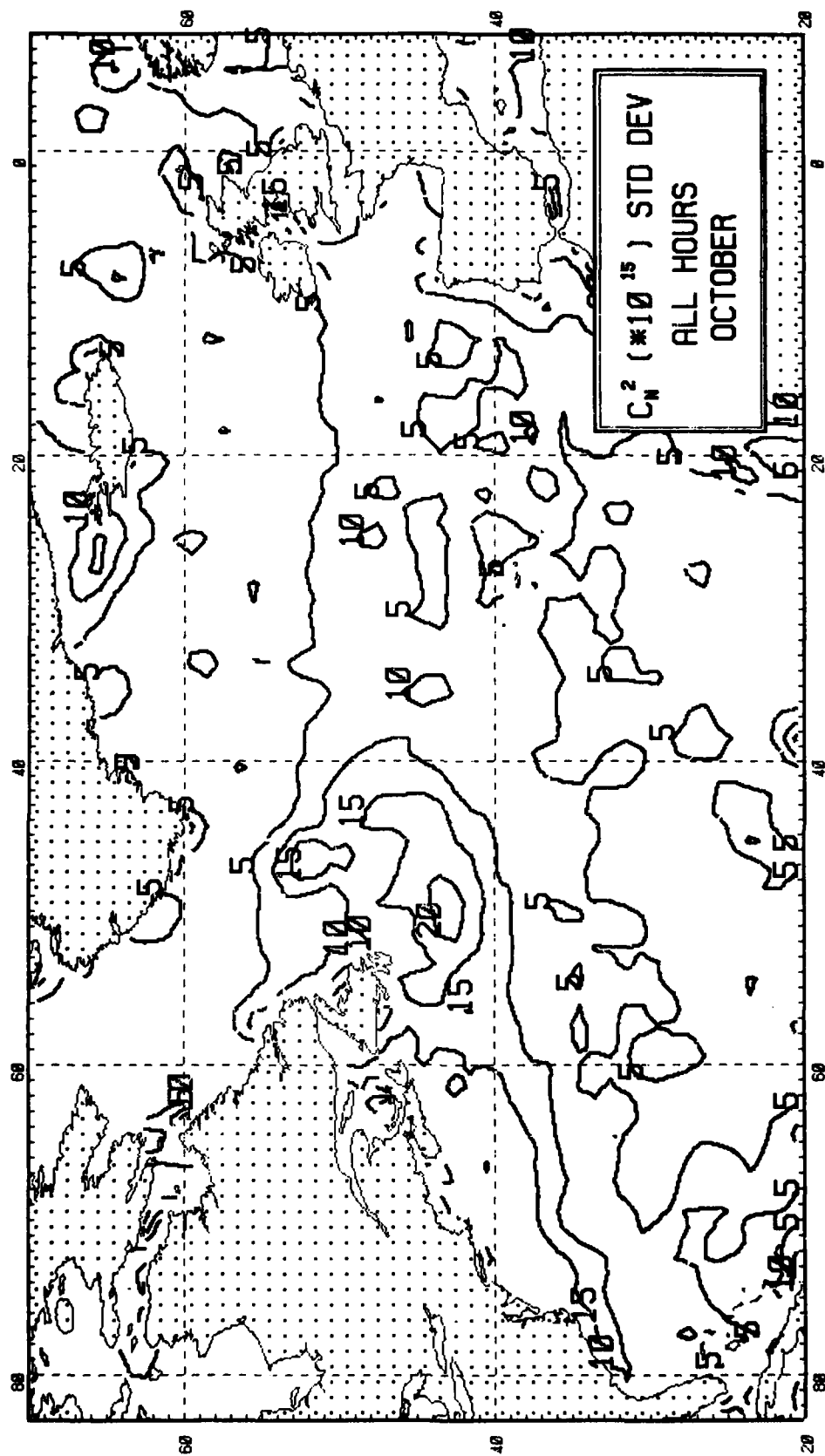


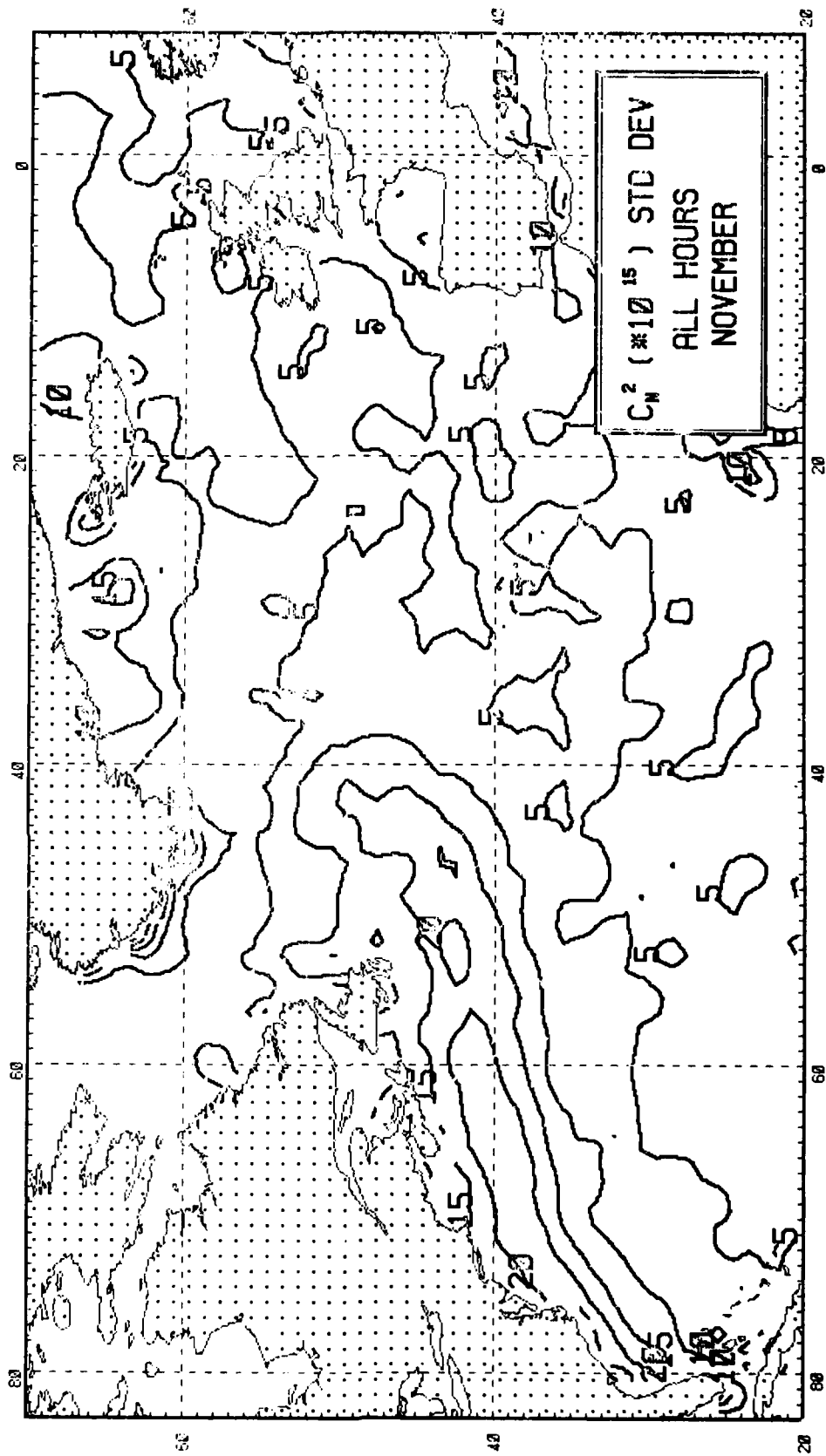


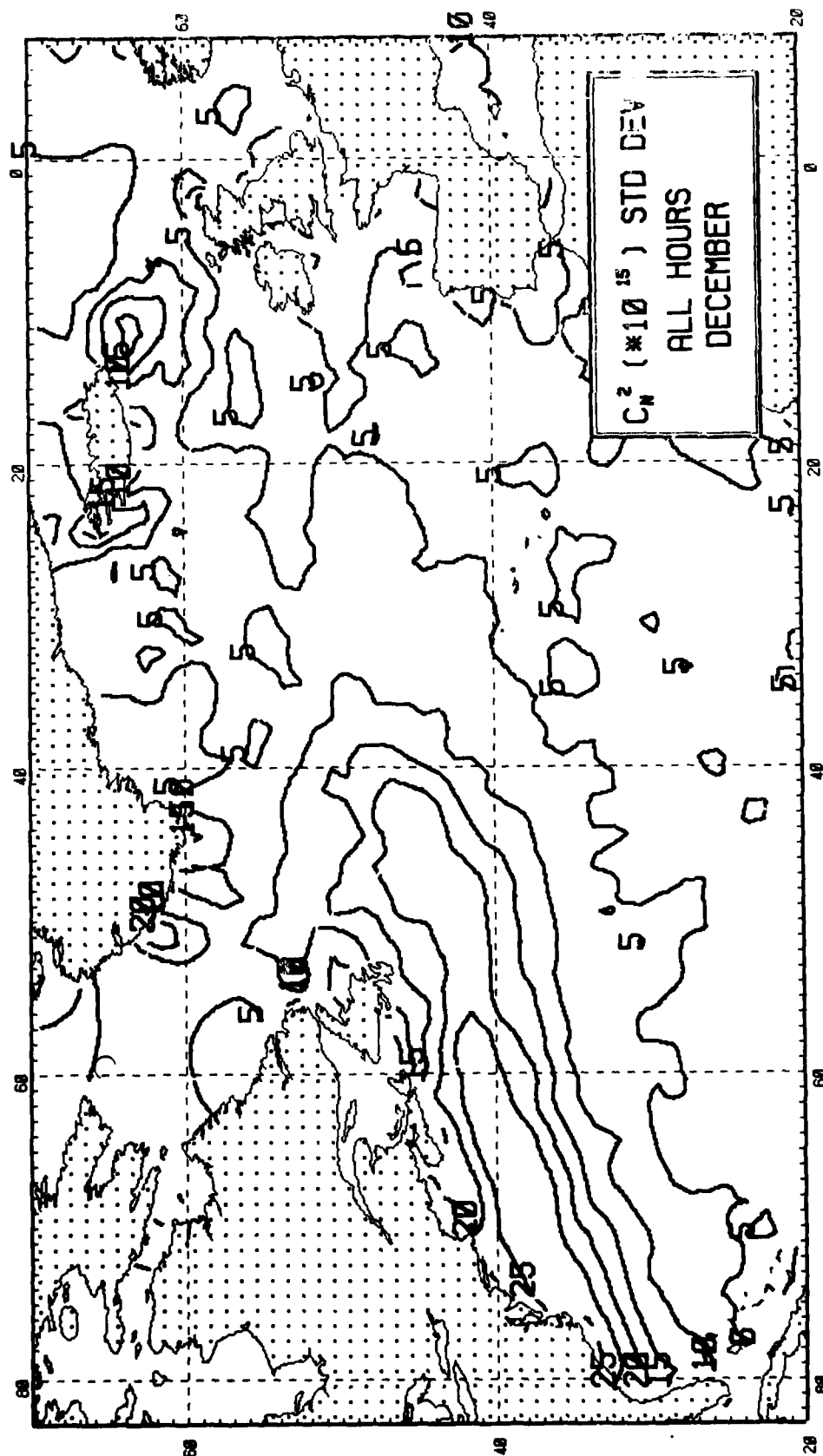


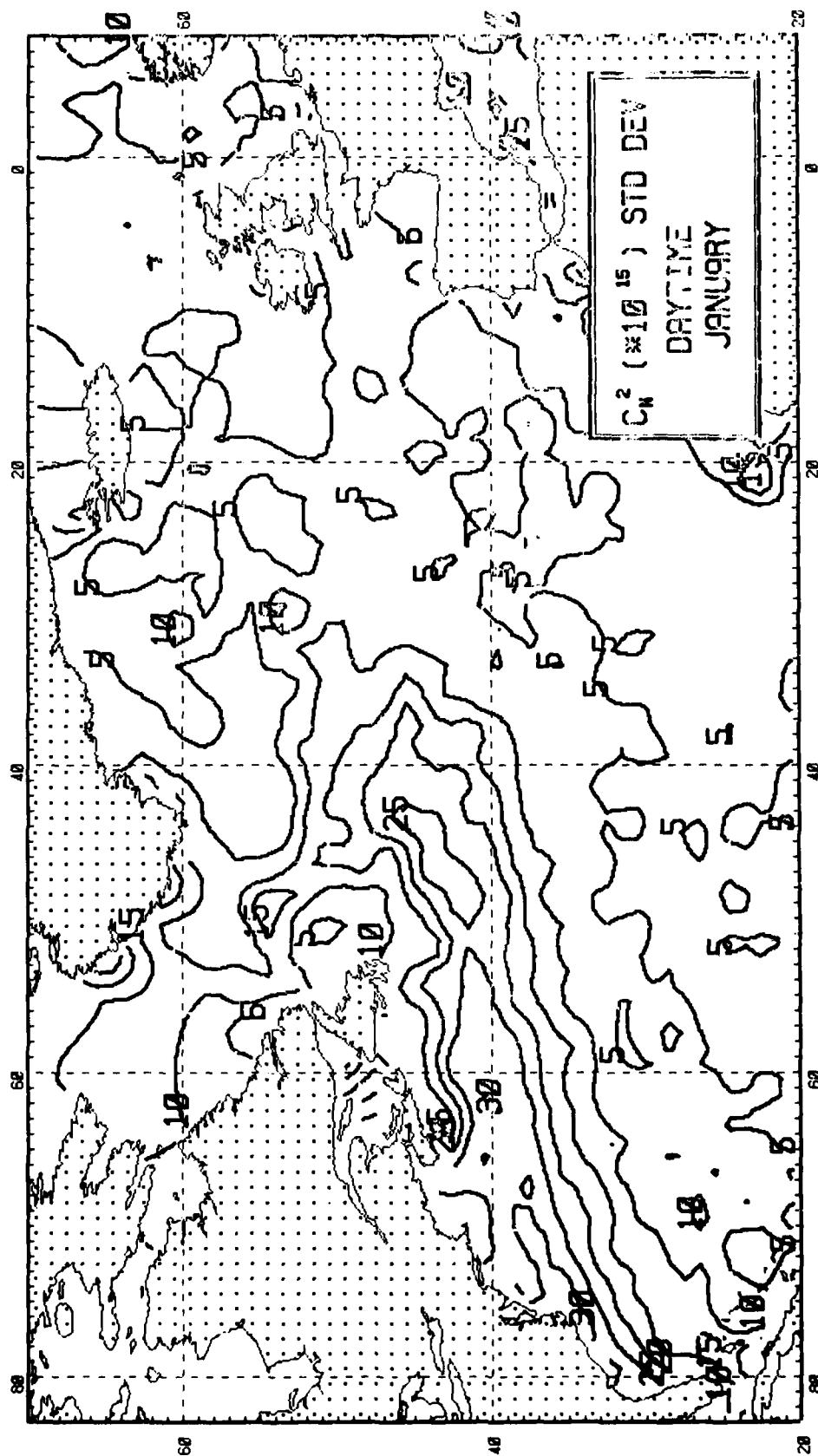




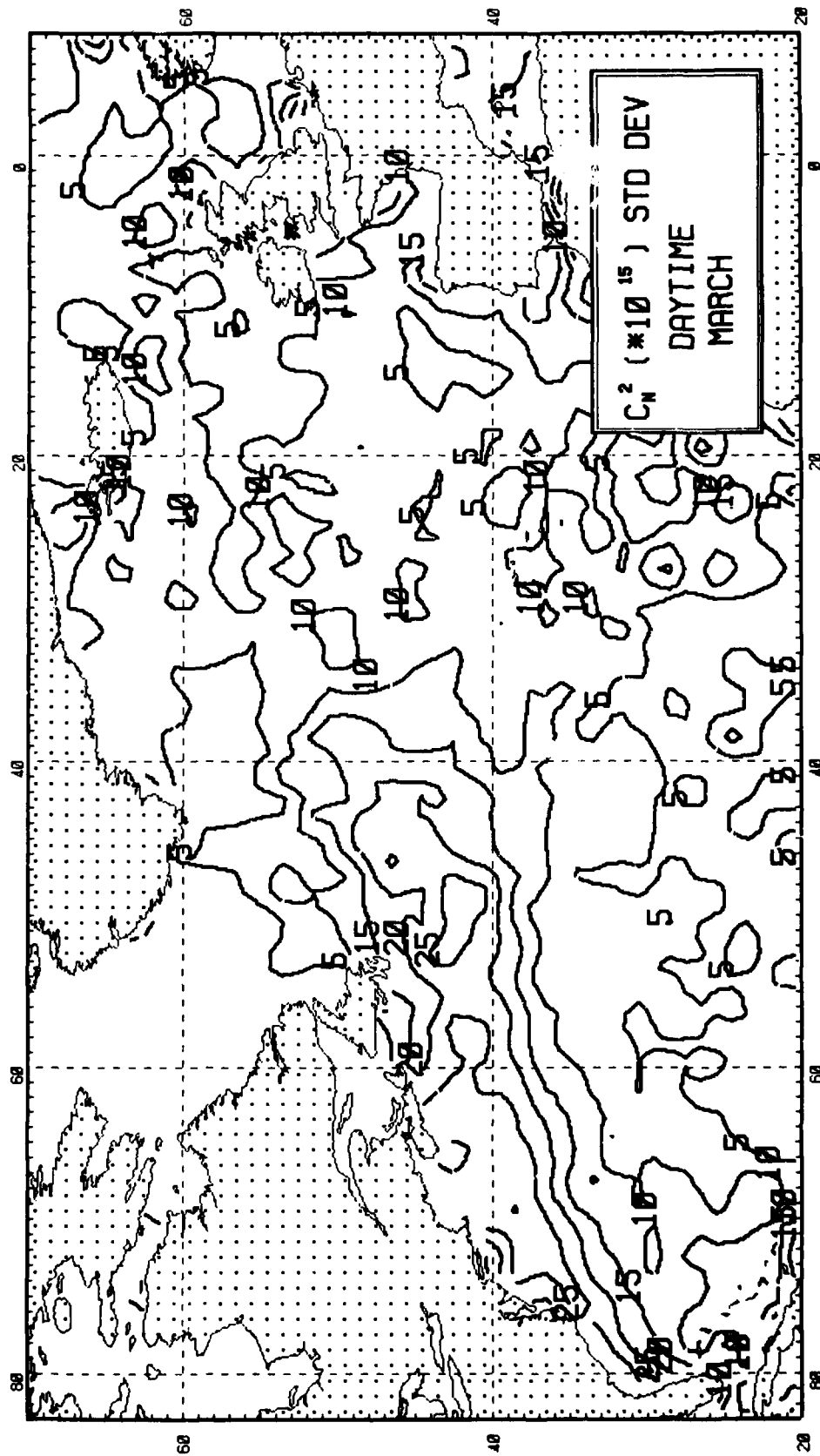


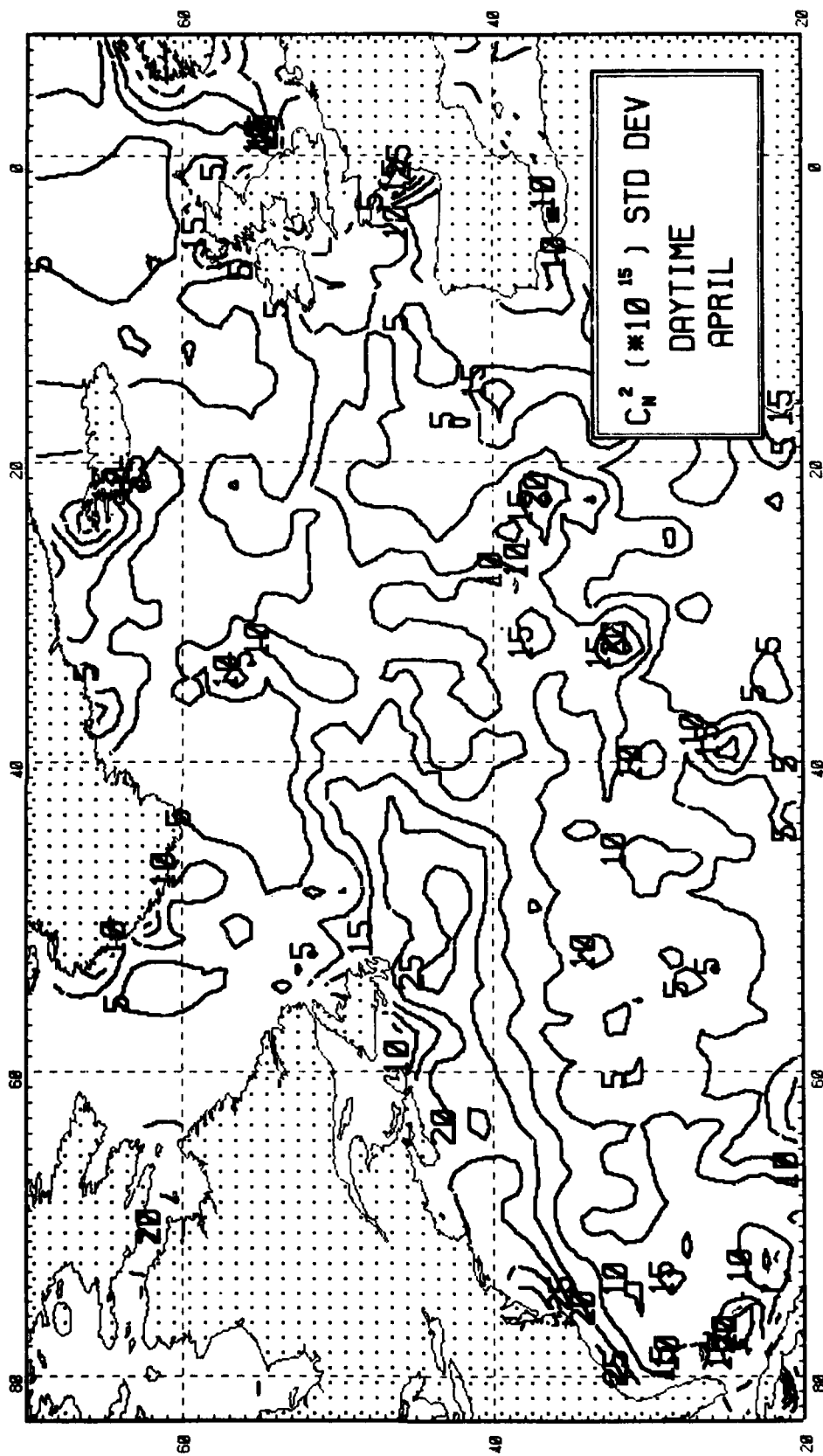


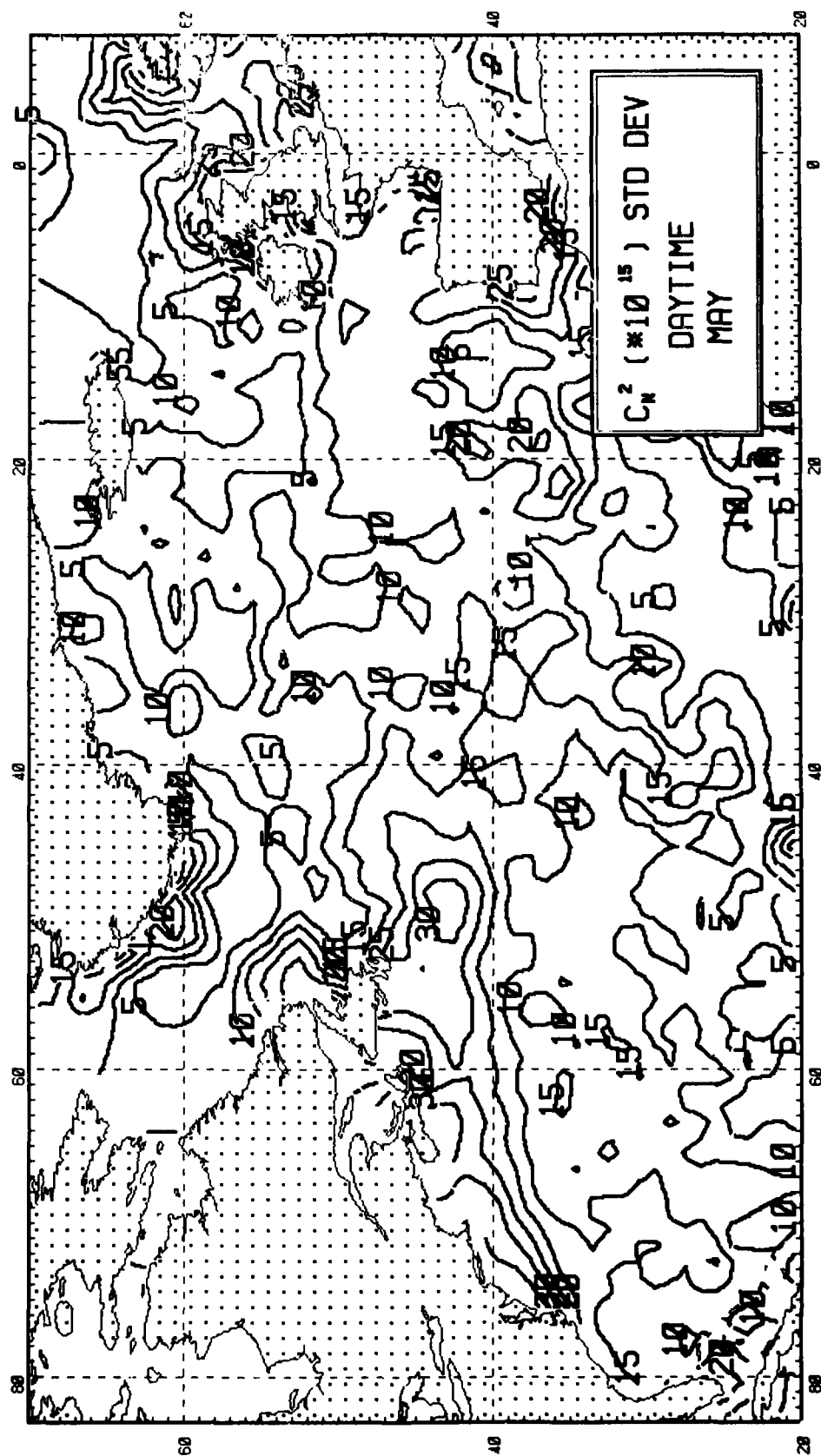




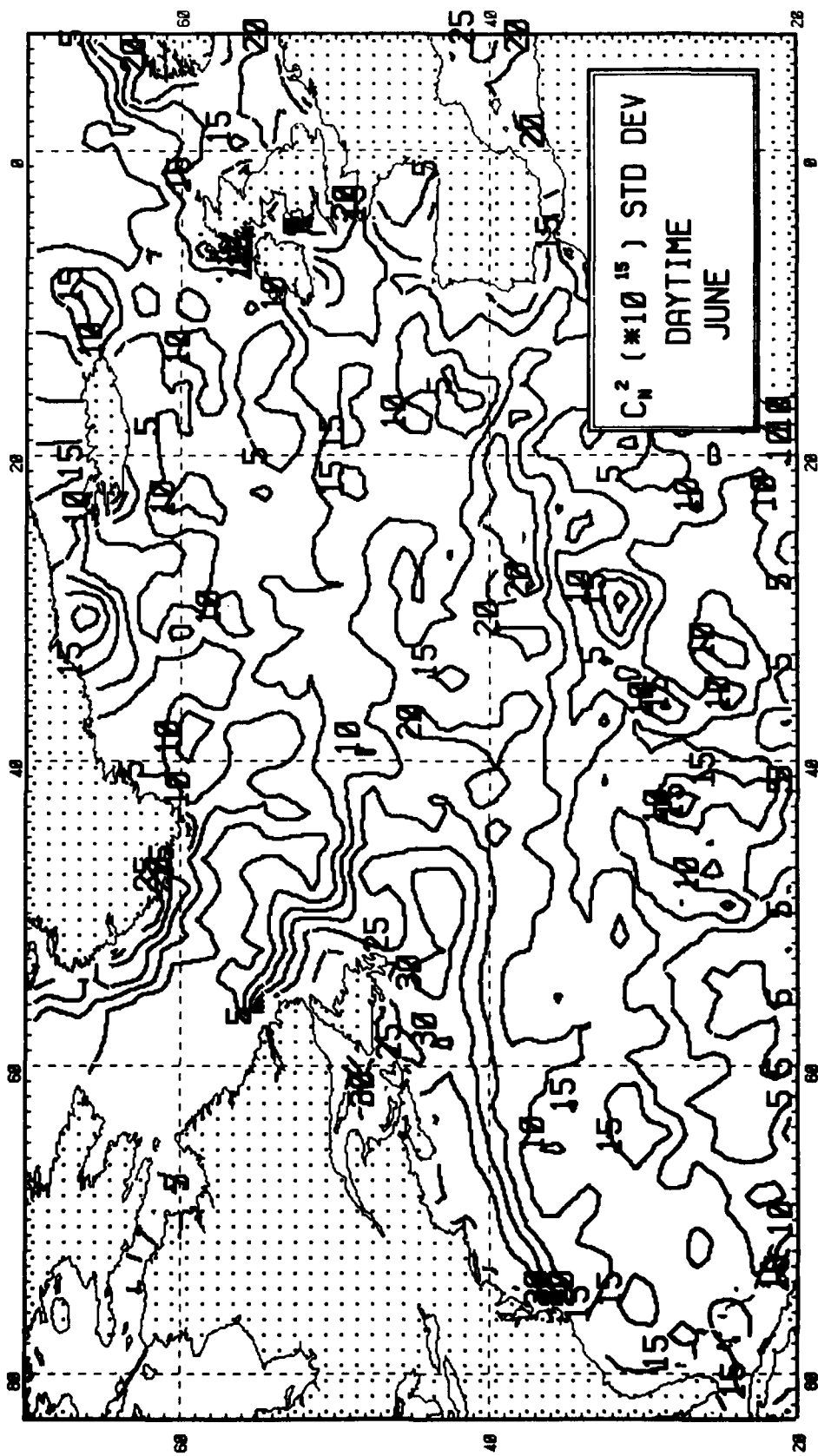


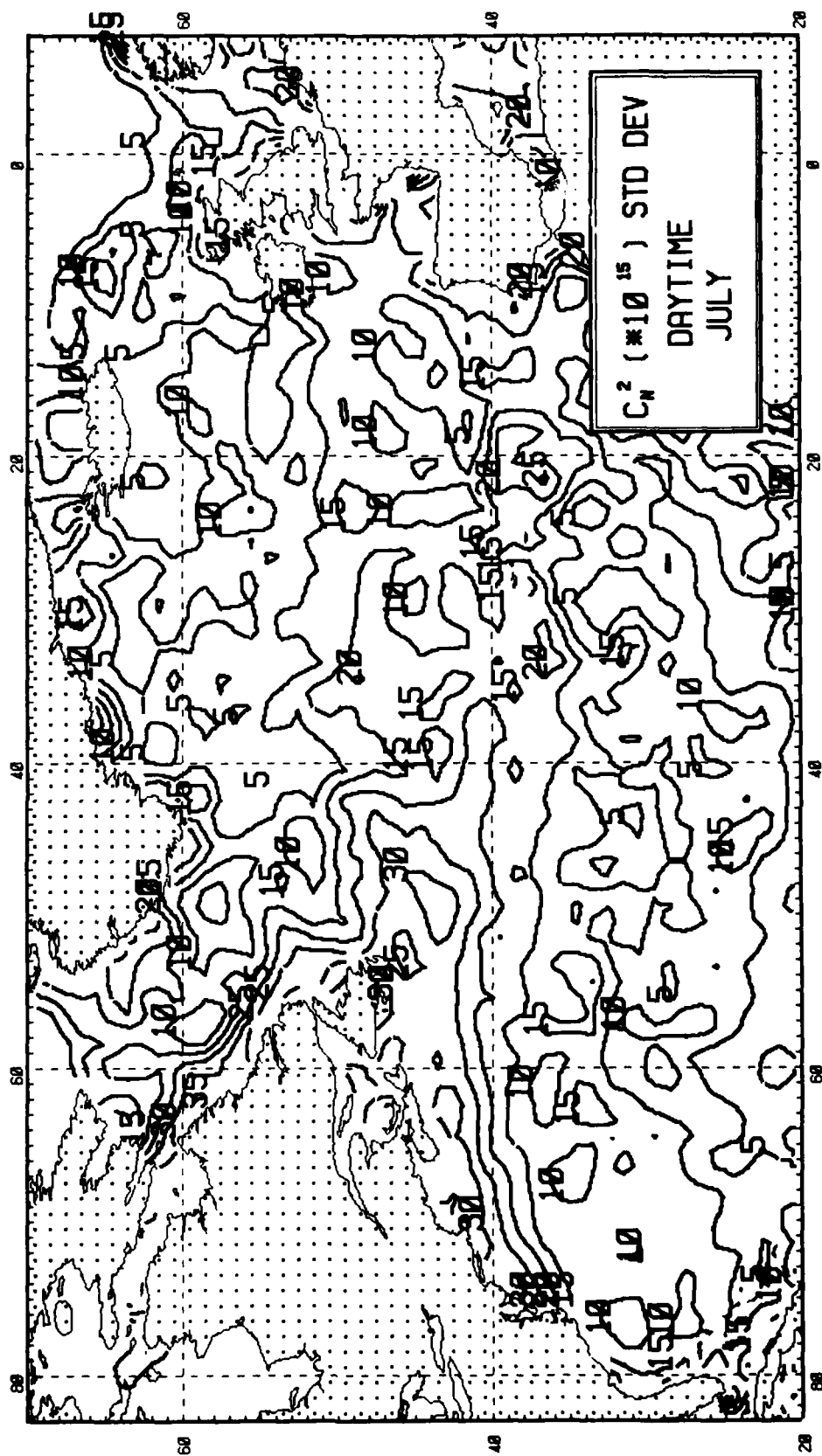


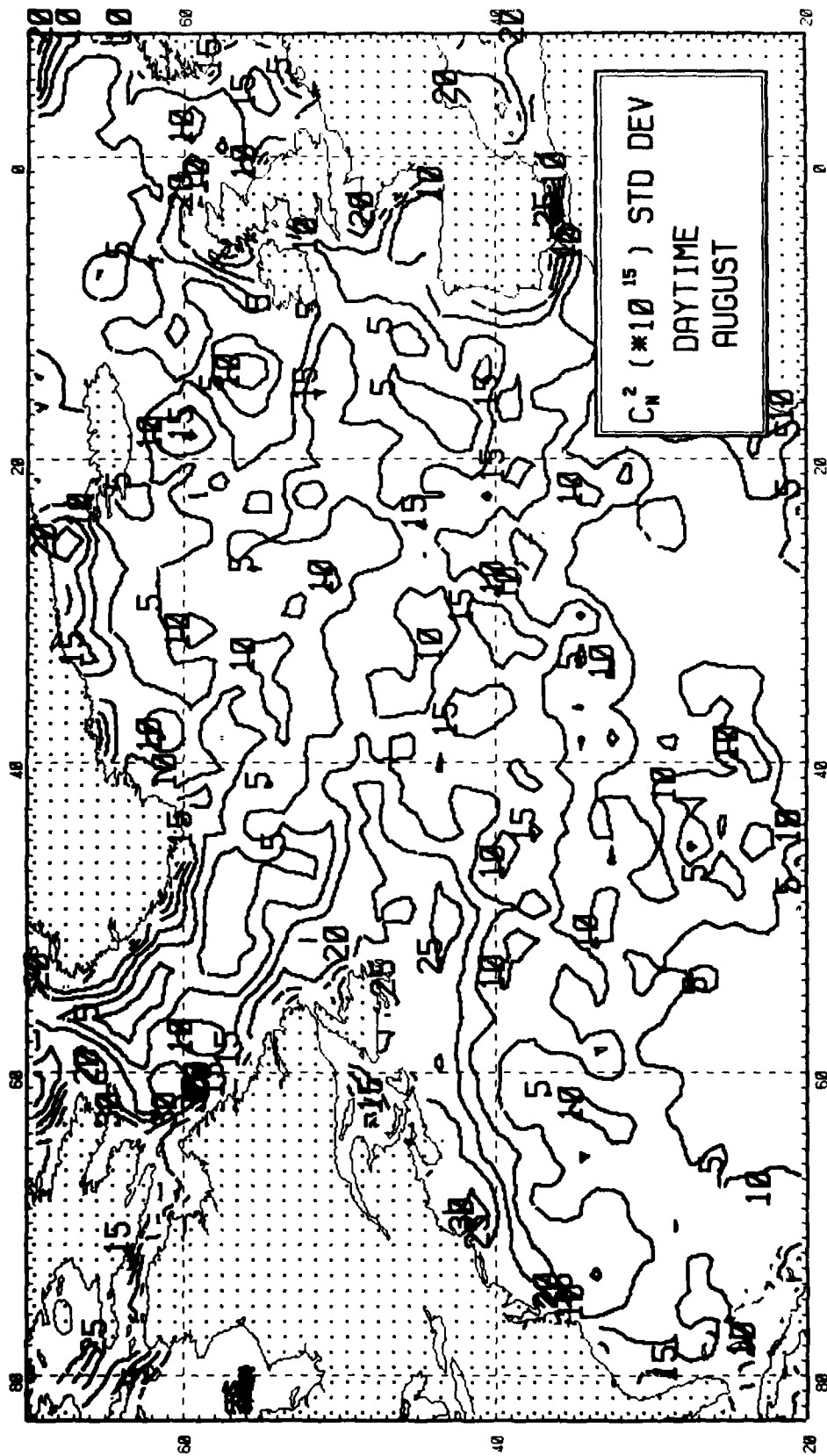


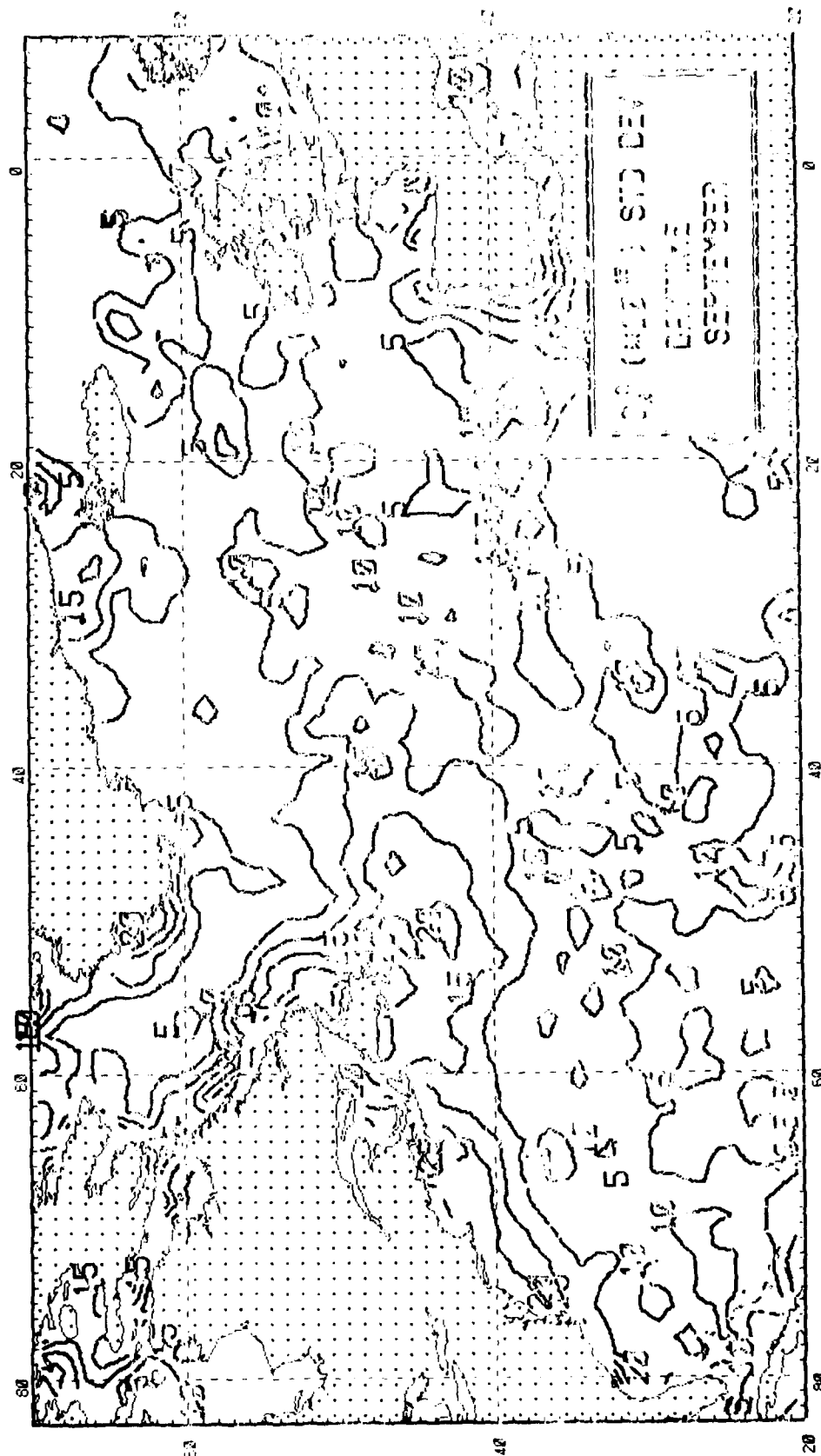


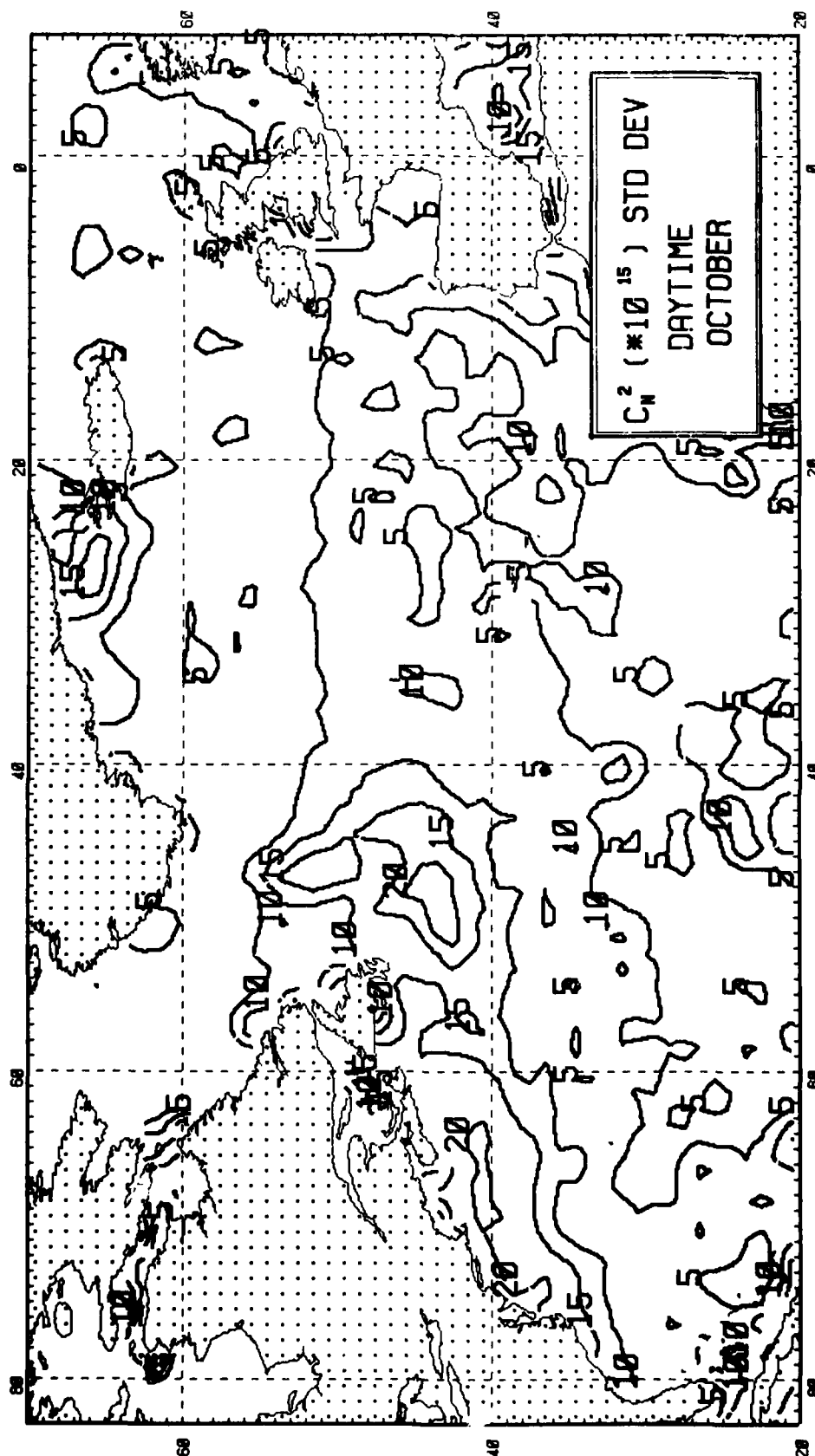


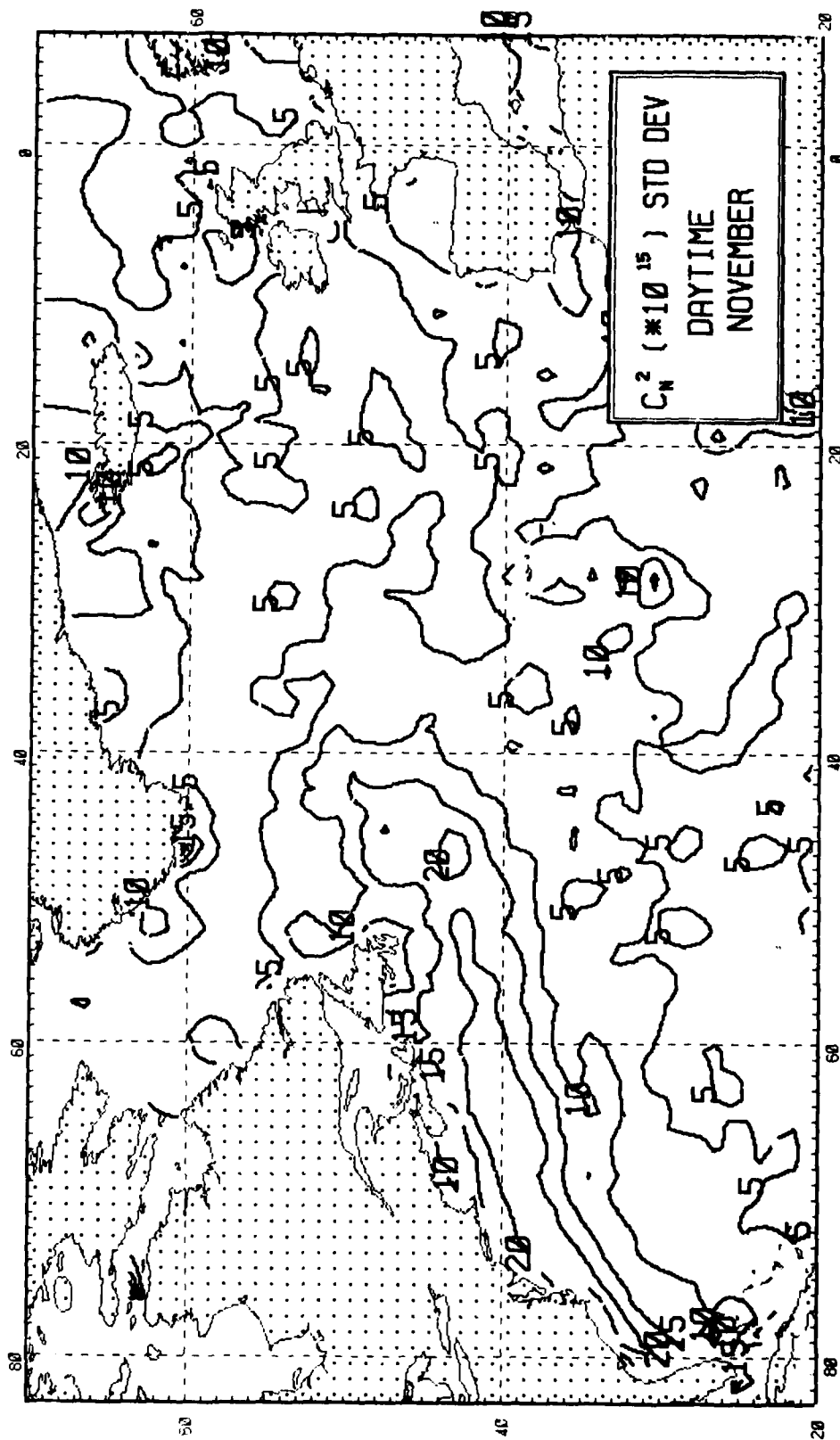


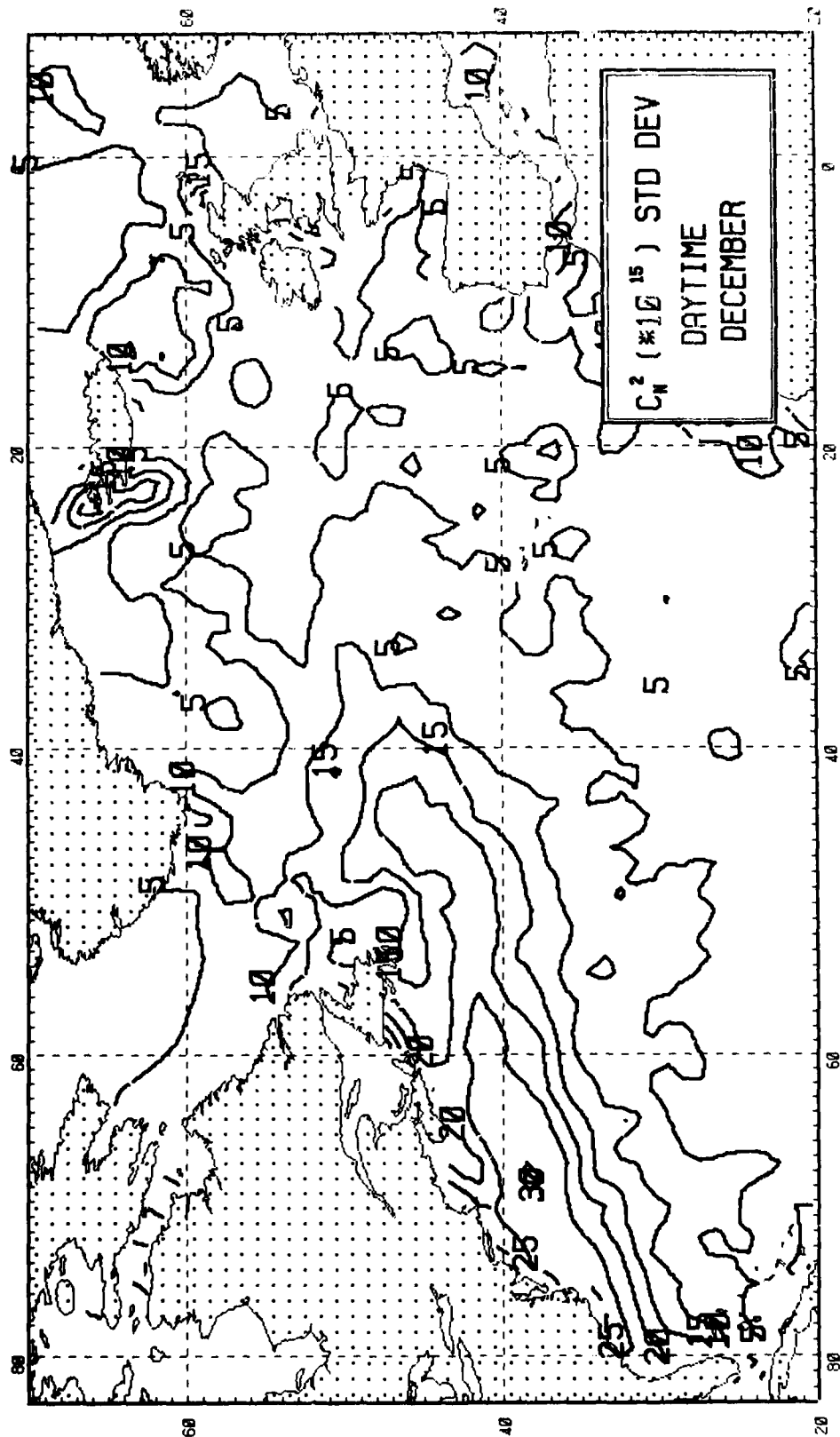


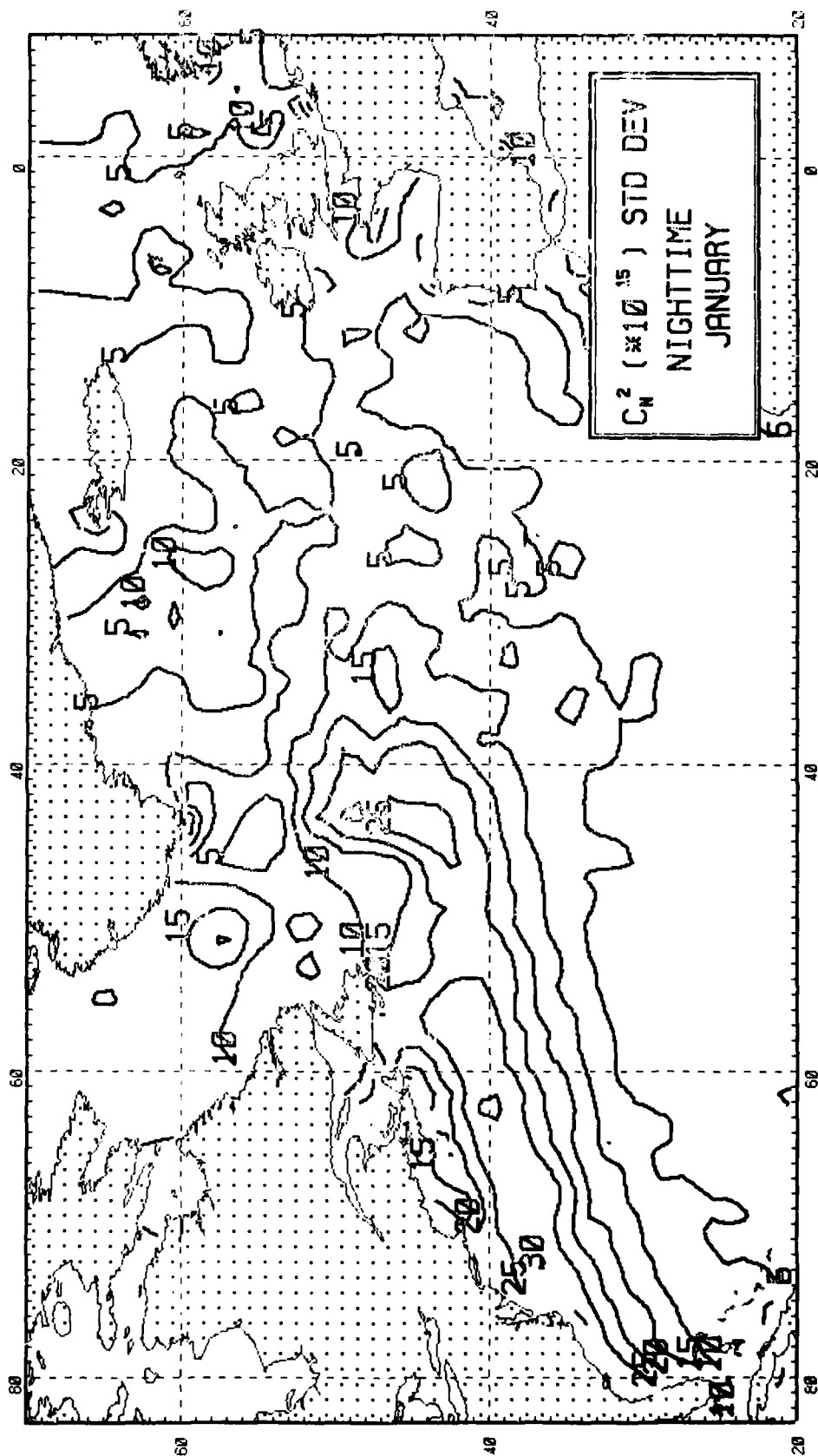




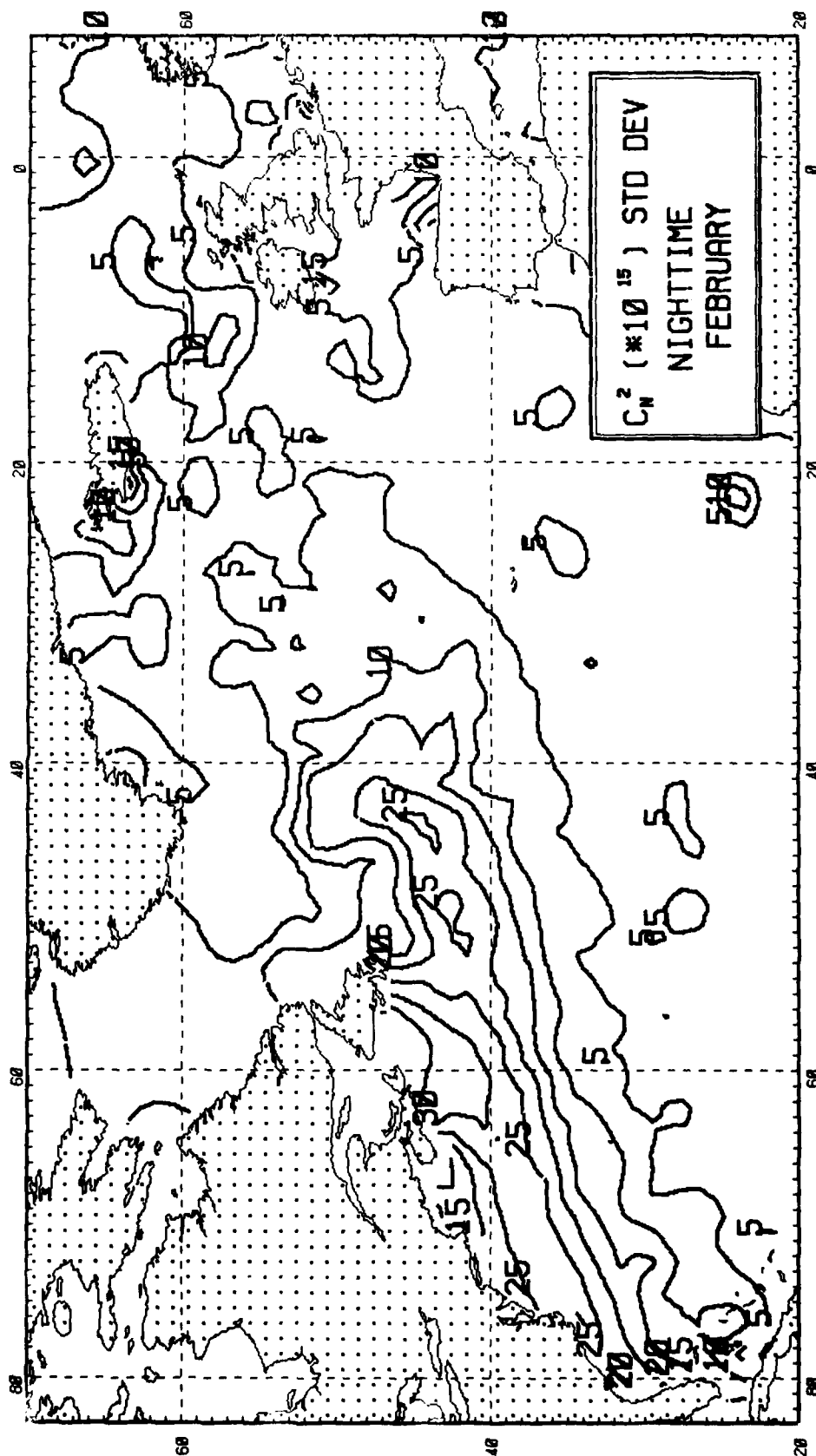


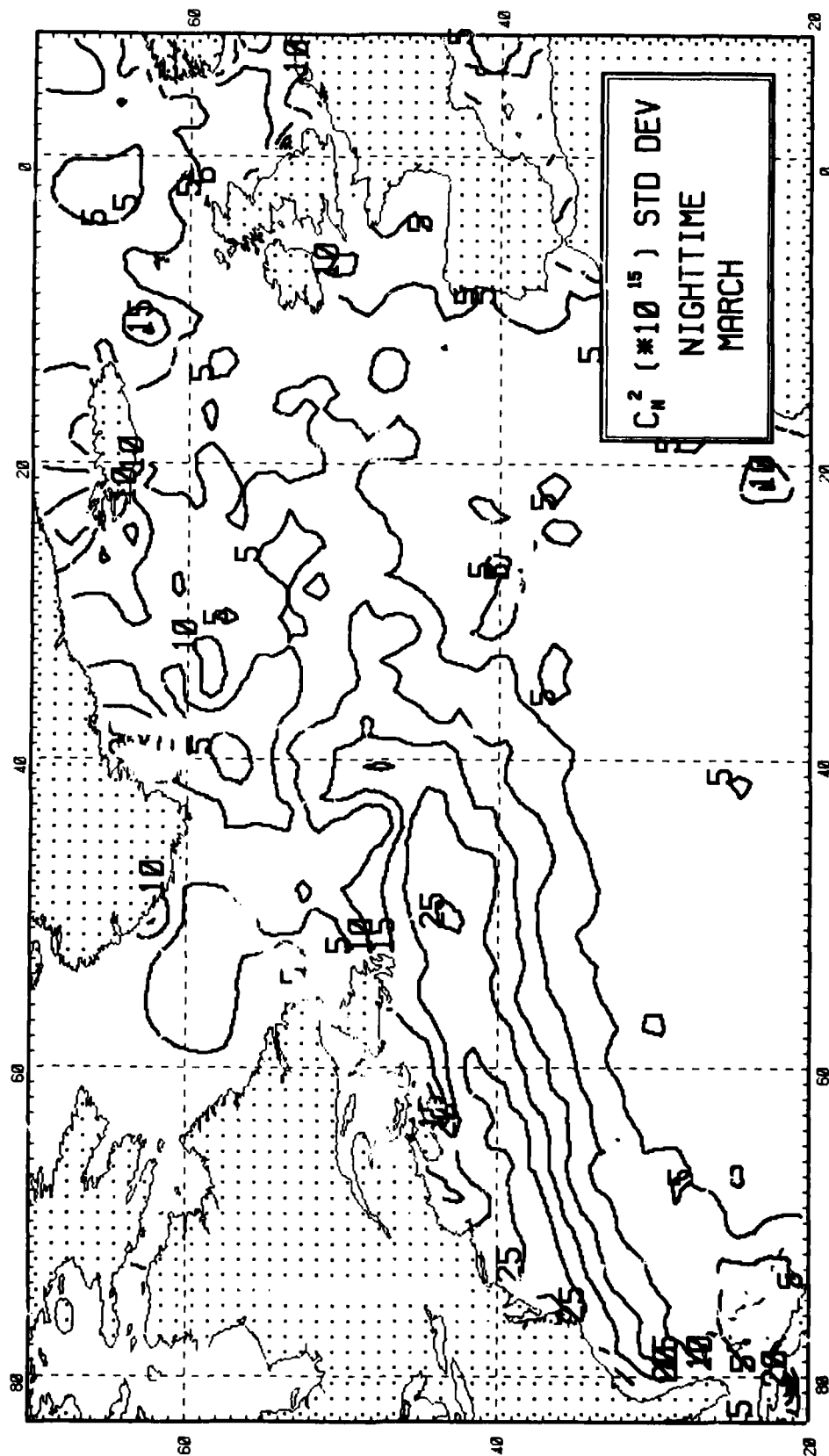


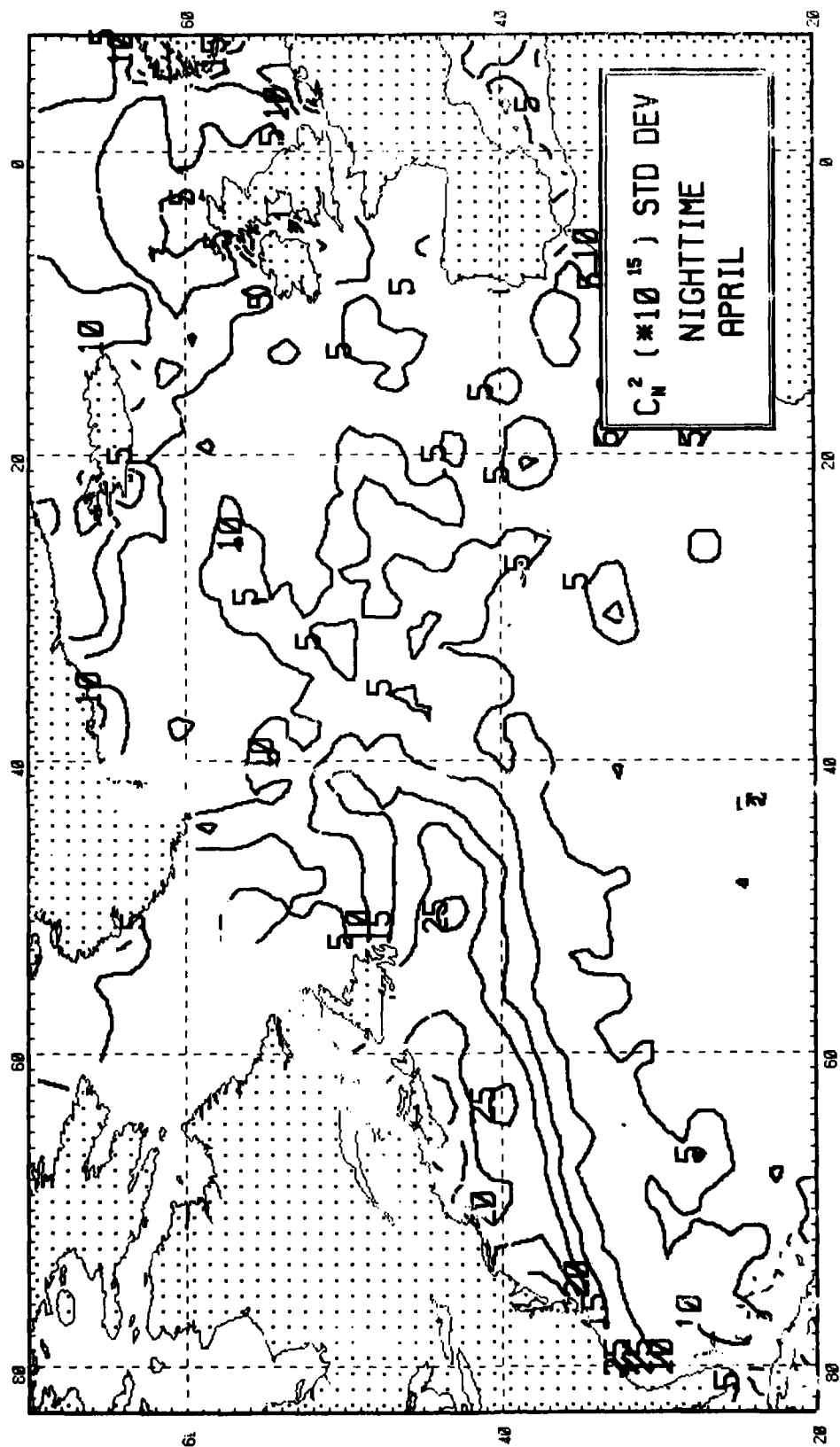


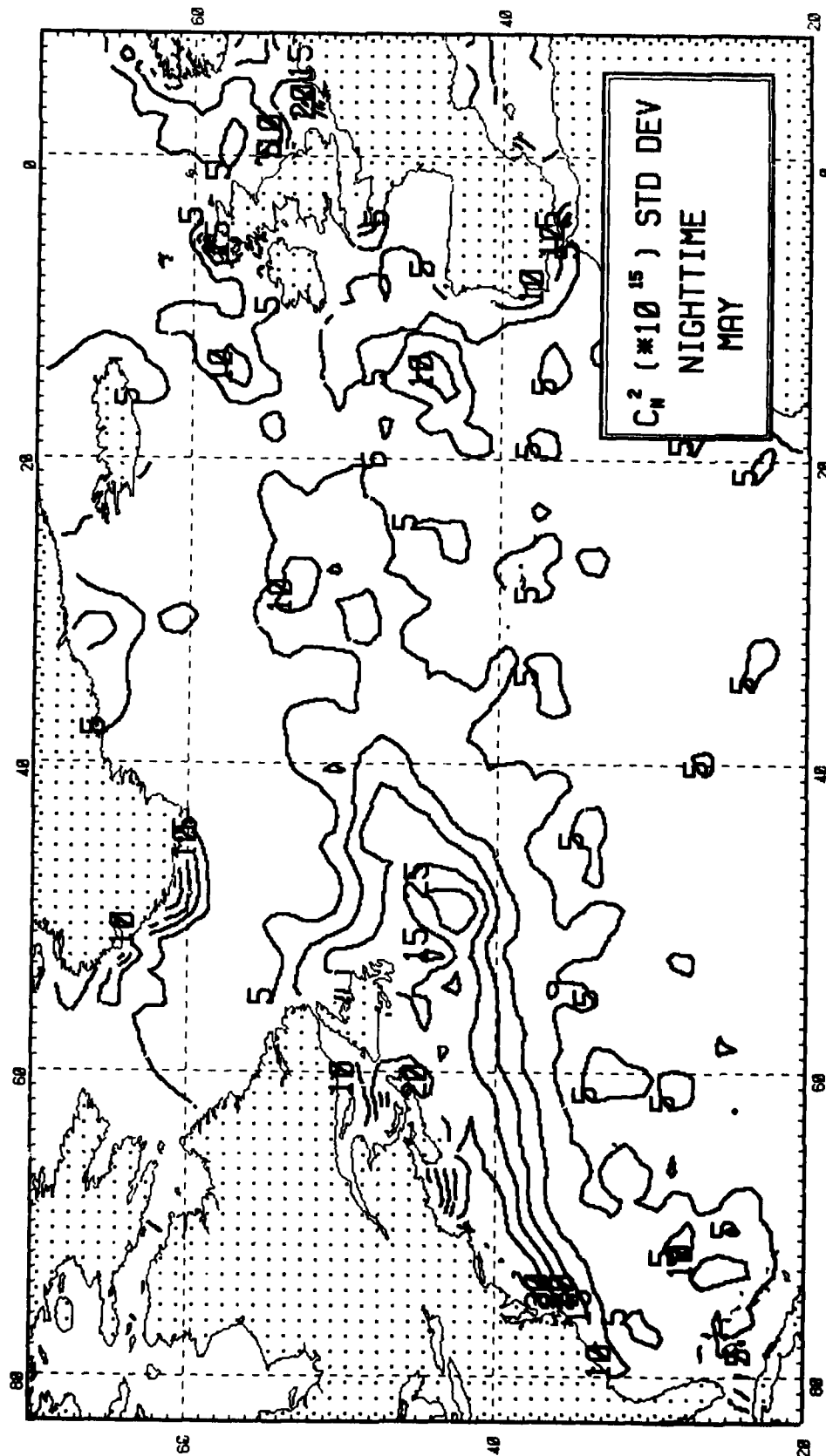


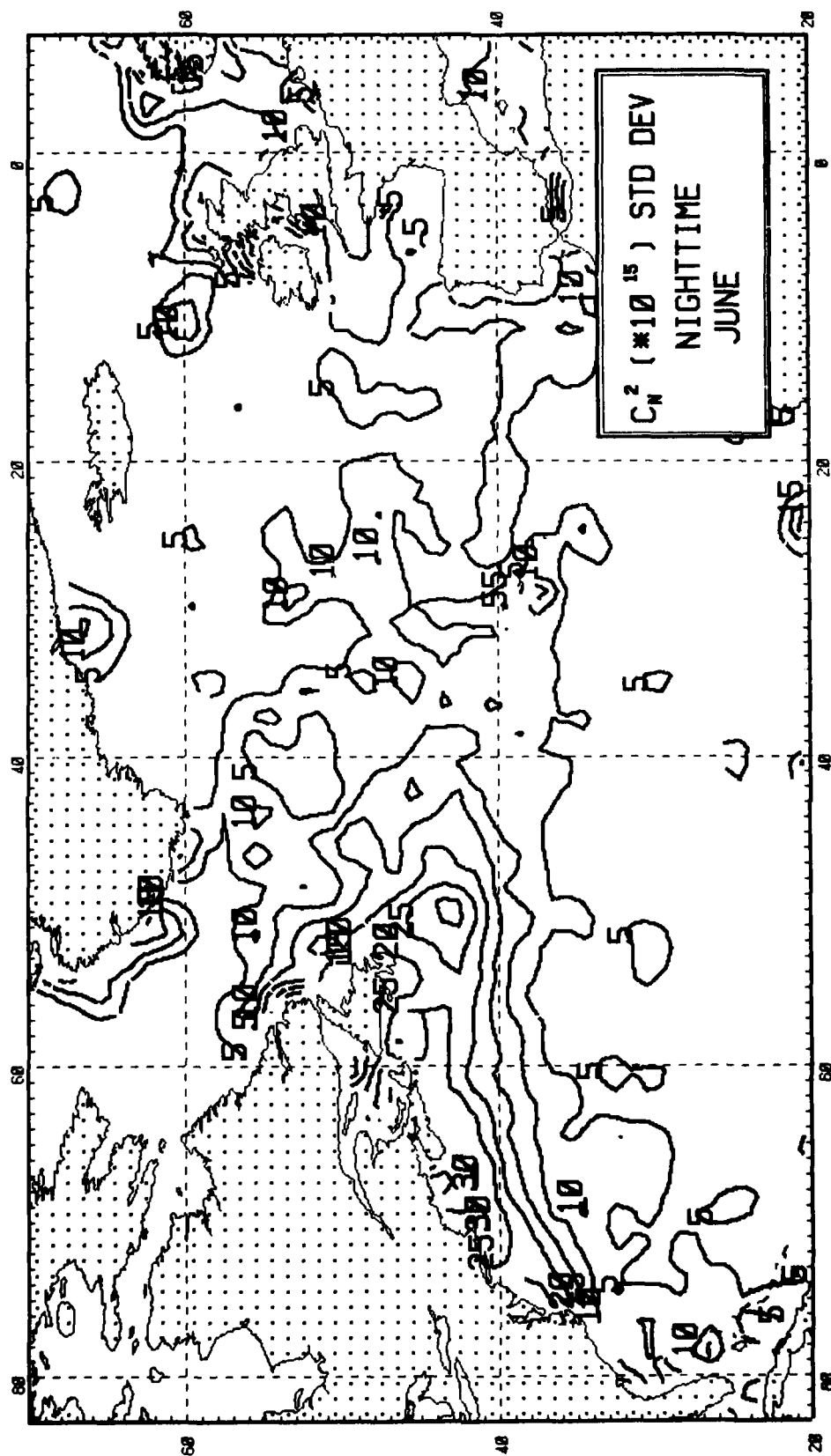












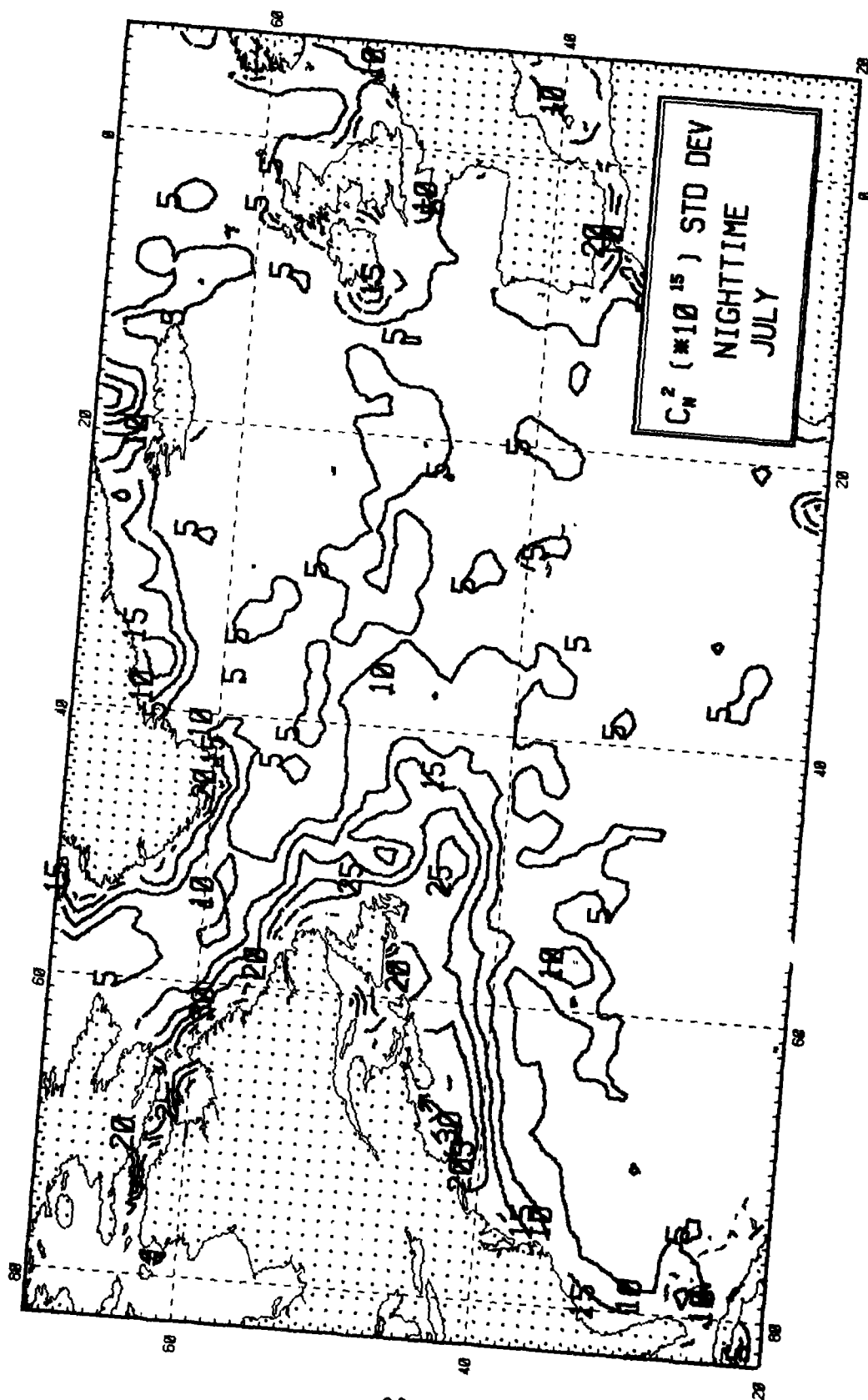
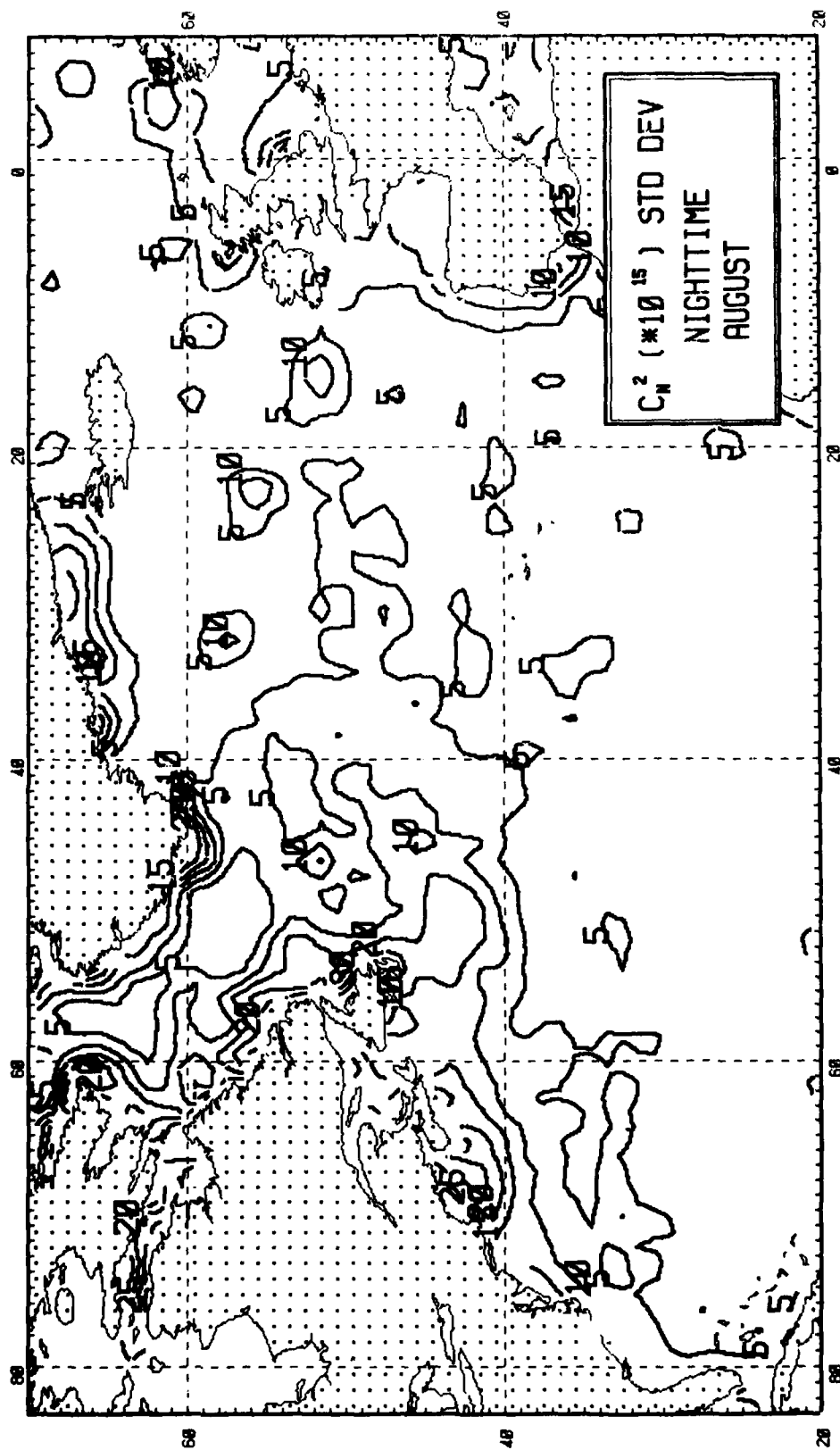
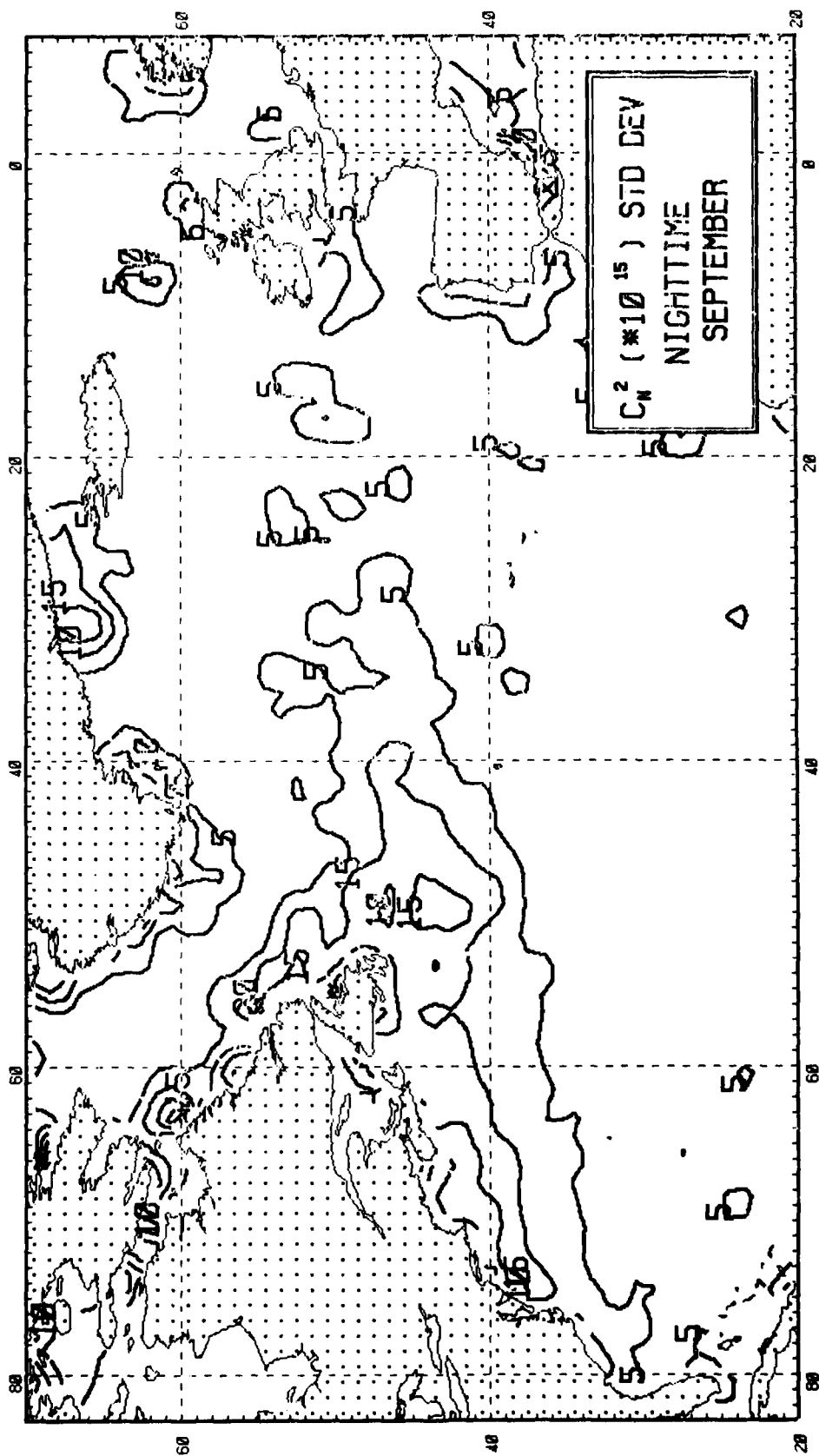
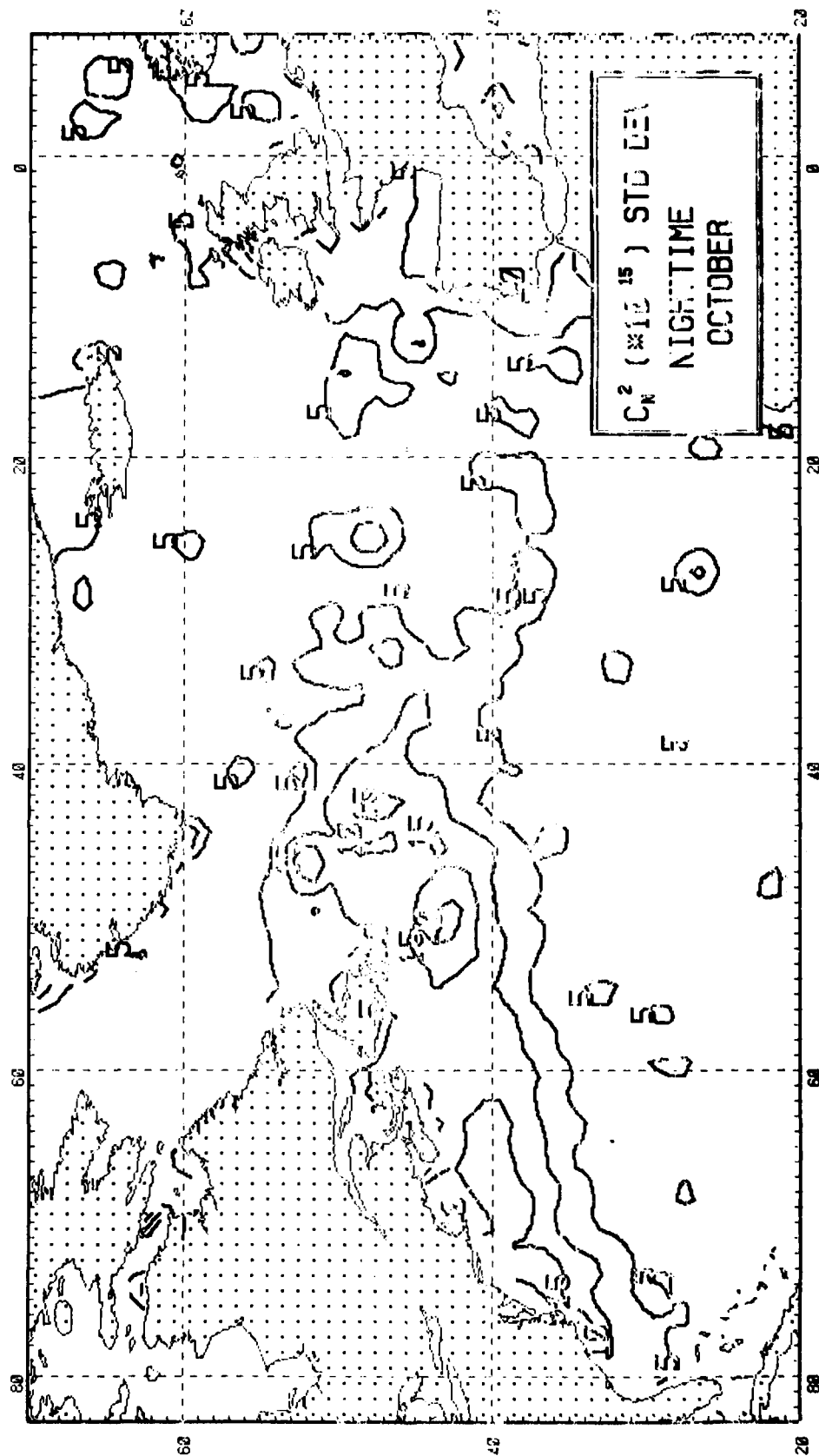


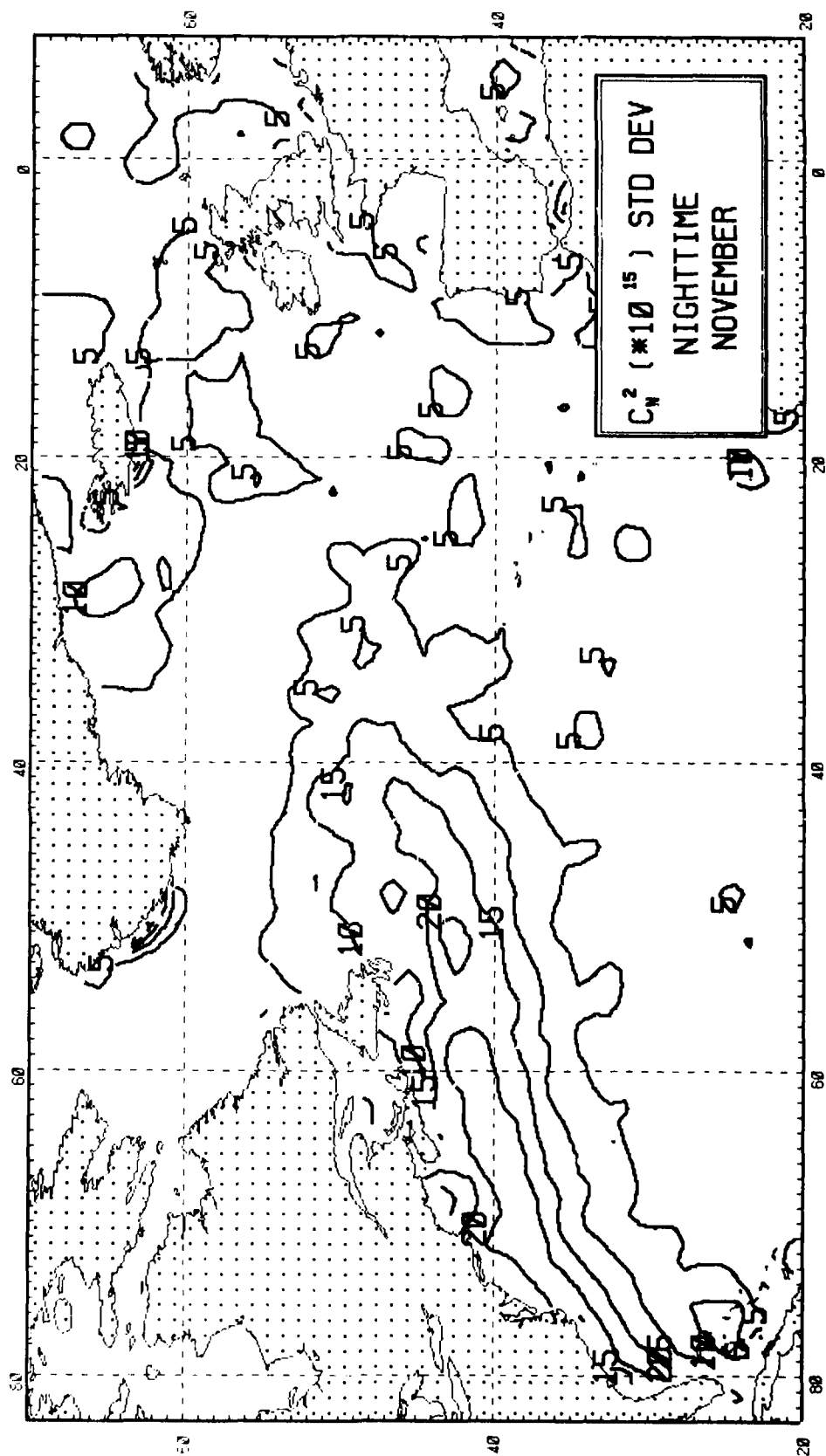
FIGURE 67











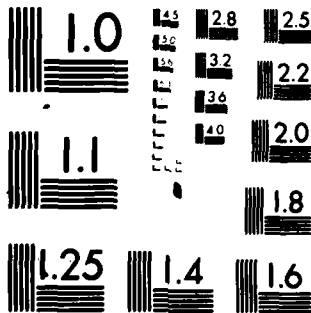
AD-A112 515 NAVAL ENVIRONMENTAL PREDICTION RESEARCH FACILITY MON--ETC F/S 4/2  
A CLIMATOLOGY OF THE REFRACTIVE INDEX STRUCTURE FUNCTION PARAM--ETC(U)  
JAN 82 T BROWN, A K GORUCH  
UNCLASSIFIED NEPRF-TR-82-01 ML

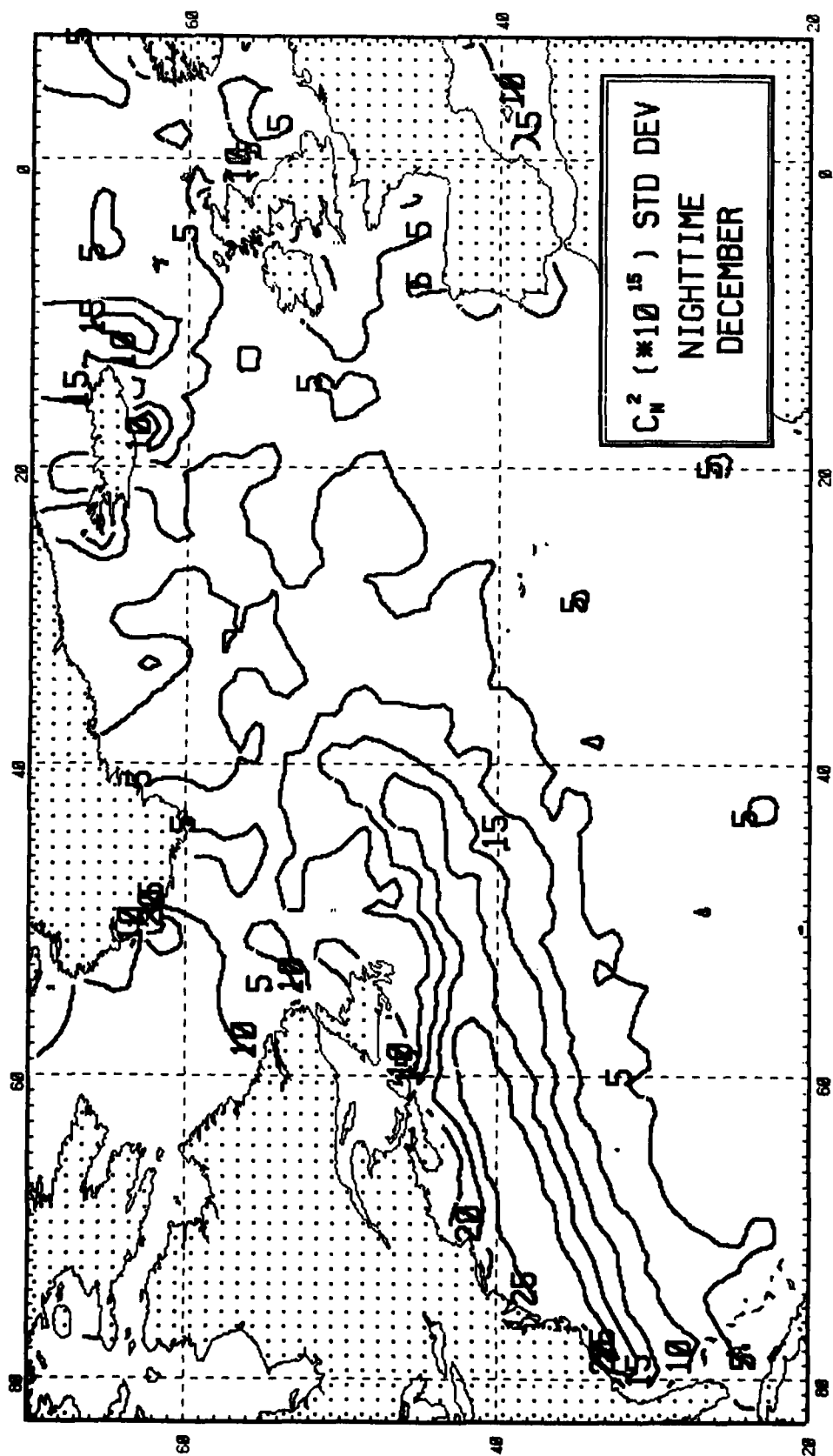
2  
1-4  
2-1



END  
DATE  
FILMED  
4-82  
DTIC

A/125





# DISTRIBUTION

CINCUSNAVEUR  
NAVELEX DET.  
ATTN: NSAP SCI. ADV.  
BOX 100  
FPO NEW YORK 09510

COMSECONDFLT  
ATTN: NSAP SCIENCE ADVISOR  
FPO NEW YORK 09501

COMNAVAIRLANT  
ATTN: NSAP SCIENCE ADV. (30F)  
NORFOLK, VA 23511

COMNAVSURFLANT  
ATTN: NSAP SCIENCE ADV. (N009)  
NORFOLK, VA 23511

COMOPTEVFOR LANT  
ATTN: NSAP SCIENCE ADVISOR  
NORFOLK, VA 23511

OFFICER IN CHARGE  
NEW LONDON TEST & EVALUATION  
FORCE DET., NEW LONDON LAB  
NEW LONDON, CT 06320

CHIEF OF NAVAL RESEARCH  
LIBRARY SERVICES, CODE 734  
RM 633, BALLSTON TOWER #1  
800 QUINCY ST.  
ARLINGTON, VA 22217

OFFICE OF NAVAL RESEARCH  
CODE 428AT  
ARLINGTON, VA 22217

OFFICE OF NAVAL RESEARCH  
CODE 420  
ARLINGTON, VA 22217

CHIEF OF NAVAL OPERATIONS  
OP-952  
U.S. NAVAL OBSERVATORY  
WASHINGTON, DC 20390

CHIEF OF NAVAL OPERATIONS  
NAVY DEPT., OP-986  
WASHINGTON, DC 20350

CHIEF OF NAVAL OPERATIONS  
ATTN: DR. R. W. JAMES, OP-952D1  
U.S. NAVAL OBSERVATORY  
34TH & MASS. AVE.  
WASHINGTON, DC 20390

NAVAL DEPUTY TO THE ADMIN.  
NOAA, RM. 200, PAGE BLDG. #1  
3300 WHITEHAVEN ST. NW  
WASHINGTON, DC 20235

OFFICER IN CHARGE  
NAVOCEANCOMDET  
FEDERAL BUILDING  
ASHEVILLE, NC 28801

COMMANDING OFFICER  
NAVAL RESEARCH LAB  
ATTN: LIBRARY, CODE 2620  
WASHINGTON, DC 20390

COMMANDING OFFICER  
OFFICE OF NAVAL RESEARCH  
EASTERN/CENTRAL REGIONAL OFFICE  
BLDG. 114 SECT. D  
666 SUMMER ST.  
BOSTON, MA 02210

OFFICE OF NAVAL RESEARCH  
SCRIPPS INSTITUTION OF OCEANO.  
LA JOLLA, CA 92037

COMMANDING OFFICER  
NAVEASTOCEANECEN  
MCADIE BLDG. (U-117), NAS  
NORFOLK, VA 23511

SUPERINTENDENT  
LIBRARY REPORTS  
U.S. NAVAL ACADEMY  
ANNAPOLIS, MD 21402

CHAIRMAN  
OCEANOGRAPHY DEPT.  
U.S. NAVAL ACADEMY  
ANNAPOLIS, MD 21402

COMMANDER  
NAVAIRSYSCOM  
ATTN: LIBRARY, AIR-00D4  
WASHINGTON, DC 20361

COMMANDER  
NAVAIRSYSCOM (AIR-376)  
WASHINGTON, DC 20361

COMMANDER  
NAVAL SEA SYSTEMS COMMAND  
ATTN: LCDR S. GRIGSBY  
PMS-405/PM-22  
WASHINGTON, DC 20362

COMMANDER  
NAVAL OCEAN SYSTEMS CENTER  
ATTN: DR. J. RICHTER, CODE 532  
SAN DIEGO, CA 92152

COMMANDER  
NAVAL WEAPONS CENTERS  
ATTN: DR. A. SCHLANTA, CODE 3918  
CHINA LAKE, CA 93555

COMMANDER  
NAVAL SURFACE WEAPONS CENTER  
ATTN: CODE N54  
DAHLGREN, VA 22448

COMMANDER  
NAVAL SURFACE WEAPONS CENTER  
ATTN: DR. B. KATZ, CODE R42  
WHITE OAKS LABORATORY  
SILVER SPRING, MD 20910

COMMANDER  
PACMISTESTCEN  
ATTN: GEOPHYSICS OFFICER, 3250  
PT. MUGU, CA 93042

NAVAL POSTGRADUATE SCHOOL  
ATTN: METEOROLOGY DEPT., CODE 63  
MONTEREY, CA 93940

NAVAL POSTGRADUATE SCHOOL  
ATTN: OCEANOGRAPHY DEPT. CODE 68  
MONTEREY, CA 93940

NAVAL POSTGRADUATE SCHOOL  
ATTN: PHYSICS & CHEMISTRY DEPT.  
MONTEREY, CA 93940

USAFETAC/TS  
SCOTT AFB, IL 62225

COMMANDER & DIRECTOR  
ATTN: DELAS-DM-A  
U.S. ARMY ATMOS. SCIENCES LAB  
WHITE SANDS MISSILE RANGE,  
WHITE SANDS, NM 88002

COMMANDER & DIRECTOR  
ATTN: DELAS-AS-P  
U.S. ARMY ATMOS. SCIENCES LAB  
WHITE SANDS MISSILE RANGE  
WHITE SANDS, NM 88002

DIRECTOR  
DEFENSE TECH. INFO CENTER (DTIC)  
CAMERON STATION  
ALEXANDRIA, VA 22314

COMMANDANT  
U.S. COAST GUARD HQ.  
ATTN: LCDR J. M. SAP (G-05T-2)  
2100 2ND ST. NW  
WASHINGTON, DC 20593

HEAD, ATMOSPHERIC SCIENCES DIV.  
NATIONAL SCIENCE FOUNDATION  
1800 G. STREET, NW  
WASHINGTON, DC 20550

PACIFIC SIERRA RESEARCH CORP.  
ATTN: A. SHAPIRO  
1456 CLOVERFIELD BLVD.  
SANTA MONICA, CA 90404

DATE  
FILMED  
→ 8